

Development of drilling optimization models for autonomous rotary drilling systems.

AMADI, K.W.

2023

The author of this thesis retains the right to be identified as such on any occasion in which content from this thesis is referenced or re-used. The licence under which this thesis is distributed applies to the text and any original images only – re-use of any third-party content must still be cleared with the original copyright holder.

Development of Drilling Optimization Models for Autonomous Rotary Drilling Systems

Kingsley Williams Amadi

MSc. Drilling and Well Engineering (RGU, Aberdeen, 2010)

BEng. Petroleum Engineering (University of Port-Harcourt, 2002)

DISSERTATION

Presented for the school of Graduate Studies of

The Robert Gordon University Aberdeen

in Partial Fulfillment for the award of degree of

Doctor of Philosophy



**Robert Gordon University
Aberdeen**

November 2023

Abstract

The growing global energy demand and strict environmental policies motivates the use of technology and performance improvement techniques in drilling operations. Traditional drilling method depends on effectiveness of human-driller in the management of operating parameters to improve system performance. Although existing work has identified the need to upscale from manual drilling to autonomous drilling system with results based on manipulation of surface drilling parameters to construct response for rate of penetration (ROP) to identify local maxima. This approach has limited applicability and is prone to intense operational redundancy. This thesis presents predictive optimization models that uses machine learning (ML) data analytics with actual field drilling data and experimental studies to develop predictive models for rock unconfined compressive strength (UCS) and ROP enabling optimal decision-making protocol. To evaluate optimized operating procedure, a comparative study of surface operating parameters using weight on bit (WOB), and rotary speed (RPM) versus drilling mechanical specific energy (DMSE), and feed thrust (FET) is presented. The study used a data-driven approach, that uses offset drilling data with machine learning model in finding a pair of input operating variables that serves as best tuning parameters for the topdrive and drawwork system. The results illustrate that derived variables (DMSE, FET) gave higher prediction accuracy with correlation coefficient (R^2) of 0.985, root mean square error (RMSE) of 7.6 and average absolute percentage error (AAPE) of 34, whilst using the surface operating parameters (WOB, RPM) delivered an R^2 , RMSE and AAPE of 0.74, 28 and 106 respectively. Additionally, ML predictive model for rock UCS using basic drilling parameters showed that Artificial Neural Network (ANN) and CATBoost gave acceptable qualitative instantaneous UCS prediction whilst drilling. The work further showed that continuous drill-off testing can

be formulated as a Markov Decision Process (MDP) which intermittently analyzes a batch real-time data using Q-value algorithm to select the pair of surface operating parameters. The findings showed that application of these models could improve drilling performance by 30-60% compared to best offset well. Moreover, it will enhance operational health and safety and provides engineered approach for efficiency of drilling process in terms of cost and time.

Acknowledgments

I would like to express my sincere gratitude towards my supervisors; Dr. Ibiye Iyalla and Professor Prabhu Radhakrishna for giving me the opportunity to be part of the incredible research team and for their endless guidance, encouragement, and support throughout my studies. I would like to thank Dr. Gbenga Oluyemi for his insightful feedback that improved the quality of this research. I have been very lucky to work with Dr. Mortadha Alsaba, the Head of Department of Petroleum Engineering at the Australian University, I am extremely grateful for the immense support and guidance. I acknowledge the contribution of my beloved friend and colleague Dr. Marwa Waly for your support in reviewing this work. I would like to recognize the support of friends and support base; Dr. Biltayib Misbah, Dr Joseph Amieibibama, Dr. Kenneth Afebu, Bar. Ifeoma Becky, Eng. Charles Adoga, Eng. Raphael Ofosu, Mr. Collins Worlu, Miss Agnes Machingauta and Miss Loveline Nji, my deepest gratitude goes to my family especially to my parent, Mrs. Matilda Amadi and siblings, Mr. Godson Amadi, Mrs. Patience Amadi Woko , Eng. Chris Azubuike and Eng. Collins Emeka Amadi for their unconditional love, trust, support, and encouragement. The love and support of Mr. Bryan Akachi Amadi and Esther Chidera Amadi have in no small measure contributed to the completion of this research studies.

Contents

1	Introduction	1
1.1	Background	1
1.2	Autonomous Drilling system.	5
1.3	Rational of study	7
1.4	Research Aim.	9
1.5	Research Objectives.	9
1.6	Scope of thesis	10
2	Literature review	12
2.1	Overview of rotary drilling process.	13
2.2	Factors affecting drilling performance	14
2.2.1	Operational parameters	15
2.2.2	Geomechanical environment	15
2.2.3	Drilling system.	15
2.3	KPI for drilling performance	16
2.3.1	Cost per foot.	17
2.3.2	Feet per day	17
2.3.3	Average penetration rate	18
2.4	Rate of Penetration models	19
2.4.1	Physics-based empirical models	19
2.4.2	Statistical Optimization models	24
2.5	Machine learning Optimizations models	26
2.5.1	Artificial Neutral Network (ANN)]	29
2.5.2	Extreme Learning Machine (ELM	31

2.5.3	Support Vector Machine (SVM)	32
2.5.4	Least-Square Support Vector Machine (LS-SVM)	32
2.5.5	Extra Tree (ET)	33
2.5.6	Randon Forest (RF)	34
2.5.7	CatBoost (CB)	34
2.6	Autonomous drilling system Predictive optimization models	38
2.6.1	Single-objective Optimizations	39
2.6.2	Multi-objective Optimizations	40
2.6.3	Aggregation techniques	41
2.6.4	Classical intelligent optimization techniques	42
2.6.5	Reinforcement learning techniques	42
2.7	Rock and drill-bit interaction model	43
2.8	Rock UCS Prediction models	45
3	Research Methodology	48
3.1	Determination of appropriate tuning parameters and Predictive drill rate models	49
3.1.1	Methodology for comparative assessment between Physics Based Model and the Artificial Neutral Model (ANN)	49
3.1.2	Determination of appropriate tuning parameters; Actual Surface Parameter and Derived Controllable Parameters	50
3.2	Rock UCS prediction and Maximum ROP Model	51
3.3	Decision-making in multi-objectives autonomous system.	53
3.4	ANNs. Model Performance Assessment Criteria	55
4	Tuning Parameter and Predictive ROP model with Drilling Data	57
4.1	Introduction	57
4.2	Data gathering and Preparation	58
4.2.1	Data collection	58
4.2.2	Data filter and quality checks	59

4.2.3	Calculation of derived functions.....	59
4.3	Statistical and graphical analysis	60
4.4	Modeling techniques	62
4.4.1	Physics Based model (PBM) Versus artificial Neural Network.....	63
4.4.2	Artificial Neural Networks configuration.....	64
4.4.3	4.4.3 ANNs Simulation cases.	66
4.5	Modeling Results	66
4.5.1	Establish relationship between input and output data (ROP)	66
4.5.2	Comparative study of Physics based model versus ANN model....	66
4.5.3	Derived controllable variable versus Actual surface parameters....	70
4.6	Sensitivity Analysis.....	73
4.7	Discussion of results.....	75
4.8	Summary of Results.....	77
4.9	Section summary.....	78
5	Real-time Prediction of Rock UCS and Maximum ROP Model	79
5.1	Introduction	79
5.2	Direct Methods for the estimation of rock strength	79
5.3	Indirect Methods for the estimation of rock strength.....	80
5.4	Proposed Model of UCS estimation using Drilling data.....	81
5.5	Research Methodology.....	81
5.6	Results and Discussion.....	87
5.6.1	Result of estimation of UCS from physics Based model.....	88
5.6.2	Results of UCS prediction from Machine Learning Algorithms....	89
5.6.3	Model result of UCS from CATBoost Algorithm	91
5.6.4	Model result of UCS from ANN Algorithm.....	92
5.7	Application of UCS estimation in maximum Achievable ROP Model	93
5.7.1	Determination of Optimum ROP window	93

5.7.2	Performance Benchmark Evaluation	96
5.7.3	DMSE and Drilling Efficiency	98
5.8	Section Summary	100
6	Decision-making model for autonomous drilling system	102
6.1	Introduction	102
6.2	Reinforcement Learning: Concept of Markov Decision Processes (MDP) Modeling for Autonomous	104
6.2.1	Concept of Markov Decision Processes (MDP)	104
6.2.2	Model Formulation.	106
6.3	Return.....	107
6.3.1	Policy	107
6.3.2	Reward	107
6.3.3	Value Function	107
6.3.4	Exploration and Exploitation trade-off.....	108
6.4	RL Solution Methods.....	109
6.4.1	Temporal Difference Method	109
6.4.2	Monte Carlo Method	109
6.5	Q-learning Algorithm.....	110
6.6	Model Application (Case study analysis).....	111
6.6.1	Data and Method	112
6.6.2	Data collection and processing	112
6.6.3	Q-Learning Algorithm.....	113
6.7	Results and Discussion	114
6.7.1	Effect of axial force(WOB) on feedrate.	115
6.7.2	Effect of rotary speed (RPM) on feedrate.	116
6.8	Section Summary	117

7	Experimental Prototype rigs design and Model validation	118
7.1	Uniaxial test machine.....	118
7.1.1	Experimental procedure	119
7.2	Labscale Experimental rig.....	120
7.2.1	Discussion on previous Labscale experimental design.....	122
7.3	Current Experimental In-House prototype	123
7.3.1	Hoisting system.....	126
7.3.2	Rotary system.....	127
7.3.3	Circuit design architecture	128
7.3.4	Data Acquisition system	129
7.3.5	Bottom Hole Assembly design	130
7.4	Miniature rig operating parameter	132
7.4.1	Drilling Mechanical Specific Energy and Miniature rig setup	132
7.4.2	Optimizing drilling efficiency using FET and DMSE.....	133
7.4.3	Experimental study of the rock-bit interaction	133
7.4.4	Investigation on the Effect of change in Weight on bit on rock-bit interaction	133
7.4.5	Effect of change in RPM on rock-bit interaction.....	136
7.5	Section Summary	138
8	Conclusions and future work	139
	Appendices	
A	Appendix A List of Acronyms and Nomenclatures	146
B	Appendix B Field Drilling Mechanics Data	148
C	Appendix C List of experiments	154
D	Appendix D Programming	157
E	Appendix E Published work	159
	Bibliography	161

List of Figures

1.1	Schematic of rock Geological structures showing hydrocarbon formation, migration, and trapping in reservoir rock.....	.2
1.2	Schematic of a topdrive rotary drilling rig with BHA rotated from a top drive motor at the surface Adopted from (Šprljan et'al (2020)	3
1.3	A Schematic of types of rotary drilling systems (a)Manual system (b) Autonomous rotary drilling system	4
1.4	Historical Development of digital oilfield and Drilling automation ..	6
2.1	(Schematic Bottom hole environment for a vertical / permeable rock (Hectoret'al2005	13
2.2	Pictorial representation of fundamental parameters.	14
2.3	Different types of bit (a) Roller cone (b) PDC (c) Diamond16
2.4	Average meters drilled per day. Exploration wells on the NCS, from 1966 to 2008.....	18
2.5	Classification of Machine Learning techniques applied in the study	27
2.6	Interconnection btw the different Machine Learning Models28
2.7	ANNs Structure with 2 hidden layers (Bishop 2006)30
2.8	The Schematic of Randon Forest classifier decision tree.34
2.9	Percentage of AI model used in ROP Prediction	37
2.10	Frequency of input used in ANN modeling.....	38
2.11	Three phases of drilling in w–d space in Detonrnay et al (2008)45
2.12	Schematic of two successive blades of a drill-bit. The drill-bit has n- identical blades45

3.1	Generalized workflow for Developing an autonomous self-optimizing drilling system	48
3.2	Simulation workflow for Physic based Model and ANN model.....	49
3.3	Workflow for determination of appropriate tuning parameters.....	50
3.4	Workflow for the prediction of rock UCS	53
3.5	Formulation of Autonomous Systems as an MDP problem.....	54
3.6	The flow chart for Modeling MDP based on the Q-learning	55
4.1	Plot of RPM and ROP vs RPM for W1 and P05.....	61
4.2	Plot of DMSE and ROP vs DMSE for W1 and P05 well.....	62
4.3	Simulation workflow for Physic based Model and ANN model.....	63
4.4	ANNs Structure with 2 hidden layers.....	64
4.5	Flowchart for ROP Modeling using ANNs Modeling.....	65
4.6	Relationship between input variable and output variable of ROP	67
4.7	Plot of Model Predicted ROP Vs Actual ROP: (a) Maurer Model (b) Bingham model (c) Bourgogne and Young (d) ANN model.	69
4.8	Model outputs vs Actual data: for (a) training and testing dataset....	69
4.9	Model outputs versus real data for case 2 using dataset-W1.....	71
4.10	Model prediction versus real data: for Case 1 Using dataset-W1.....	71
4.11	Model prediction versus real data: for Case 1 Using dataset-P05	72
4.12	Model outputs versus real data: for Case 2 using dataset-P05.....	73
4.13	Sensitivity Analysis for the selection of optimal number of neurons. (a) 10 neurons (b) 20 neurons (c) 30 neurons (d) 40 neurons	74

5.1	Schematic of Unconfined Compression Test Setup. adopted from Gullu, and Hazirbaba (2010)	80
5.2	Research Flowchart showing the step-by-step approach.....	82
5.3	Relative Feature Importance Plot Generated by CatBoost Model.....	84
5.4	Scatter Matrix of Selected Features in the Experimental database.....	85
5.5	Schematic of ANN network Architecture	86
5.6	Plot of estimation of UCS from established empirical based model ..	88
5.7	Cross-validation plot between measured and predicted UCS value using Catboost Model: a) training, and b) testing... ..	91
5.8	Measured and predicted UCS value with depth using Catboost Model: a) plot and b) sample	91
5.9	Cross-validation plot between measured and predicted UCS using ANN Model: a) training, and b) testing dataset.....	92
5.10	Measured and predicted UCS value with depth using Catboost Model: a) plot and b) sample	92
5.11	Plot of Optimum ROP curve and actual measured ROP	95
5.12	Comparison of CatBoost Predicted UCS versus DMSE Derived UCS measured ROP.....	96
5.13	ROP Benchmark Actual measured ROP vs ROP Baseline	97
5.14	DMSE and ROP as functions of WOB, at constant RPM of 130rpm	99
6.1	Schematic of a Decision control for Autonomous drilling system....	103
6.2	Formulation of Autonomous Systems as an MDP problem.	106
6.3	Q-Learning flowcharts showing the State, actions, and rewards.....	111
6.4	Pseudo-code for Matlab Q-value programming	114
6.5	Plot of the Feedrate versus Reward at different states.....	115

6.6	Plot of the Rewards of various RPM (Distance drilled) Versus episodic state (WOB).....	116
7.1	Schematic of ADR1500 with its main components.....	119
7.2	Experimental testing of Core UCS using ADR1500. Machine... ..	120
7.3	Schematics of prototype rig in SPE Drillbotics... ..	122
7.4	Schematic of the in-house prototype rig (design) includes. electric motor, load cell, ball screw assembly.	124
7.5	Hoisting system includes electric motor, LVDT sensor, load cell, ball screw assembly and rock holder.	126
7.6	Components of the hoisting system	126
7.7	Schematic of rotary system and component	127
7.8	Picture of rock holder and load cell	129
7.9	Instrumentation box and key sensor connection.....	129
7.10	Instrumentation sensors used in this rig	130
7.11	Bottom Hole Assembly design	134
7.12	Plot of ROP versus WOB at different rotational speed	135
7.13	Plot of DOC versus WOB at different rotational speed	136
7.14	Plot of DOC versus RPM at different rotational speed	13
7.15	Plot of DOC versus RPM at different weight on Bit (WOB	137

List of Tables

2.1	Summary of Physic based penetration rate models	23
2.2	Summary of Artificial intelligence model for ROP prediction.	25
2.3	Summary of Statistical model for penetration rate prediction.....	36
2.4	Summary of rock-cutter interactions models.....	44
2.5	Published Correlations to Predict UCS.....	46
4.1	W1 -Sample 200ft of filtered and quality check dataset....	58
4.2	Range of input parameters for W1	61
4.3	Range of input parameters for P05.	61
4.4	Bourgogne and Young model coefficient for the field.....	64
4.5	First 15 datapoints sample of Calculated derived variables.....	66
4.6	Physic Based model and ANN model performance results.....	68
4.7	Summary of Model result for selection of Tuning parameters.....	70
4.8	Sample of predicted Vs Actual ROP using [FET, DMSE]	72
4.9	Sample of predicted Vs Actual ROP data using [WOB, RPM]	73
4.10	Summary of findings.....	77
5.1	Statistical analysis describing range and distribution of data.....	83
5.2	ANN modeling parameters....	87
5.3	The Performance Assessment of six ML on Training and test data ..	89
6.1	MDP elements.....	106
6.2	Published Experimental Data for MDP model... ..	112
6.3	Summary of model result	114
7.1	Summary of Drillbotics winning teams on drilling automation.....	121
8.1	Summary of conclusions.....	143

Chapter 1

Introduction

1.1 Background

Hydrocarbons are formed on earth's subsurface by the decomposition of organic sediments deposited several millions of years ago. Upon increasing burial with depth, it became subjected to increasing temperature and pressure forming kerogen which later produces hydrocarbons within the pore spaces of the rock. A rock material is a naturally occurring aggregate of minerals, constituting an important part of earth crust. According to Emery (1966), a rock is defined as a composition of granular and cementation materials. Lithologic rock is a heterogeneous and anisotropic material and can be classified into three types of igneous, sedimentary, and metamorphic rock Alfreds (1983). Hydrocarbons are commonly found in sedimentary rocks enclosed within geologic traps as shown in **Figure 1.1**. Drilling a borehole is the only way to harness the hydrocarbon trapped beneath the subsurface. The drilling process involves creating a borehole achieved by simultaneous rotary action of the top-drive and the application of axial force by the draw-work hoist. wherein the former transmits. torque to the drill bit via the drillstring and the latter facilitates drillstring longitudinal motion thereby establishing drill bit normal force referred to as weight-on-Bit (WOB), Akgun (2002).

1.1 Background of study

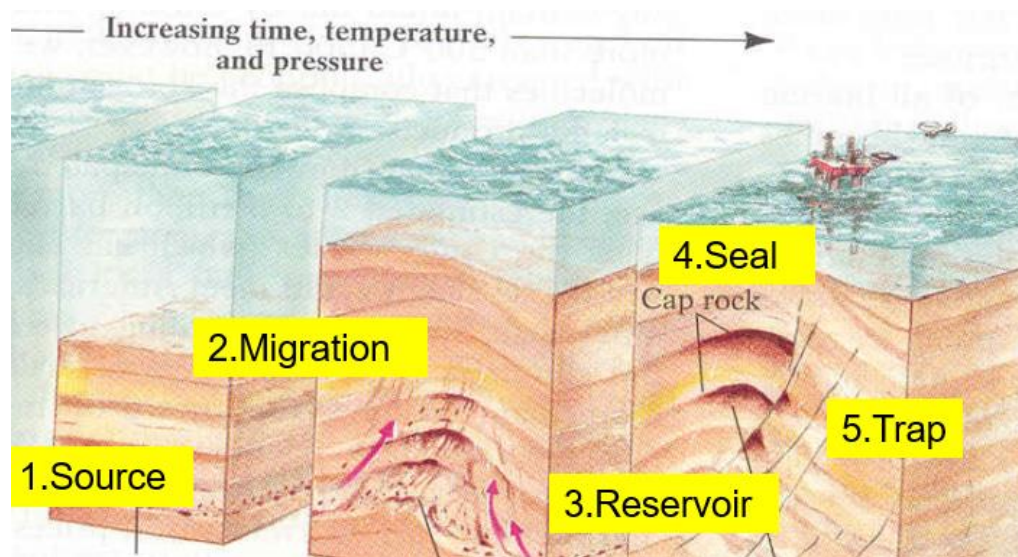


Figure 1.1: Schematic of Rock Geological structures showing hydrocarbon formation, migration, and trapping in reservoir rock.(Robert Gordon University (2008))

During the drilling operation, the drill-bit cuts the rock material and the resulting drill cuttings are removed from the borehole by the circulation of drilling fluid which is pumped into a well through the rotary hose and drill string as shown in **Figure 1.2**. Boreholes are drilled using a drilling rig that suspend and rotate the drillstring and the drillbit. The lower part of the drillstring is commonly referred to as the bottom hole assembly (BHA). Initially the BHA hangs in tension with the support of the hoisting hook which also support the topdrive. The total weight suspended by the hook is known as the hook load. (HL). The sequence of rotary drilling begins with breaking circulation by increasing the pump strokes until the desired flowrate (Q). Then established rotation by increasing the rotary speed of the topdrive until the desired rotary speed in revolution per minute (RPM). The drilling sequence continues with lowering the drillstring in the hole using the drawwork hoisting system. When the bit contacts the bottom

of the hole, a proportion of the drillstring weight is transferred to the rock-bit interface as the drillbit penetrates the formation. The amount of load transferred is commonly referred as the weight on bit (WOB) measured in pounds (lbs). This is estimated by subtracting the initial hookload with the bit off bottom with the final hookload when the bit is on bottom. Similarly, the torque required to turn the drillstring whilst off bottom is referred to as the off-bottom torque while the torque drilled to turn the drillstring with the bit on bottom is referred to as the on bottom torque (TOB).

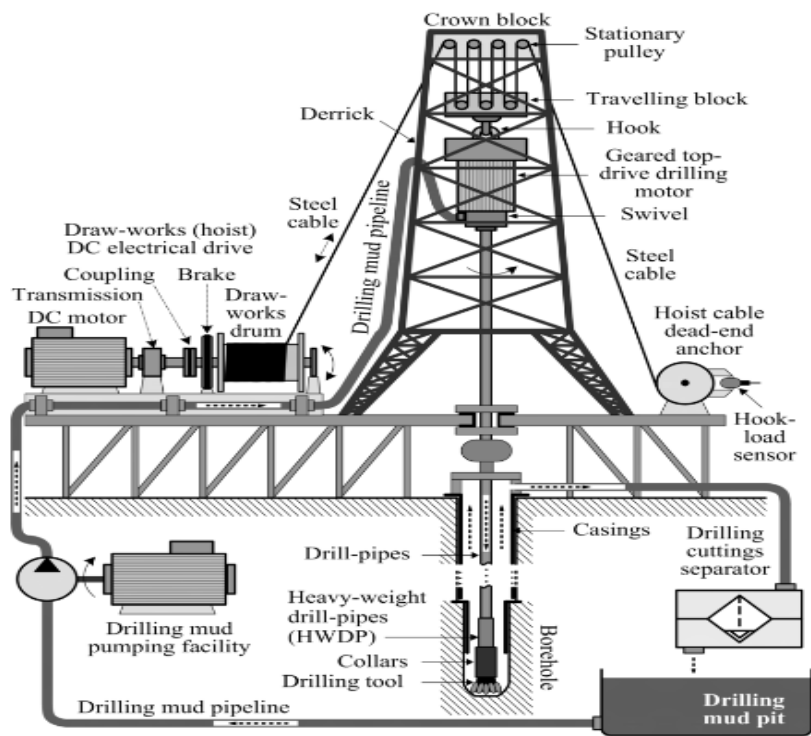


Figure 1.2: Schematic of a topdrive rotary drilling rig with Bottom Hole Assembly rotated from a top drive motor at the surface Adopted from (Šprljan et' al (2020)

The penetration rate is dependent on the amount of WOB and the rotary speed and flowrate. When the rate at which the drillstring is lowered at surface, exceeds the rate of drillbit penetration the WOB increases until the state of equilibrium is attained. In the conventional drilling system, the parameter management, and efforts to optimize drilling

1.1 Background of study

operation depends on the effectiveness of a highly trained human operator that continuously adjust the rotary speed and the drillstring decent velocity to maintain the desired weight on bit and acceptable drilling performance as shown in Figure.1.3(a). But the current practice for selecting optimal set of parameters to improve system performance is based on intuition, experience or trial and error method which often creates redundancy. The redundancy in the system creates hidden time and suboptimal operating conditions.

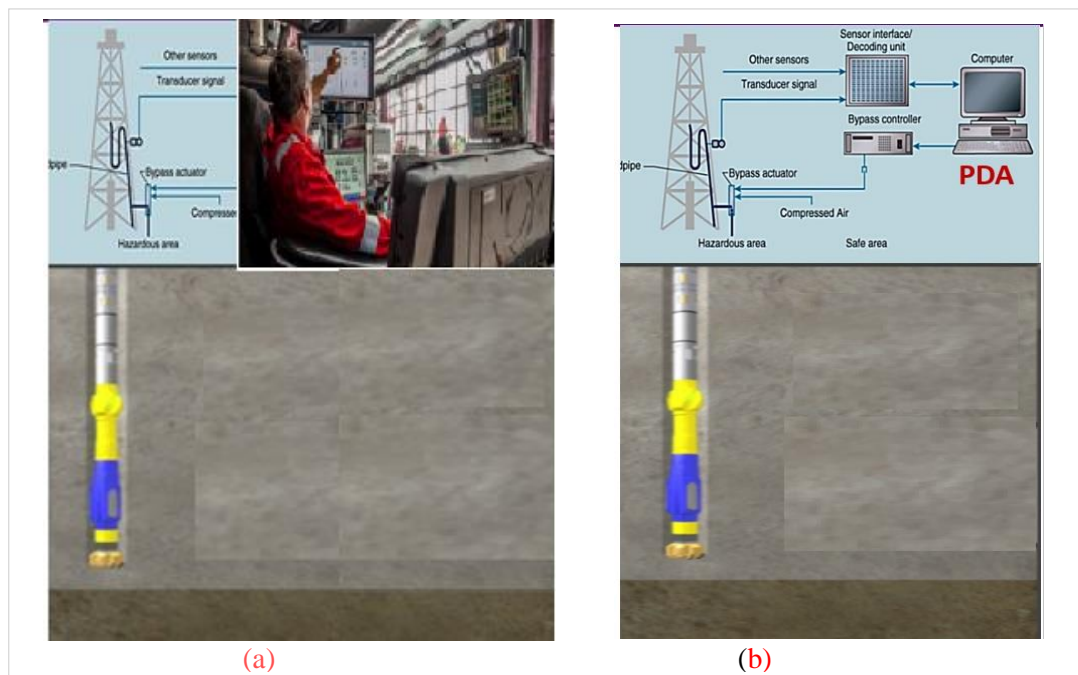


Figure 1.3: Schematic of types of rotary drilling systems (a)Manual system (b) Autonomous rotary drilling system

The human operator could cause operational delay thereby increasing both the number of days and well delivery cost and environmental footprints. Although several research works have identified the significance of upscaling from manual drilling to autonomous drilling system, little has been done to support this transition. According to [Pavković \(2017\)](#) improvement in "legacy" drilling rig hardware could be extended through retrofitting with control and feedback system leads to tremendous improvement in performance and operational safety, raising the delivery efficiency.

1.2 Autonomous Drilling system

In spite of improvement in the mechanization of the rig system by installation of the control and feedback system, an engineered approach is required in determining tuning variable, selection of operational parameters and performance benchmark of the autonomous drilling system (Šprljan et'al (2020)). In recent time, availability of big data, high precision sensors, control systems and machine learning can be used in autonomous drilling system to improve performance by prompt adjustment to varying conditions based on real-time measurement using models that are based on scientific principles. Auto-Diller computer logic with potential of learning, reasoning, and planning inspired to corresponding human cognitive functions. The development of the autonomous drilling system will increase drilling speed, provide greater efficiency, and reduce equipment failure as shown in Figure 1.3(b).

1.2 Autonomous Drilling system

There are two main modes of rotary drilling system, manual drilling, and autonomous drilling system. The traditional manual mode of drilling system is manned by the driller who controls the rotary action of the topdrive and the axial force of the drawwork. The driller determines the operating parameters either by intuition, previous experience or by trial-and-error approach. Alternatively, the autonomous rotary drilling system is designed to reduce mental and physical workload of human operator by the use of control systems. The drive to optimize oil and gas portfolios through automation dates back to the late 90's. According to [Norwegian Oil Industry Association \(2006\)](#), Equinor developed a program called integrated operation with the initial level-1 mainly composed of real-time monitoring and communication. This level of automation is classified as Level 1-2 and designated as monitoring. Whilst Level 3-4 is designated as Advise, Level 5-6 designated as control, and level 7-8 designated as autonomous.

1.2 Autonomous Drilling system

The breakthrough in digitalization and the big data acquisition through high frequency sensors raised the interest in optimizing drilling processes using real-time drilling data, Arabjamaloei and Shadizadeh, (2011). The timeline for the historical development is presented in **Figure 1.4**. Autonomous drilling system consist of three parts: The real-time monitoring, decision-making, and actuator as presented in Amadi et al. (2022). The real-time monitoring provides the environmental information for decision making and control execution. Amer et'al (2017), used the application of control system and information technology to operate both the topdrive and the drawwork system., McKenna et al. (2015).

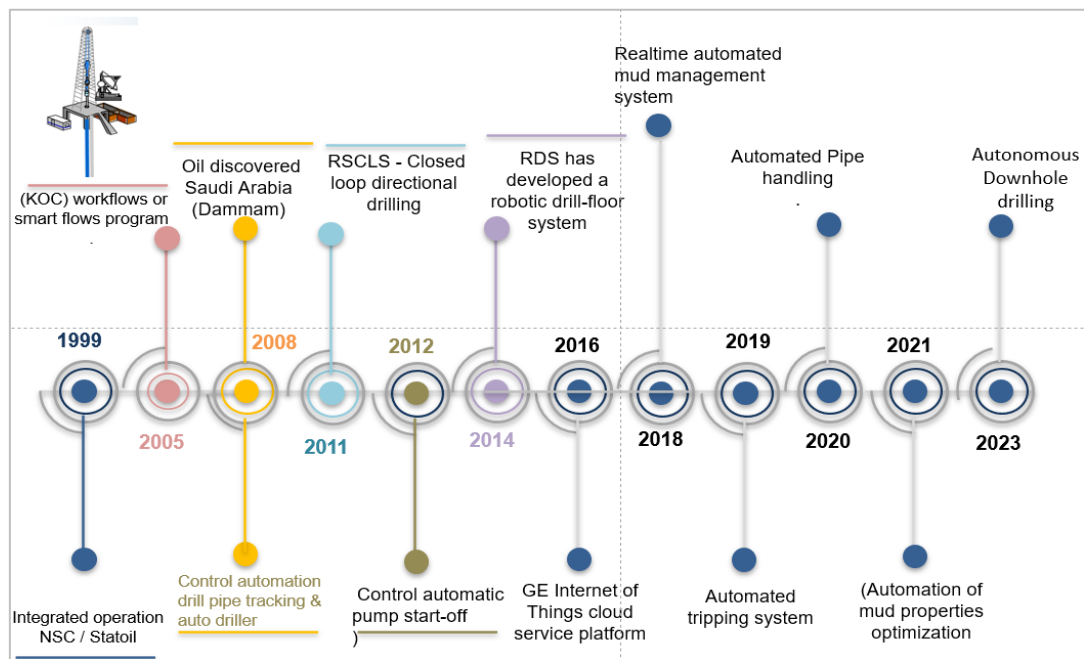


Figure 1.4: Historical Development of digital oilfield and Drilling automation

In spite these achievements, real-world problems, which pose hard scientific challenges to autonomous drilling operations are highlighted under the rational for the study.

1.3 Rational for the study

Automation is changing many aspects of our lives as well as the oil and gas industry. The medium and short-term changes to the petroleum industry are challenging its profitability and sustainability. Recognition of more efficient approaches and solutions is essential to creating future business resilience. Upscaling from manual to autonomous drilling system is expected to bring several benefits including safety, efficiency and cost savings. According to [Lyons and Plisga, \(2004\)](#), drilling cost is time dependent and large saving in time is achieved from operating closer to constraints and reducing well delivery time and cost in drilling operation. For an autonomous system an adaptive parameter optimization becomes a critical success factor as the use of reduced operating parameters would implies operating at suboptimal rate, whilst too high operating parameters may result in wear and damage to Bottom Hole Assembly (BHA) resulting to premature trip with consequence of increase in time and cost. Therefore, determination of optimal operating parameters and the corresponding rate of penetration is essential. Furthermore, an autonomous drilling system will offer a step change in downhole monitoring of drilling conditions and improving operational safety, [Amadi et'al \(2023\)](#). Automation responds faster to problems with fast and small corrections versus large corrections or costly remedial actions. The manual drilling system are prone to dense, unpredictable adjustment of drilling parameter due to changes in drilling dynamics, different rocks, and other process elements. In these situations, delay in identifying the redundant source causes hidden time. Redundancy reduction requires that the drilling system stays fully operational at a technical limit. In the scope of these arguments, it proposed to take advantage of the latest control system and machine learning in the prediction of optimum drilling rate eliminating redundant elements such suboptimal operating rate, human error,

Additionally, quality of Experience (QoE) aims at assessing the quality perceived by a user, while experiencing a service (e.g., penetration rate, drill string dynamics, etc). Even though QoE is human centric, in general, due to the exponential increase of services, it is not practical to employ humans to assess the services quality. Thus, objective computational methods capable of assessing the quality of those services such as humans do are needed. [Liotta, A \(2013\)](#). Thus, improving operational health and safety by elevating the driller from direct involvement in the drilling operation into a supervisory role. This can result in improvement in rate of penetration and well integrity of an autonomous drilling system leading to a more efficient drilling operation. [Wee and Kalogerakins \(1989\)](#), discussed that modeling results can be applied in the optimization of drilling operations to attain minimum drilling cost and increase the profitability of the drilling business. With the aim of addressing these fundamental challenges, this research will attempt to answer the following research questions such as follows;

- 1) How to determine optimal operating parameter and corresponding rate of penetration (ROP) in an autonomous drilling system in a heterogenous rock?
- 2) What variables are suitable for tuning parameters; surface operating parameter (WOB, RPM) or energy derived variable (DMSE, FET).
- 3) How can a change in formation change be promptly identified?
- 4) How will the automatic decision-making process in selecting and implementing best operating parameters be modeled.

There are approximately 1105 rig counts worldwide (Baker Hughes 2020) that are manually operated despite the benefits of automation. Although there are several research efforts to support the transition from manual to autonomous drilling system. This research will support this initiative in two key areas. Modeling of rate of penetration (ROP) development of predictive models for performance benchmark and decision making protocol and implementing optimal drilling parameters.

1.4 Research aim

The aim of this research is to develop predictive optimization models for Autonomous rotary drilling system using machine learning approach. The study will leverage on drilling data, machine learning algorithms, modeling and experimental investigation.

1.5 Research objectives

To achieve the above aim the following objectives will be investigated in this research:

1. Critical evaluation of digital drilling optimization models for automatic system.
2. Determination of appropriate tuning parameters and Predictive drill rate models.
3. Real-time prediction of rock UCS & ROP benchmark using basic drilling data.
4. Evaluate decision-making model for autonomous drilling system
5. Design an experimental test rig in order to observe rock-bit interactions by.
 - Evaluating dynamic relationship of WOB with ROP
 - Evaluating dynamic relationship of rotary speed (RPM) with ROP

1.6 Scope of thesis

Chapter 1 contains the introduction for the thesis including the rational for study, research aim and objectives and scope of this research.

Chapter 2 presents literature review to rock drilling process including methods and mechanisms and the effect of surface operating parameters on drilling rate of penetration. In addition, it provides a comprehensive literature review on drilling Optimisation models, modeling of rock cutting along with experimental studies.

Chapter 3 provides an overview of the research methodology utilized in this research. It includes methods for the determination of optimum tuning parameters, prediction of changes in Rop of lithologies using unconfined compressive strength of the rock.

Chapter 4 presents a study on the analysis of drilling mechanics data and predictive ROP models. It provides a new mechanism for prediction of ROP of an autonomous drilling system using basic surface drilling parameters.

Chapter 5 concentrates on real-time prediction of rock UCS whilst drilling using drilling mechanics data. It proffer an alternative method of predicting instantaneous UCS enabling creation of achievable ROP benchmark, This chapter used ANN modeling in comparison with other machine learning algorithms such as Extreme Learning machine, Catboost algorithm, support vector regression (SVR), Decision tree and Randon Forest (RF) algorithms.

Chapter 6 considered decision making process with respect to optimal drilling parameters for different rocks and strategy for intermittent performing an automatic drill-off test whilst exploring the optimal operating parameter to optimize the drilling progress, it discussed the concepts of Markov decision process and Q-value algorithm.

Chapter 7 focuses on experimental drilling analysis of rock-PDC drill-bit interaction and exploring understanding the dynamic non-linear relationship between weight on bit and rate of penetration. Also investigate the effect of different operating parameters on their drilling responses and the dynamic non-linear relations between rotary speed and rate of penetration.

Chapter 8 summarizes the main conclusions drawn from this work and gives some recommendations and plans for future work.

Chapter 2

Literature review

Designing an adaptive optimization model that uses energy conservation principles to evaluate the dynamic relationships of weight on bit, rotary speed, torque, penetration rate and the force transfer through the drilling system in real time has been an overarching interest of the oil and gas industry as optimization techniques are often used as a cost reduction tools. A careful understanding of the use of real-time drilling data, in determination of operating parameters and in predicting optimal penetration rate behavior would be highly vital in this matter.

In this chapter, an overview of the current knowledge in this field will be reviewed. First an introduction to rotary drilling system and rock cutting process is presented. Followed by a general overview of the various drilling optimization models proposed by previous researchers who tried to gain an understanding of the complexity of penetration rate prediction using mathematical, statistical and machine learning techniques. Next the application of machine learning techniques in the development of high reliability prediction model for penetration rate. Finally, the current state of research on the development of optimization model for autonomous downhole rotary drilling system

2.1 Overview of rotary drilling process

The rotary drilling system is the most frequently used method in oil and gas drilling operations. In rotary drilling process, a rotating drill bit is used to dig down through the Earth's crust by the application of a downward axial force provided by the weight of drill collars and an applied rotary torque from the drillstring rotation from the top drive motor on surface. High pressure drilling fluid is circulated through the drill pipe and returned via the annulus with rock cuttings to the surface as shown in Figure (2.1). The input energy required for crushing the rock is derived from the axial force (WOB) from the draw work hoist and the rotary torque from the rotation of the drill string. Šprljan et al. (2020) noted that weight on bit, rotary speed, bit type and bit hydraulics are the most influencing factors affecting the rate of penetration. Penetration rate is a useful energy utilization and improves drilling performance, however drillstring vibration represent a loss of energy in the system and causes wear and tear and premature failure of drilling tools. Selection of the correct combination of (WOB, RPM) is therefore essential component for drill rate management.

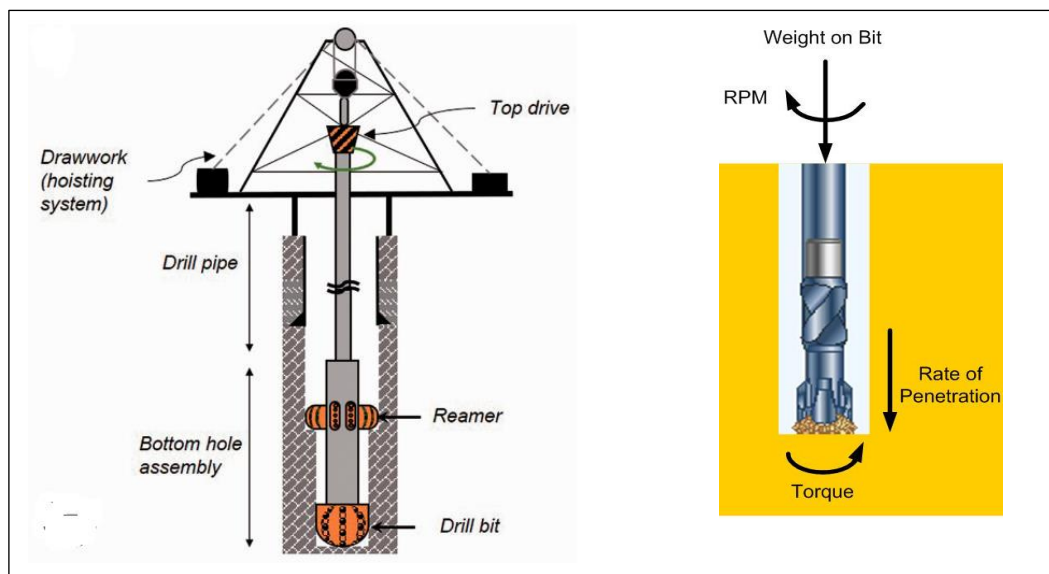


Figure 2.1: Bottom hole environment for a vertical / permeable rock (Al Dushaishi et al 2021)

2.2 Factors affecting drilling performance.

The factors affecting the rate of penetration can be broadly categorized into three (3). These include operational parameters, geomechanical parameter and drilling system characteristics, Gatlin (1996) Desmette et'al (2009). According to MensaWilmot et al. (2009), drilling performance improvement or optimization of drilling performance can only be achieved by applying a detailed analysis focused on these characteristics, components and behaviour of the drilling system to overcome barriers and thus enable sustainability. Figure 2.2, shows the pictorial representation of fundamental parameters. Each of the influencing factors are further discussed below.

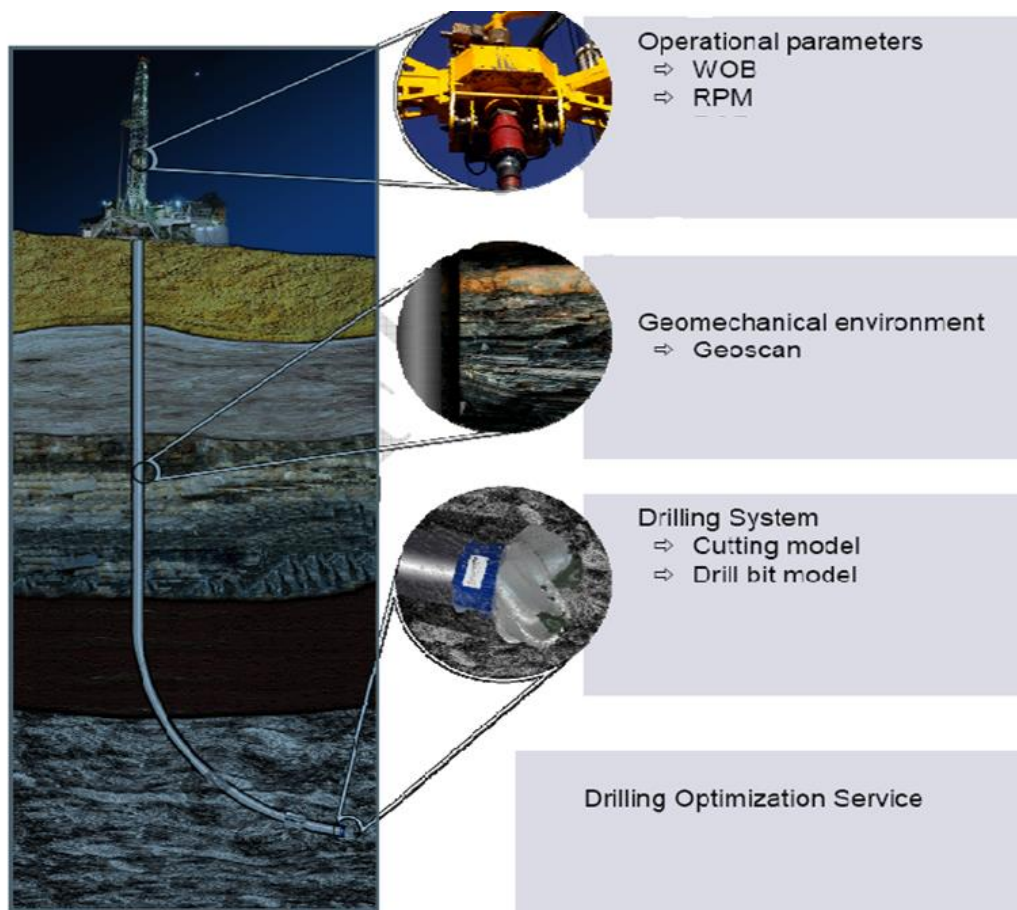


Figure 2.2: Pictorial representation of holistic drilling system. (Desmette et'al 2009)

2.2 Factors affecting drilling performance.

2.2.1 Operational parameters

The drilling rate depends on the interacting surface variables such as the weight on bit (WOB), rotary speed (RPM), flow rate (hydraulic term). These variables influence the dynamic, directional, stability and the durability of the drilling system which also affects the achievable penetration rate. Ebrahim and Noveiri (2010) noted that weight on bit, rotary speed, bit type and bit hydraulics are the most influencing factor affecting the rate of penetration.

2.2.2 Geomechanical environment

These are uncontrollable variables resulting from the local geology. Geologic formations vary across the world and even within a producing basin. The ultimate strength of the formation, formation abrasiveness, porosity, permeability, and mineral composition of the rock are amongst the several properties affecting penetration rate (Bourgoyne et'al 1986). Formation hardness is calculated as unconfined compressive strength (UCS) by a direct correlation of rock geophysical properties (Oniya 1988). The knowledge of the geomechanical environment is a leading parameter to understanding the downhole drilling condition and the good choice to optimize drilling operations.

2.2.3 Drilling system

Critical factor that influence the drilling progress both surface and downhole driving systems. The drilling equipment technical capability and the operational limit of the equipment, the bit performance and the Bottom Hole Assembly (BHA) tendency.

2.2 Factors affecting drilling performance.

According to Mazzini et al (2009) inappropriate bit type, BHA component failure reduces penetration rate and impact on overall drilling cost due to unscheduled bit or BHA trip. They further highlighted the importance of holistic view in drilling system selection to enable optimal equipment and system selection. Suitable bit selection for the specific application is essential in the delivery of superior drilling performance, Capuano (2016). Figure 2.3 shows the various types of bit models namely the roller cone bit, polycrystalline diamond compact (PDC) and the diamond drill bit. Hariharan and Aziza (1996) noted that PDC bits with parabolic profile and bladed hydraulic design have a lesser tendency to ball-up during drilling of reactive shale.

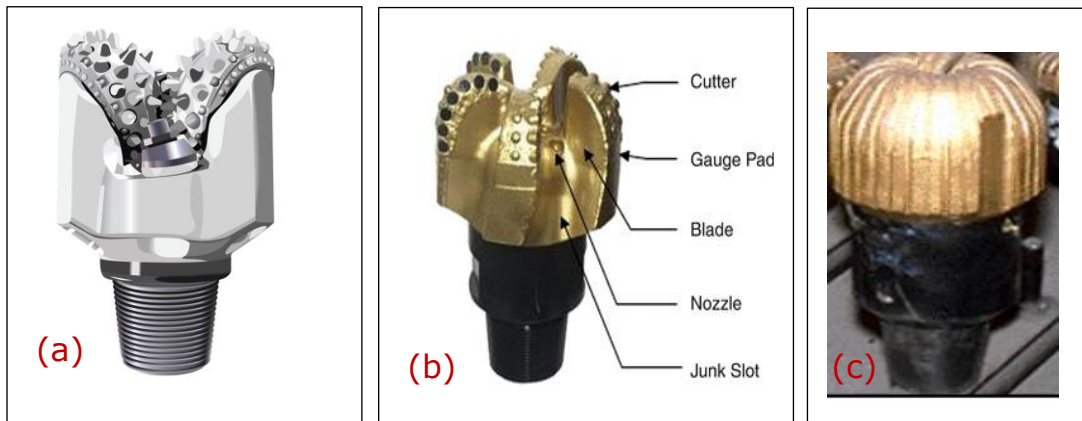


Figure 2.3 shows the different types of bit (a) Tungsten carbide insert (b) PDC (c) Diamond bit. (Capuano (2016).

2.3 Key Performance Indicator (KPI) for drilling performance.

Benchmarking is a vital process involving the evaluation and documentation of drilling performance from a historical perspective and enabling the identification of performance deficiencies (Mensa-Wilmot et al. 2009). It is important to identify possible drilling deficiencies by analyzing patterns in the drilling performance, quantifying metrics (key performance indicators (KPIs) or performance evaluation tools used in the assessment of the ROP for any drilled well. The quantifying metrics includes the cost per foot, footage per day and rate of penetration rate

2.3.1 Cost per foot (CPF) : The total cost of drilling a well (by foot of a hole drilled) excluding production cost such as the cost of leasing rigs, bits, casings, downhole equipment, site preparations, etc. Out of these methods, the most popular method in use is cost per foot (CPF) estimation for drilled intervals. The method is popular, as it is based on the operating cost of the drilling operation. CPF can be measured using equation (2.1)

$$CPF = \frac{BitC + RigC(BitRT + CNT + TripT)}{F} \quad (2.1)$$

Where, CPF is in Dollar/ft,

BitC is the bit cost in dollars,

RigC is the cost of rig per hour,

BitRT is the bit running time in hours,

CNT is connection time in hours

TripT is the trip time in hours,

F is length of wellbore drilled in feet.

CPF is used in combination with other methods as it does not depend on the operational parameters, but the drilling economics is highly affected by them. CPF has been proven efficient in the analysis of historic drilling data obtained from the offset wells and current supervision of bit run Perrin et.al(1997).

2.3.2 Feet per day (FPD): The number of meters drilled per day is a measure of the efficiency of the rig and the crew experience. Although there is lack of studies on drilling efficiency available, anecdotal evidence indicates that a decreasing trend in drilling efficiency is a global tendency (Osmundsen et.al2014). Figure 2.4 shows the average meters drilled per day in exploration activities on the North Sea Continental Shelf (NCS) from 1966 to 2008. (Osmundsen et.al2014). A sharp decline in drilling efficiency as

2.4 Rate of Penetration models

measured by the industry standard drilling meters per day, can be observed from 2004 to 2008 as the exploration drilling activities slowed down from an average of 144 to 67 meters by day, over 50% reduction. According to Osmundsen et.al (2014), meters drilled per day is the standard key performance parameter in drilling and a dramatic drop in meters per day, combined with very high rig rates, it is apparent that the main challenge of exploration drilling on the North Sea Continental shelf (NCS). Figure 2.4 shows the average drilled distance with year.

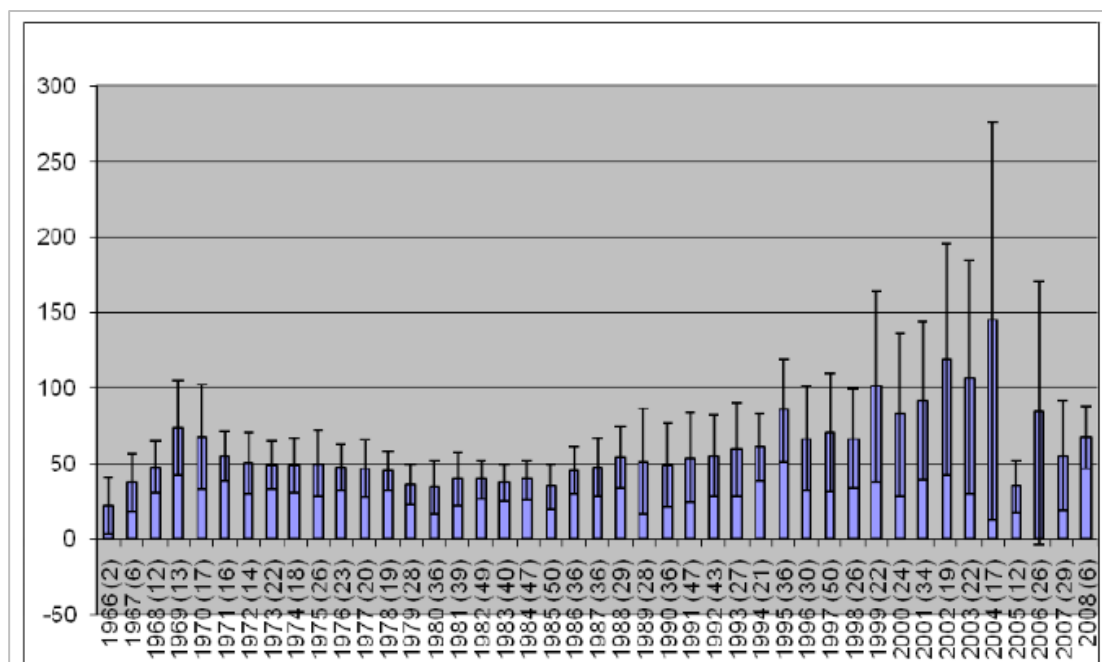


Figure 2.4 : Average meters drilled per day. Exploration wells on the NCS, from 1966 to 2008. Annual number of wells in brackets. Black vertical lines indicate standard deviation. (Osmundsen et.al 2014).

2.3.3 Average Rate of penetration (AROP): The rate at which a drill bit breaks down the rock underneath it, to deepen the borehole. this is taken over the total interval drilled from trip-in hole (TIH) to pull-out-of-hole (POOH) by the respective bottom hole assembly (BHA). This is the ROP at which improvement of drilling efficiency depends. According to Hossain and Rafiqul (2018), most factors categorized under planning, environment and execution that affect ROP have influencing effects on the PQs. The

2.4 Rate of Penetration models

planning factors include hole size, well profile, casing depths, drive mechanisms, bits, BHA, drilling fluid. In most engineering studies involving rotary drilling, the factors affecting AROP are said to be divided usually into Personal efficiency, Efficiency of the rig. characteristics of the formation, balling tendency, fluid content and interstitial pressure, porosity, and permeability. Mechanical factors (e.g., WOB, bit type and rotary speed. Hydraulic factors (e.g., jet velocity, bottom-hole cleaning.) and Mud properties (e.g., mud weight, viscosity, filtrate loss)

2.4 Rate of Penetration models

There is extensive literature on drilling optimization models following its importance in drill rate management in the oil and gas industry. According to [Barbosa et'al \(2019\)](#), the main goal of drilling optimization is to reduce the total operating time and reduce risk as low as practically possible. Several researchers have carried out extensive investigation on methods of controlling and predicting stick-slip and penetration rate, respectively. [Chiranth et'al \(2017\)](#) classified the different established drilling optimization models into three groups: physic-based models, statistical and data-driven models. These models are explained in the subsequent section.

2.4.1 Physics-based empirical models

The physic-based optimization model uses mathematical equations to predict penetration rate, bit wear and borehole hydraulics with a goal of improving the overall drilling efficiency and minimizing drilling cost. Several physic-based empirical models proposed a relationship between different penetration rate and parameters that influences it significantly ([Soares et'al. 2016](#)). [Graham and Muench \(1959\)](#) presented the earliest form of mathematical model commonly referred to as the Rotary-Weight-Rotary speed (R-W-N) equation based on the assumption of perfect hole cleaning. [Graham and Muench](#)

2.4 Rate of Penetration models

analyzed and predicted penetration rate as a product of weight on bit, rotary speed raised to an empirically derived exponent and then multiplied by a proportionality constant which accounts for formation effect as given in equation (2.2).

$$ROP = f (W.N)^n \quad (2.2)$$

Where, f is a function.

N is the rotary speed (rev/min)

W is weight on bit in (lbf) and index n is less than 1 and obtained from drill off test.

Graham and Muench penetration rate model were based on the assumption of a condition of perfect hole cleaning where the rates of cutting removal was greater or equal to rate of cutting generation and does have several setbacks such as not accounting the effect of formation strength and the effect of depth on the rate of penetration.

Maurer (1962) in his research on a theoretical model for roller cone bits, considered the effect of rock strength and based the model on rotary speed, weight on bit, rock strength, and bit size. He developed equation (2.3) based on observations of the volume of cuttings generated during the drilling operation. However, Bingham (1965) modified equation (2.3) for all bit types and expressed as equation (2.4)

$$ROP = k \frac{N W^2}{D_b^2 \times S^2} \quad (2.3)$$

$$ROP = K \left(\frac{W}{D_b} \right)^{a5} N \quad (2.4)$$

Where k is drillability constant,

N is rotary speed (RPM),

W is weight on bit (Klbf),

D_b is the diameter of the bit (in),

S is rock compressive strength (kPa)

and $a5$ is a formation constant determined from the rock sample.

2.4 Rate of Penetration models

Warren (1987) discovered a relationship between the rock compressive strength (UCS) and the drill bit for soft formation where the rate of cutting removal has no influence on ROP. Warren's model calculates ROP using equation (2.5).

$$ROP = \left(a \frac{S^2 D_b^3}{N^b W^2} + \frac{c}{N D_b} \right)^{-1} \quad (2.5)$$

where a, b and c are constants of the bit. To account for the dynamic bit wear and the effect of drilling fluid on ROP. Hareland (1993) modified Warren model by adding a dimensional analysis containing bit impact force, mud properties, and bit wear as in equation (2.6).

$$ROP = \left[1 - \frac{W_c \sum_{i=2}^n W_i N_i A_{abr,i} S_i}{8} \right] \left[f_c(P_e) \left(a \frac{S^2 D_b^3}{N^b W^2} + \frac{c}{N D_b} \right) + \frac{d \mu \gamma D_b}{F_{jm}} \right]^{-1} \quad (2.6)$$

Where W_c is wear coefficient,

A_{abr} is relative abrasiveness,

$f_c(P_e)$ chip hold down function (lbf),

μ is mud viscosity (cp),

γ is fluid specific gravity,

F_{jm} is modified impact force (lbf), and a, b, c, d are constants.

The work of Bourgoyne and Young (1986) was considered the most comprehensive and widely accepted drilling model for rotary drill bit. According to Soares and Gray (2019) the Burgoyne and Young model (BYM) predict ROP using multiple regression analysis of drilling eight parameters expressed as equation (2.7) and later proposed an adaptation to the original ROP model as in equation (2.8)

$$\frac{dD}{dt} = \exp^{(a_i + \sum_{j=2}^8 a_j x_j)} \quad (2.7)$$

$$ROP = f1 * f2 * f3 * f4 * f5 * f6 * f7 * f8 \quad (2.8)$$

2.4 Rate of Penetration models

Where; $F1 = e^{2.303 a_1}$ $F2 = e^{2.303 a_2(1000-D)}$ $F3 = e^{2.303 a_3 D^{0.69}(gp-9)}$

$$F4 = e^{2.303 a_4 * D(gp-\rho c)}, F5 = \left[\frac{\frac{W}{d_b} - \left(\frac{W}{d_b}\right)_t}{4 - \left(\frac{W}{d_b}\right)_t} \right]^{a_5} \quad F6 = \left(\frac{N}{60}\right)^{a_6}, F7 = e^{-a_7 H},$$

$$F8 = \left(\frac{F_j}{1000}\right)^{a_8}$$

Where a_1 to a_8 are constants,

a_1 – formation strength parameter

a_2 – exponent of the normal compaction trend

a_3 – under compaction exponent

a_4 – pressure differential component

a_5 – bit weight exponent

a_6 – rotary speed exponent

a_7 – tooth wear exponent

a_8 – hydraulic exponent

D is true vertical depth,

d_b is bit diameter (inches),

N is rotary speed (rpm),

h is fractional bit tooth wear,

F_j is Jet impact force (lbf),

gp is Pore pressure gradient (psi/ft),

ρc is equivalent circulation density(ppg),

W is weight on bit (Klbf)

Rate of penetration (ROP) in (ft/hr),

$\frac{W}{d_b}$ is threshold bit wear per inch of bit diameter (1000lbf/in).

Where, F1 defines the effect of formation strength, F2 represent the effect of compaction,

2.4 Rate of Penetration models

F3 models an exponential increase in penetration rate with pore pressure gradient, F4 defines the effect of over balance on penetration rate, F5 defines the effect of weight on bit and rotary speed while F6 models the effect of rotary speed. F7 and F8 models the effect of fractional bit tooth wear. Accurate modeling of drill rate of drilling system led to drilling performance efficiency as drilling cost is time dependent but not product cost dependent (Lyons and Plisga, 2004). Despite the great achievement in the drilling rig mechanization over the years, and the concerted effort by researchers in modelling ROP as a mathematical function of dependent variables has been an upheaval task, due to the multi-variable constraints and ambiguity in the knowledge of heterogenous formation drilled resulting in a highly non-linear problem. Table 2.1 provides the summary of Physic based model and their operating parameters.

Table 2.1: Summary of Physic based penetration rate models

ROP Model	Model Type	Methods / Optimal parameters
Graham and Muench (1959)	Physic-based model	Earliest form of mathematical model commonly referred to as Rotary-Weight-Rotary speed (R-W-N)
Maurer model (Maurer 1962)	Physic-based model	Theoretical model for roller cone bits. Based on the volume of cuttings generated during Model parameters; WOB, RPM, bit size and UCS. See equation (2.3)
Bingham model (Bingham 1965)	Physic-based model	Modified Maurer model to include an exponent to account for hole depth. See equation (2.4)
Warren (1987)	Physic-based model	Accounts for hole cleaning in soft formation. Based on the relationship between rock and bit. See equation (2.5)
Hareland (1993)	Physic-based model	Dimensional analysis of fluid properties and modified impact force and bit wear and Mohr-Coulomb. See equation (2.6)
Burgoyne and Young (1986)	Physic-based model	Based on eight functions that affects ROP effect of formation strength, compaction, pore pressure, overbalance, bit wear and jet impact force. See equation (2.8)

The challenges of traditional Physic-based models were discussed by Soares et'al (2016) Which includes use of empirical constants and low accuracy in heterogenous lithologies. Consequent on the review of the physic-based models, it can be deduced that physics-based model is a data fitting model. As the functional relationship of the input parameters remains constant, empirical values are tuned to fit the data. The requirement

2.4 Rate of Penetration models

for the empirical coefficient results in low ROP prediction accuracy and conformity to one lithologic type. The empirical coefficients are continuously varied through calibration when there is a formation change. Soares et'al (2019) confirmed these disadvantages of traditional models which includes the use of empirical constants and coefficient such as the bit design constants, mud properties and formation constants, low prediction accuracy and their conformality to a homogenous formation.

2.4.2 Statistical Optimisation models

The statistical approach to penetration rate prediction is a data driven model that uses pre-selected model to predict ROP as a function of drilling variables. Although it differs from the traditional method in that it does not attempt to represent the physics of the mechanics of rock bit interaction Barbosa et'al (2019). Linear regression is the simplest form of statistical model used in rate of penetration (ROP) prediction. It is modelled as a linear function of the feature vectors as in equation (2.9)

$$\text{ROP} = \sum_{n=1}^n a_n x_n \quad (2.9)$$

Where x_n feature is vector and a_n are formation dependent constants.

The application of statistical techniques in ROP prediction was applied by Maraveji and Moraveji and Naderi (2016) who tested a quadratic form of multiple regression by minimizing the error sum of squares and determined the regression coefficient. They further predicted ROP as a function of six variables including depth, weight on bit, RPM, jet impact force, plastic viscosity, and yield point. Seifabad and Ehteshami (2013) evaluated several regression equations for each of the different lithology in Ahvaz oil with the aim of developing a general ROP model suitable for each formation in the field. There were also work of Hedge et'al (2015) who compared the several techniques of statistical techniques including least square regularization techniques, principal

2.4 Rate of Penetration models

component analysis (PCA) regression and bootstrap. They stated that the accuracy in ROP prediction are improved with regularization techniques which can constrain the regression coefficient. The advantage of bootstrapping was also highlighted in that it provides specific intervals for ROP prediction. Arabjamaloel and Shadizadeh (2011) compared the use of linear coefficient, non-linear regression, and combination of linear and non-linear in ROP modelling to select the most important features in ROP.

In summary, statistical model is data driven built as a function of feature vector extracted from the dataset to predict the output (ROP). In this case the functional relationship between the input and the output is not constant but based on the dataset.

Table 2.2 presents the summary of the statistical model.

Table 2.2: Summary of Statistical model for penetration rate prediction

ROP Model	Model Type	Methods / Optimal parameters
Hegde and Gray (2018)	Regression Function	Participle swarm optimization. Optimal Parameters: WOB, RPM, Mud weight
Jiang and Samuel (2016)	AntColony Optimization	R = 0.999
Ahmed et'al (2020)	Multiple Regression Analysis	Independent variables used include RPM, FR WOB, AZI, INC and YP with a significant level of P-value less than 0.052. The variable with the highest impact are RPM, FR,WOB
Moraveji and Naderi (2016)	Quadratic form of multiple regression	Optimization parameters used includes well depth, weight on bit, bit rotation speed, and bit jet impact force bat algorithm
Seifabad and Ehteshami (2013)	Regression analysis	The effect of mud specific gravity, mud viscosity, depth, bit diameter, bit rotation. For each formation the coefficient of adjusted determination was examined. Hypothetical regression tests ran, and graphs plotted to present the actual and predicted values using the model for different cases.
Hedge et'al (2015)	Trees, bagged trees, and random forests (RF).	Accuracy can be increased by using bootstrap aggregating (bagging) or Random Forests. These techniques are applied, using the statistical software computing package R (WWSLM) with nine predictors such as WOB, RPM, depth, different formations in shale, sandstone, and limestone.
Arabjamaloel and Shadizadeh (2011)	Compared liner and non-liner model	Captured the most influential factors on ROP Prediction.

Therefore, it performs better than the physics-based model in terms of accuracy and reliability. The algorithm used to build that model determines the type of data driven model. These have prompted researchers to start utilizing the machine learning approach such as the ANN, SVM and LS-SVR etc. for modeling rate of penetration due to well established experience with the universal function approximation.

2.5 Machine learning Optimization models

In recent years, machine learning (ML) algorithms have been applied in many areas of petroleum engineering and geosciences. Successful implementations of the technology have supported considerable application of the techniques in predicting seismic pattern recognition, lithofacies identification and reservoir permeability prediction. The principles of the ML techniques involve the system to learn complex patterns from the dataset during the training (learning) phase without any specified mathematical model [Barbosa et. al \(2019\)](#). Once the training phase is completed, the trained machine learning model can make predictions given a model input. According to [Okoroafor et'al \(2022\)](#), there are two main broad classifications of machine learning algorithms commonly used in the field engineering and earth science applications: supervised and unsupervised learning. Supervised learning are commonly used in predictive and regression tasks after undergoing an appropriate learning phase required for features extraction with label by providing the model with several examples in the form of datasets. Unsupervised learning uses algorithms to analyze and cluster unlabeled datasets, no training labels are used. The algorithm discover hidden patterns or data groupings without the need for humans ([Jain et al \(1999\)](#)). **Figure 2.5** show the different classification of the machine Learning algorithm.

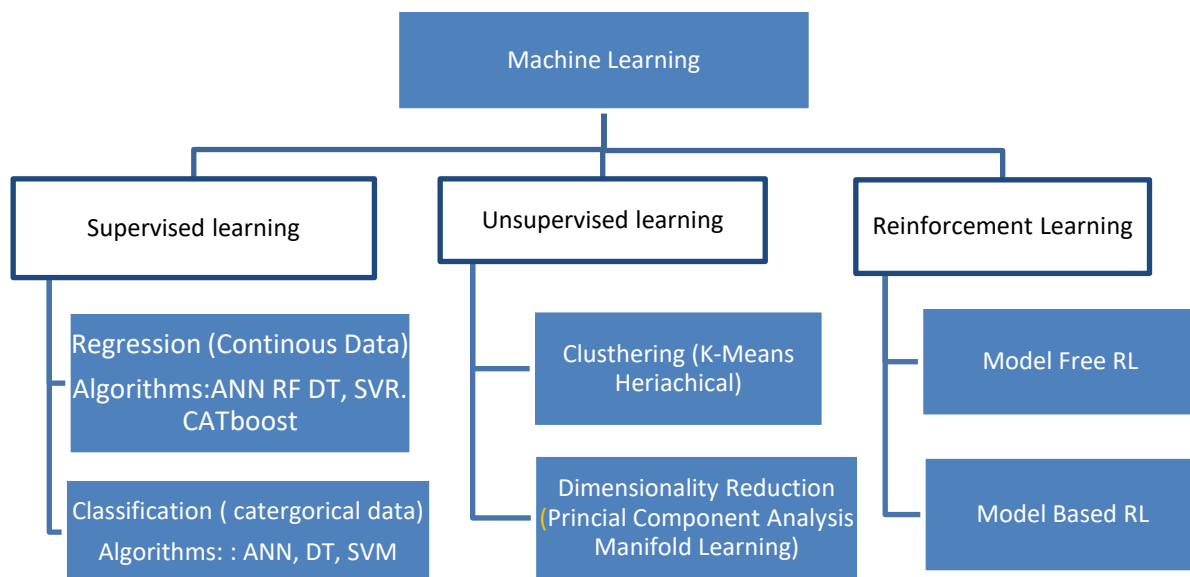


Figure 2.5 : Classification of Machine Learning techniques applied in the study.

The unsupervised machine learning is divided into two main groups: Clustering algorithms and Dimension reduction. Chropra et'al (2019) described unsupervised classification algorithm as attempts to explicitly group dataset into a finite number of clusters using a metric “that best defined the given dataset”. The Clustering algorithms performs classification of input data into a group without labels. It is commonly used in putting unstructured data into classes and in identifying structures and patterns in labels and unlabel data. Clusters have proven powerful in medical diagnosis e.g in Alzheimers diseases (Alashawat et al (2019)). The Dimensionality reduction serves as a feature engineering technique that reduces multi-dimensional data into a lower subspace, examples of these techniques include principal component analysis (PCA) and Independent Component Analysis (ICA). The Supervised Learning classification algorithm is one part of the machine learning algorithm that is used in identifying or categorizing new observation based on training dataset. The Supervised Learning model attempts to map each data point to a suite of features defined by the interpreter (Chropra et'al (2019)). These algorithms include the traditional ANN, Decision Tress and the

Support Vector Machine. The regression ML is supervised Machine Learning used in predicting continuous values. It performs the task by plotting a best fit line or a curve between based in the given independent data. Three matrixes are used to examine trained regression' these are the variance, bias, and error Okoroafor et'al (2022). Examples of regression techniques includes Randon forest, support vector regression, linear regression, CATBoost, polynomial regression, multiple linear regression, and ANN, commonly referred to as multi-layer perceptrons (MLP) Okoroafor et'al (2022). The supervised learning regression will be mostly used in the prediction in this work. **Figure 2.6** shows the interconnection of the different Machine learning models.

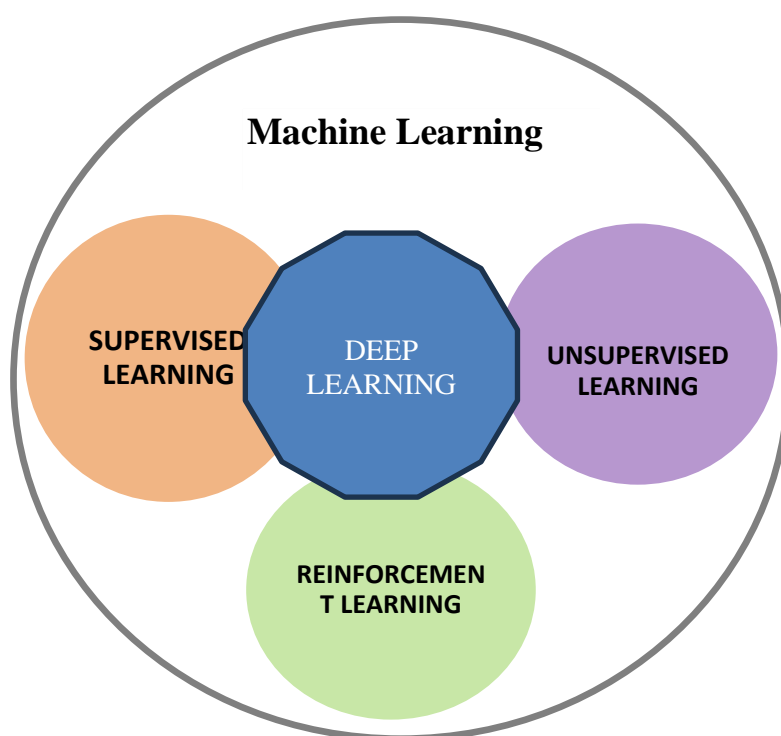


Figure 2.6: Interconnection between the Machine Learning Models and the other models.

The Reinforcement learning is another area of machine learning deals with decision making by intelligent computer agent taking decision in its environment and receiving rewards, then uses the feedback to modify its decisions in order to optimize its

cumulative rewards. In other words it is about learning optimal behaviour in an environment to obtain the best reward. There are two broad classifications of reinforcement learning the model-based RL and the model free RL. The applicability of the various artificial intelligence techniques namely, artificial neural network (ANN), extreme learning machine (ELM), support vector regression (SVR), and least-square support vector regression (LS-SVR) Decision tree etc. are discussed. A detailed explanation of the different artificial intelligence techniques is presented below.

2.5.1 Artificial Neural Network (ANN)

ANN are adaptive, information processing structures that are universal function approximator and simplifies simulation of a biological learning process with performance behaviors like those of biological neural networks (Ahmed, Adeniran and Samsuri 2018). The processing elements of ANNs are artificial neurons. These neurons consist of four basic components that include input data, connection lengths (weights), a transfer function (activation function), and output values. Neural networks are linked in a way that allows it act as a universal function approximator. Which implies that given the right linkage between nodes and connections, ANNs can simulate any input and output relationship. The ANN structures may differ from each other in architecture and in training algorithms. The most common type of ANN network structure is referred to as feedforward neural network with multilayer perceptron (MLP) (Barbosa et al. 2019). Bishop (2006), stated that network function for figure (2.7) can be expressed using equation (2.9). The back-and-forth movement in a neural network between the input and

output layers is referred to as an epoch. ANN undergoes several epochs till an acceptable error is achieved and like this the training of an artificial neural network is achieved.

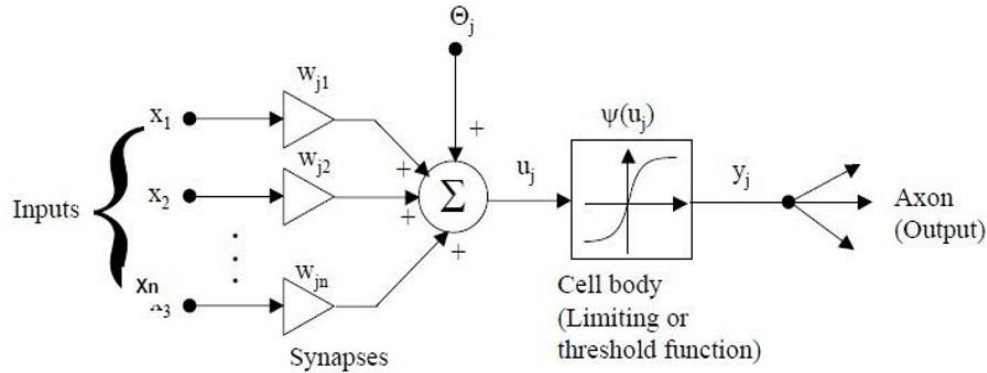


Figure 2.7: ANNs Structure with hidden layer (KUMAMOTO University (2010))

Where Θ is external threshold, offset or bias, w_{ji} is the synaptic weights, which are estimated during the training phase, ψ is the action function, x_i is the input and y_j the output variable as shown in equation (2.10)

$$y_i = \psi\left(\sum_{j=1}^n w_{ji}x_i + \Theta_i\right) \quad (2.10)$$

Where y_i is the output prediction of the i th iteration, and w are the weights which are estimated during the training phase and ψ is the activation function.

Another classification of ANN is the radial basis function (RBF) which uses a backward propagation function that involves propagating backward the error between the actual output and the predicted output. (LeCun, Bengio and Hinton 2015), Rumelhart et'al (1986) reported the application of this technique. In such ANNs architecture, the information will propagate in one direction from usually from input neurons through the transfer function of the hidden neurons to the outputs. Depending on the relative influence of each unit in the hidden layer in creating the original output, the unit receives a portion of the total error signal based on their contribution. The neurons use transfer functions to generate their output from the net input. The most used transfer functions for backpropagation are PURELIN, TANSIG, and LOGSIG. The ANN techniques are used in forecasting reservoir performance, ROP prediction and robust tool in reservoir

field development (Ghazwan, 2012). However, a known limitation of ANN reported by investigator are lack of global optima and the problem of overfitting (Zhan,2015).

2.5.2 Extreme Learning Machine (ELM)

Extreme learning machine (ELM) is derived from the ANN as a modified single-hidden layer feedforward neural network (SLFN) proposed by (Huang, Zhu and Siew 2006). The ELM algorithm trains a single forward network comprising of a random generation of hidden layer weights and biases, followed by a linear system of equations by least squares approximation of the output layer weights. This learning strategy of ELM uses a fixed nonlinear transformation, which is often fast and provides a good approximate accuracy. The key benefit of this model is that it automatically determines all the network parameters analytically avoiding trivial human intervention, which makes it efficient in online and real-time applications (Ahmed, Adeniran and Samsuri 2018). Practically, the hallmark of the model includes good simplification performance and speed as it has been shown to be much faster than most conventional machine learning algorithms for feedforward neural networks. According (Cao et al. 2015) ELM has been widely studied and proven by investigators for accurate prediction performance in most real-life applications, Success story of the application of ELM in many real-world problems especially in classification and regression problems on very large scale datasets. ELM is very efficient and effective as an innovative training algorithm for single-hidden layer feed-forward neural networks (SLFNs) (Huang, Zhu and Siew 2006) however, there are limited application in the oil and gas industry. Mathematically, the output function of an ELM model with hidden nodes can be expressed as equation (2.11)

$$f_L(x) = \sum_{i=1}^L \beta_i h_i(x) \quad (2.11)$$

2.5.3 Support Vector Machine (SVM)

SVMs are commonly used machine learning algorithms developed by (Cortes and Vapnik 1995) that uses a new learning theory referred as statistical learning theory for classification and nonlinear function estimation. SVMs are algorithms based on three mathematical principles (Ccoicca 2013); Principle of Lagrange (1788), Principle of Fermat (1638) and Principle of Kuhn-Tucker (1951). Support Vector Machines (SVM) have been widely discussed in literature with superior performance indices when compared to other ML algorithms and overcome the problems of the classical neural networks; e.g. multilayer perceptron (MLP) like the existence of many local minima and the choice of the number of hidden units (Bishop 1995). SVM solutions provides for convex optimization problems and further provides few additional fine-tuning parameters. Although SVMs have limited application in oil and gas engineering unlike the ANN, but SVM offers a simplification of regularization methods that ensure easy training and global optima overcoming one of the shortcomings of the ANNs (Zhou et al. 2011). Derivation of the SVM performed for regression case are referred to support vector regression (SVR) (Drucker et al. 1997). SVR model can overcome the problem of overfitting, hence producing good performance.

2.5.4 Least-Square Support Vector Machine (LS-SVM)

LS-SVM algorithms are alternate formulation of SVM proposed by (Suykens et al. 2002) for nonlinear function estimation and classification problems. LS-SVM uses the equality constraints and least squares cost function. Like regularization networks and Gaussian processes, LS-SVM exploits a primal-dual interpretation in that it maintains the attributes of the original SVM theory but performs better as it eliminates quadratic programming problem by converting to a set of inverse matrix operation in dual space.

The LS-SVR involves not as much of effort in training model in comparison to the traditional SVR, due to its simplified algorithm. which takes reduced processing time compared to solving the SVR quadratic programming problem (Bishop 2006). Bayesian framework with three levels of inference has also been developed (Suykens et al. 2002). In feature space LS-SVM models take the form of equation (2.12)

$$y(x) = w^T \varphi(x) + b \quad (2.12)$$

where the nonlinear function $\varphi(\cdot)$ maps the input data into a feature space; $W \in \mathbf{R}^N$; where w is adjustable weight vector and b = the scalar threshold.

2.5.5 Extra Tree (ET)

Decision tree is another supervised learning algorithm that can be applied to both regression and classification problems. James et al.(2013) discussed two steps for building a regression tree: (i) Divide the set of possible values X_1, \dots, X_n for into I distinct and non-overlapping regions, R_1, R_2, \dots, R_i .

(ii) For every sample that falls into R_i , the same prediction is made, which is the average of the dependent feature for the training sets in R_i . But for simplicity, we may split the predictor space into high-dimensional boxes and for easy analysis of the predictive model. The aim is to obtain boxes R_1, \dots, R_i that minimizes the Residual Sum of Squares (RSS) as given in the mathematical expression in (2.13)

$$\sum_{i=1}^I \sum_{j \in R_i} (y_j - \hat{y}_{R_i})^2 \quad (2.13)$$

Where (\hat{y}_{R_i}) is the mean response of the training sets in the i th box.

In a classification tree, the predicted observation belongs to the ‘most frequently occurring’ class of training sets in the region to which it belongs. Since we intend to

allocate samples in each region to the ‘most frequently occurring’ class of training sets in that region. The classification error rate is the portion of the training sets in the region that does not belong to the most frequent class, as given in equation (2.14)

$$E = 1 - \max_l(\hat{p}_{ml}) \tag{2.14}$$

where (\hat{p}_{ml}) denotes the ratio of training samples in the mth region from lth class

2.5.6 Random Forest (RF)

Random forest is a supervised ML algorithm that can be used for both regression and classification problems. It is constructed from decision tree algorithms and utilizes ensemble learning; a method combines many classifiers to provide solutions to complex problems. Classification problem in RF relies various decision trees with each tree consisting of decision node, leaf node and root node. The output returned is the output chosen by most of the decision trees and hence the final output. Figure 2.8 shows the schematic of Random Forest classifier decision tree.

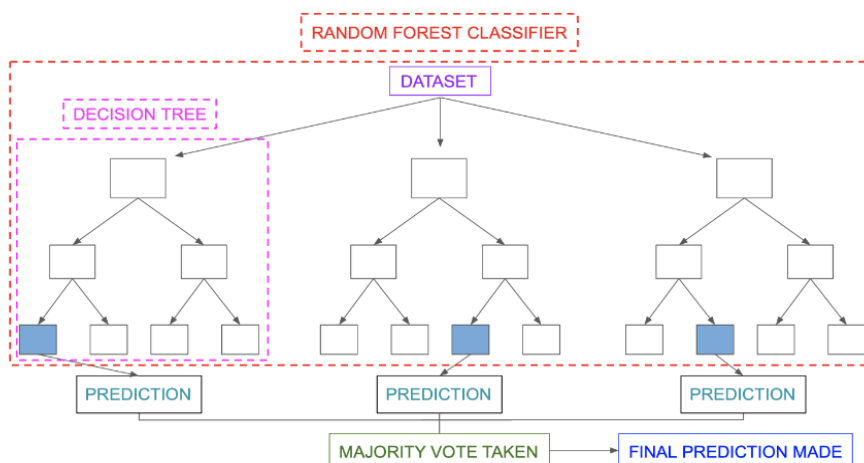


Figure 2.8 shows the schematic of Random Forest classifier decision tree.

2.5.7 CatBoost (CB)

Categorical Boosting (CatBoost) was developed by Yandex. Designed for regression and classification problems having a very large number of independent features.

Catboost is a variant of gradient boosting with built-in method for handling categorical features both categorical and numerical features. It uses symmetric weighted quantile sketch (SWQS) to handle the missing values in the dataset. CB can be applied to machine learning problems using python platform. Xia et al. (2019), predicted approvals for a peer-to-peer lending system by comparing Random Tree (RT), Logistic Regression (LR), Bayesian Neural Network (BNN), Random Forest (RF), Gradient Boosted Decision Trees (GBDT), XGBoost, and CatBoost. The results revealed that CatBoost gave the best performance over the other classifiers. The goal of the learning task is to train a function $H: \mathbb{R}^n \rightarrow \mathbb{R}$, which reduces the expected loss in equation (2.15)

$$L(H) := \mathbb{E}L(y, H(X)) \quad (2.15)$$

where $L(\cdot, \cdot)$ is a loss function and

(X, y) is a testing data sampled from the training data.

Machine learning and the implementation of data-driven solutions such as ANN, SVM, and LS-SVR are taking bigger footprint in the drilling industry to solve complex problems. The application of ANNs have been used in drilling in the selection of drill bit and drill bit diagnoses. Bilgesu et al. (1997) investigated the application the artificial neural network (ANN) in predicting ROP and drill bit dull for different types of lithologies and operating parameters. (Dashevskiy, Dubinsky and Macpherson 1999) applied ANNs in modeling dynamic behavior of non-linear drilling system. (Bataee and Mohseni 2011), (Manshad, Rostami and Toreifi 2017), (Elkatatny et al. 2017) all used artificial neural network to predict penetration rate, using WOB, RPM, Mud weight. ANNs was used to predict wellbore instability using a case history in Niger delta oilfield and utilized to predict bed heights and formation top as well as diagnose trouble zone during drilling process (Yuswandari, Prayoga and Purba 2019). Real-time drilling fluid rheological properties have been estimated using ANNs based on historical data as well

2.5 Machine learning Optimization models

as drilling hydraulics (Shi et al. 2016). (Ahmed et al. 2019) utilized three different machine learning approaches (ANNs, ELM, SVR) to predict ROP using the parameters of hydro-mechanical specific energy. (Shi et al. 2016) evaluated the prediction results of ROP using ANN and extreme learning machine (ELM), whilst (Jiang and Samuel 2016) utilized Ant colony optimization model in ANN, to predict ROP using WOB, RPM, Flowrate, depth, and gamma-ray. The various Application of machine learning in drilling operation is summarized in **Table 2.3**

Table 2.3: Summary of Artificial intelligence model for penetration rate prediction

ROP Models	Prediction Details		Method	Input parameters used in the Model	Model Performance parameters
	Output	#Inputs			
Bataee and Mohseni (2011).	ROP	5	Genetic Algorithms	RPM, WOB, Mud weight, Depth & Bit diameter	ANN, RMSE of 14.4 for training and 23.4 for testing using SVR, 27.3 for training and 27.6 for testing.
Bilgesu et'al (1997)	ROP& Bit wear	9	ANN	WOB, RPM, torque, flowrate, rotating time, tooth wear, bearing wear, formation abrasiveness and UCS	500 dataset records. 90% for training and 10% for testing Correlation coefficient (R) that ranged from (0.902) to (0.982)
Moran et'al (2010)	ROP	6	ANN	RPM, WOB, MW, Rock strength, rock type formation abrasiveness.	500 datapoints. 90% for train and 10% test 23.2 for training and 27.1 for testing using correlation coefficient of R2 equal to 0.8
Jahanbakhshi et'al (2012)	ROP	21	ANN	WOB, RPM, Pump pressure, ECD, mud type, YP, PV, mud pH, solid %, bit type, bit wear Gel strength, bit hydraulic power, UCS, hole size porosity, permeability, rock drillability, differential pressure, hole depth	ELM 0.94 for training 0.81 for testing using SVR ,0.74 for training and 0.7 2for testing using ANN and 0.82 for training and 0.71 for testing
Arabjamaloei & Shadizadeh (2011)	ROP	7	ANN	RPM, WOB, flow rate, mud density, viscosity, depth, bit size, bit hours, bit efficiency and annulus pressure.	330 dataset records. 10- input parameters Training (R2=0.94) and testing (R2= 0.74)
Elkakatny et'al (2017)	ROP	7	ANN	RPM, WOB, Q, SPP, torque, drilling fluid density and plastic viscosity	3333 datapoints.70% training, and 30% for testing. Model achieved (R=0.997 & R= 0.993) for training and testing respectively
Ahmed et'al (2019)a	ROP	8	ANN, SVR, ELM	Depth, flow rate, weight on bit, rotation per minute, torque, standpipe pressure, mud weight, and bit size	8869 datapoints 9- input parameters,70% for training,15% for testing and 15% for Validation R2 =0.95 & AAPE= 0.22, SVR: R=0.96, AAPE =0.078
Bodaghi et'al (2015)	ROP	12	ANN, SVR & others	Pump rate, tooth wear, mud weight, WOB, RPM, pump pressure, well deviation, mud viscosity, lithology, bit size, bit tooth wear, and interval drilled	93 datapoints from 13wells.154 points for training, 39 points for testing. Model Results: ANN (R ² =0.95 & AAPE= 0.22) For SVR (R=0.96, AAPE =0.078)
Shi et'al. (2016)	ROP	10	ANN and ELM	RPM, WOB, pump pressure, mud wt, mud viscosity, formation abrasiveness, formation hardness, UCS, bit wear, bit type, and bit size	5000 datapoints: ANN: R2 = 0.90 RMSE 3.56 SVR: R = 0.96, AAARE= 0.078.

Manshad, Rostami and Toreifi (2017) created a multi-layer ANN to model ROP. They applied a genetic algorithm to optimize the input parameter with 332 dataset and ten input parameters. The application of machine learning for ROP prediction are widely supported by researchers, of the 53 reviewed work with some listed in Table 2.3, 47% of the researcher used ANN followed by the Ensemble at 15% and SVR at 12% as in shown Figure (2.9)

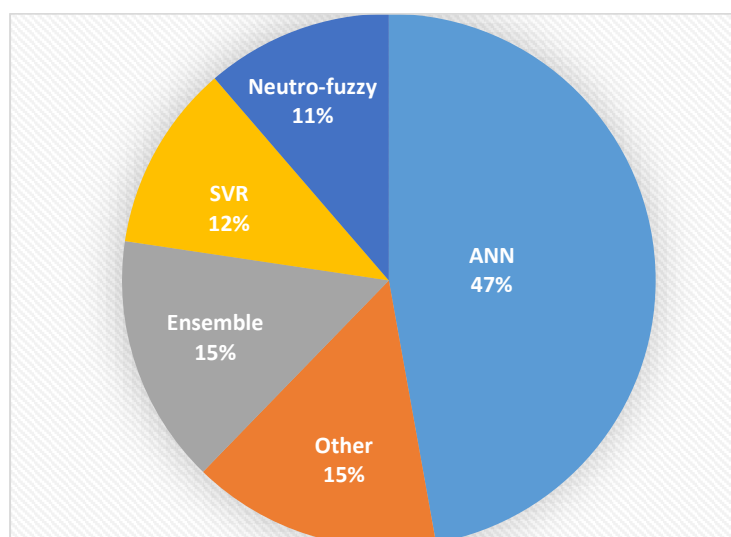


Figure 2.9: Percentage of AI model used in ROP Prediction

The extraction rule is a method used to evaluate the effect of input drilling parameters on ROP. Sensitivity analysis of the variable by holding one variable constant whilst varying other drilling variables was used by (Eskandarian, Bahrami and Kazemi 2017) who explored the range of controllable drilling variables at which the ROP is near to the maximum point. The frequency of input parameters used in ANNs modeling are as shown in **Figure (2.10)**. This work will explore the ANNs in predicting the optimal operating parameters for an autonomous downhole drilling system delivering an adaptive system that will be sensitive to change of lithology and drilling dysfunction, hence varying drilling parameters to optimize the drill rate across different formation.

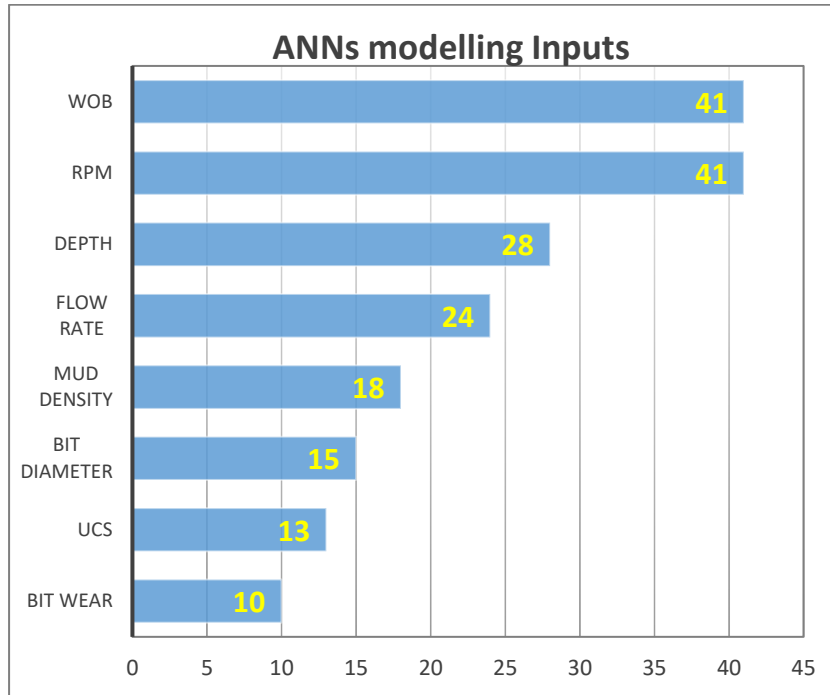


Figure 2.10: Frequency of input used in ANN modeling.

2.6 Autonomous system and predictive Optimization model

Unlike the traditional manual drilling system which requires the driller to change controllable parameter to improve the drillability rate across different formation by performing regular drill off test while drilling a specific formation, the autonomous drilling system uses a predictive model to determine the optimum combination of input drilling parameters for example, WOB, RPM that maximize the ROP. For this case maximization of ROP is a single objective optimization problem. However, in the case where more than a single drilling performance indicator is involve, for instance maximizing ROP and minimizing stick-slip, a multi-objective Optimization function formulation is required as more than one objective function is considered and these functions may be opposing to each other. In this section, the general framework for the formulation of single and multi-objective optimization problem is presented.

2.6.1 Single-objective Optimization

The single objective Optimization seek for either maximum or minimum objective function $f(x)$. According to (Cui et al. 2017) the general framework of a single objective optimization can be expressed as a minimization problem as the transformation $Max f(x) \Leftrightarrow Min (-f(x))$, which implies that it is likely to transform a maximization problem into to a minimization problem and vice versa. (Chiandussi et al. 2012) defined the general form of a single objective optimization problem subjective to inequality constraints as follows.

$$g(x) \leq 0, i = (1, 2, 3 \dots p) \text{ and equality } h_j(x) \leq 0, j = (1, 2, 3 \dots q) \quad (12)$$

Where the universe Ω denotes the space of all possible values of decision variable $X = (x_1, x_2, x_3 \dots x_n)$ respecting the constraints

The commonest single objective function in drilling optimization has been the maximization of ROP, Others includes minimization of total time, minimization of torque and minimization of drilling mechanical specific energy (DMSE). (Hegde, Soares and Gray 2018) evaluated these single objective functions to know the most appropriate for drilling optimization, they found that minimization of DMSE was the best approach as this option provides the best trade-off between optimum ROP and drilling efficiency.

Awotunde and Mutasiem (2014) compared between two objective functions of minimization of total drill time and maximization of ROP. They concluded that the best option depends on the depth of the hole drilled. For a shallow depth, maximization of ROP produces the lowest total time. However, at deeper depths minimization of the total time yields the lowest overall time, this is true due to the huge contribution of tripping time at deeper sections.

2.6.2 Multi-objective Optimization

Multi-objective optimization formulations are used for simultaneous optimization of multiple objective functions. (Zhou et al. 2011) proposed a model for multi-objective optimization as given in equation (2.15).

$$\text{Minimize } f(x) = [f_1(x), f_2(x), \dots, f_m(x)]^T \quad (2.15)$$

Where the universe Ω denotes the space of all possible decision values of X , in the case of n -objective functions the objective space will have n -dimensional vector space \mathbf{R}^m .

The multi-objective optimization problem can be subjected to equalities and inequalities (Antonio and Coello 2018), (Cui et al. 2017) According to Zhou et al. (2011) the search space can be formulated as follows.

$$\begin{aligned} g(x) &\leq 0, \quad i = (1, 2, 3, \dots, p) \\ h_j(x) &= 0, \quad j = (1, 2, 3, \dots, q) \\ x_i^{\min} &\leq x_i \leq x_i^{\max} \quad i = (1, 2, 3, \dots, q) \end{aligned} \quad (2.16)$$

Where Ω is a n -dimensional search space for the decision variable X . The objective of equation (2.15) is often conflicting with each other as an enhancement of one objective function may result in decline of the other. Therefore, there is no single optimum solution able to satisfy all the objective functions simultaneously, rather a set of optimal solutions may be obtained instead of an optimum single solution. These set of optimal solutions are called the pareto optimal solution and are explained in (Zhou et al. 2011), (Chiandussi et al. 2012). According to Lyons, Plisga and Lorenz (2004), drilling optimization problem is complex involving several constraints such as reducing total time, production capacity, health, safety, and environment constraints and therefore more suitable for a multi-objective optimization approach. Some of the pioneer work that proposed multi-objective optimization problem for drilling operation events includes (Gendelman 2012); (Payette

et al. 2017) and (Guria, Goli and Pathak 2014). Gendelman (2012) considers two optimization objective functions simultaneously: Minimum specific energy (SE) and minimum error function (E) between the predicted and the desired which the driller could set. The target was to determine the optimum WOB and RPM that will attain the desired ROP. During the research he tested two optimization methods, the particle swarm optimization and the self-developed exhaustive search engine that combines “if-then” rules with grid search in the space region of the decision variables. The selected variables to be optimized were WOB and RPM. In their work on drilling advisory by (Payette et al. 2017) adopted a simplified strategy for multi-objective optimization problem using three (3) different objectives namely ROP, specific energy (SE) and Stick-slip. They combined the three-objective function into a single scalar function that simplifies the optimization task using a real-time controllable drilling variable especially RPM, WOB and flowrate. The works of Gendelman (2012) and Payette et al. (2017) utilized decision making process which combined the multi-objective problem into a single objective function.

2.6.3 Aggregation techniques

These techniques involve combining several criteria into one. For instance, the global criterion method, sum weighted or e-constraints that are used in optimization problem in engineering. According to (Chiandussi et al. 2012) the major benefit of the aggregation techniques is the simplicity of arriving at an optimal solution as the multi-objective functions are transformed into a single-objective function. They however identified the main setback of this approach, which is the difficulty in giving suitable ranking for each criterion (Chiandussi et al. 2012).

2.6.4 Classical intelligent optimization techniques

Predictive optimization searching techniques such as genetic algorithms (GA) differential evolution (DE) and particle swarm optimization (PSO) have capability of mapping decision space into objective space using two types of methods: analytical method and numerical method. Analytical method relies on gradient information or mathematical model whilst the numerical method can be applied in a black-box problem (Cui et al. 2017)

2.6.5 Reinforcement learning techniques

Reinforcement learning approaches are used in autonomous decision making in a multi-objectives problem using a value function and a feature learning technique. Sequential decision making is modeled as a Markov Decision Process (MDP) with multiple goals. For instance, maximization of ROP, Minimization of vibration, health, and safety. To achieve the optimized policies for the autonomous system, a policy iteration algorithm is required. The features for value function approximation are learned using a real-time drilling data where a kernel-based feature is constructed based on the drilling data samples. (Xu et al. 2019). An MDP provides a mathematical framework for solving a sequential decision-making problem, irrespective of the type of control optimization system whether partially random or partly controlled by humans (Perera and Kamalaruban 2021). Chapman et al. (2012) tested the ROP optimization system automatically without the intervention of a driller with significant success in the field test, but the system was unable to avoid vibration limit zones and would require human intervention to bring it back to a stable region when damaging vibrations were observed. Jeffery and Creegan (2020) investigated an intelligent drilling optimization application that performs as an adaptive auto driller using artificial intelligence (AI) algorithms to improve on-bottom

drilling performance and proactively eliminate drilling dysfunction. The framework models the optimal decision of RL agent that receives feedback of rock-bit interaction on a drilling environment and take an action on a current state, based on the observation the agent receives in form of reward from the environment, it uses the information to improve its decision. The agents not only need to make sequential decision, but it also needs to learn how to make the decision to maximize its reward. The framework will be used in the formulation of the decision making in autonomous system.

2.7 Rock and bit interactions models

Mechanical properties of the rock are strongly influenced by their depositional environment. According to Kou (1995), four major factors affecting the behavior of the rocks includes confining pressure, pore fluid pressure, temperature and loading rate. It is essential to comprehend the concepts of rock physics, particularly rock-bit interactions, to reach a more efficient drilling process. Theories and models have been established and experiments conducted on rock-bit interactions by many researchers. **Table 2.4** presents the summary of the models and the application area. Nishimatsu (1972). Detournay and Atkinson (2000) and Evans (1962) modeled the rock cutting forces based on the theoretical models for single cutter. Nishimatsu (1972) observed that cutting penetration rate into the rock can be classified into two zones; primary zone when the depth of cut (DOC) reaches a critical value resulting in the formation of chip and the secondary zone which occur underneath the chip initiation point, where the rock is crushed into fine debris. Detournay and Atkinson (2000) modeled the applied force as a differential force, which is the difference between the force required to move the cutting minus the force exerted by the mud pressure, They further assumed a linear Mohr-coulomb relationship across the failure plan.

2.7 Rock and bit interactions models

Table 2.4: Summary of rock-cutter interactions models.

Model	Application area	Material failure and chipping mode
Detournay et al (2008)	rock-single cutter	Friction + cutting linear relation between TOB and WOB
Evans (1984)	rock-conical bits	Brittle failure. Tension-along a circular failure plane Minimum energy principle
Richard et al (2007)	rock-drill bit	n identical blades with symmetrical distribution
Detournay & Atkinson (2000)	rock-single cutter	in presence of fluid Shear- along a shear failure plane linear Mohr-Coulomb
Nishimatsu (1972)	rock-single cutter	Brittle failure Shear-along a shear failure plane linear Mohr-Coulomb
Detournay et al (2008)	rock-drill bit	Generalization of the cutter model to each blade linear relation between TOB and WOB
Wiercigroch et al (2017)	rock-drill bit	n identical blades with non-symmetrical distribution
Merchant (1945)	metal-single cutter	Ductile failure shear-along a single shear failure plane linear Mohr-Coulomb

The Merchant model (1945) assumed that the plastic flow has a single moving shear failure plane, which has an angle θ from the horizontal plane and shear stresses follow a straight line in front of the tool tip. Whilst in Evans cutting model (1984) it is supposed that the rock breaks adjacent to a circular arc tensile failure surface and the direction is tangential to the cutter surface and it reaches to surface. According to Wiercigroch et al (2017) rotary drilling model the bit is described by n identical blades, which are not distributed equally around the axis of rotation as shown in **Figure 2.12** Detournay et al. (2008) proposed that there are three phases in drilling as shown in **Figure 2.11**. In phase 1 drilling action is characterized by an increase in cutting forces as depth of cut increases. In phase II normal contact stress and contact length reaches maximum values in such that increase in weight on bit translate to cutting action. In this region drilling efficiency increases with WOB, Detournay et al. (2008) as the cutting component which makes the drill bit work like a sharp and efficient cutter. The third phase III, borehole cleaning becomes inefficient as the rate of cutting generation becomes higher than the rate of cleaning which leads to increase in contact forces. Drilling dysfunction like vibration and bit balling can also be a cause of inefficiency.

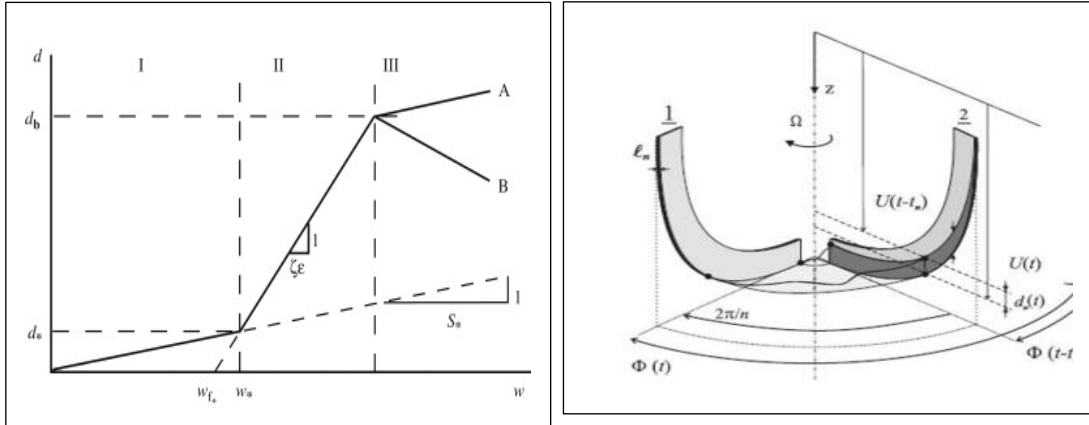


Figure 2.11: Three phases of drilling in $w-d$ space in [Detournay et al \(2008\)](#)

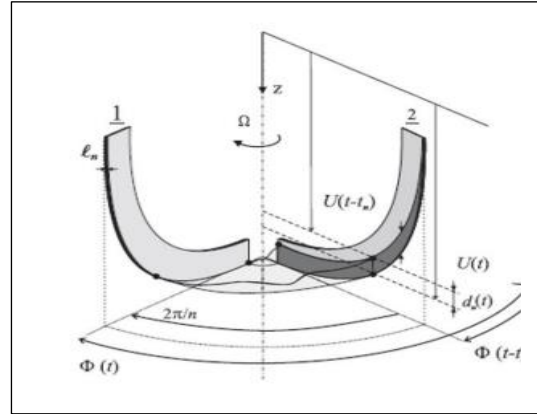


Figure 2.12: Schematic of two successive blades of a drill-bit. The drill-bit has n identical blades Adopted from [Richard et'al\(2007\)](#)

2.8 Rock UCS Prediction models

Conventional methods used to estimate UCS require either laboratory experiments or derived from sonic logs and the main drawbacks of these methods are the data and samples availability, high costs and time. The laboratory techniques have their limitations that restrict their application such as the high cost of coring operation and limited number of samples collected, which often results in a discontinuous measurement. In addition, these tests are only representative of the cored interval and cannot produce a continuous profile of the rock strength along the drilled wellbore [Abdulraheem et al. \(2009\)](#). Indirect methods of using derived correlations were developed to fill the missing gaps between the rock mechanical properties using petrophysical well-log data. The use of empirical correlation that interrelates UCS to rocks petrophysical properties that can be measured directly or indirectly from wire line logs can be used for estimation of UCS. [Trixier et al. \(1973\)](#) proposed a correlation for UCS using the rock strength as a function of formation transit time. It can be observed that correlation derived using Sonic log has negative time exponent. This is because the transit time is shorter in a harder formation and take more time a soft formation. [Chang et al. \(2006\)](#) similarly determined rock strength based on rock failure criterion and image log data. It deduced that the

2.8 Rock UCS Prediction models

terminal formation pressure where breakout stops is equal to the uniaxial strength of the formation. Oyler et al. (2010) developed a correlation between the UCS and the sonic velocity for use in the United States mining industry. Many investigators in the literature have reported various correlations (**Table 2.5**) to predict UCS of different lithologies using logging data.

Table 2.5. Published Correlations to Predict UCS

References	Correlation	Equation number	Rock Type	Comments
Oyler et al. (2010)	$UCS = 468000 e^{-0.054\Delta t}$	(2.15)	Sandstone	UCS is in (Psi) and t is travel time of P-wave in microsec/ft
Militzer and Stoll (1973)	$UCS = \left(\frac{7682}{\Delta t}\right)^{1.82}$	(2.16)	Carbonate	UCS is in (MPa) and t is travel time of P-wave in microsec/ft
Golubev and Rabinovich (1976)	$UCS = 10 \left(2.44 + \left(\frac{109.14}{\Delta t}\right)\right)$	(2.17)		
Nabaei and Shahbazi (2012)	$UCS = 7600 e^{-0.064\Delta t c}$	(2.18)	Carbonate	UCS is in (MPa) and t is sonic wave travel time in micro-sec/ft
Mostofi et al. (2011)	$UCS = \left(\frac{80204}{\Delta t}\right)^{1.285}$	(2.19)	Carbonate	UCS is in (MPa) and t is travel time of P-wave in microsec/ft
Zhang et al. (2008)	$UCS = 0.68 \left(\frac{304.8}{\Delta t}\right)^{2.5}$	(2.20)	Sandstone	UCS is in (MPa) and DT is travel time in microsec/ft. Used for weak sandstone in GOM and North Sea.
Amani and Shahbazi (2013)	$UCS = 292.04 e^{-9.541\phi}$	(2.21)	Carbonate	UCS is in (MPa) and ϕ in porosity in fraction
Chang (2006)	$UCS = 143.8 \exp^{(6.95\phi)}$	(2.22)	Carbonate	UCS is in (MPa) and ϕ in porosity in fraction

Rock strength can be estimated using drilling parameters, where some rate of penetration models such as the Bingham model (1965) established a correlation between the UCS and surface drilling parameters. S is the confined rock strength. Deng et al. (2016) proposed a theoretical model for determining the ROP for roller cone bit and validated the model using experimental ab drilling results. The authors used the rock dynamic compressive strength as an alternative of static compressive strength, which increased the accuracy of the theoretical model. Al-abduljabbar (2019) proposed a new ROP model based on the finding s and the regression analysis. In addition, the concept of drilling mechanical specific energy (DMSE) could also be used to estimate the UCS. Since the DMSE present the amount of energy required to destroy a unit volume of rock,

2.8 Rock UCS Prediction models

Amadi and Iyalla (2012) used a pattern recognition by plotting UCS versus DMSE to investigate the effect of UCS on penetration rate and lateral vibration enabling the determination of optimum penetration rate. Recent studies by Rashidi and Asadi (2018) proposed ANN model to estimate the formation pressure using drilling mechanical specific energy (DMSE). According to Wei et al (2023), ANN was employed to predict unconfined compressive strength (UCS) of sedimentary rock using three corresponding inputs : dry rock density (g/cm^3), Brazilian tensile strength (BTS) (Mpa) and rock wet density (g/cm^3), The result showed a best fit correlation with R2 value of 0.83. Ferentinou and Fakir (2017) in their work noted that the directly direct estimation of the UCS may be problematic as obtaining fresh sample is not always feasible due to operational constraints and further proposed a relationship between the UCS and the index measurement. In this work investigation on the use of basic drilling parameters with different machine learning discussed will be employed to predict UCS and penetration rate with the overall goal of developing a drilling optimization model that will improve drilling performance, drilling environmental footprint and cost.

Chapter 3

Methodology

This chapter presents the general overview of the research methodology used in this study. There are four key sub-sections in the study namely, determination of tuning parameters and predictive drill rate models, rock UCS prediction and maximum achievable ROP Model, decision-making model in a multi-objectives autonomous system and Experimental prototype rigs design and model validation. Figure 3.1 shows the generalized workflow for developing predictive optimization model for drilling system. Each sub-section will be described and developed into four subsequent chapters. Details of the methodology used are discussed in their respective chapters.

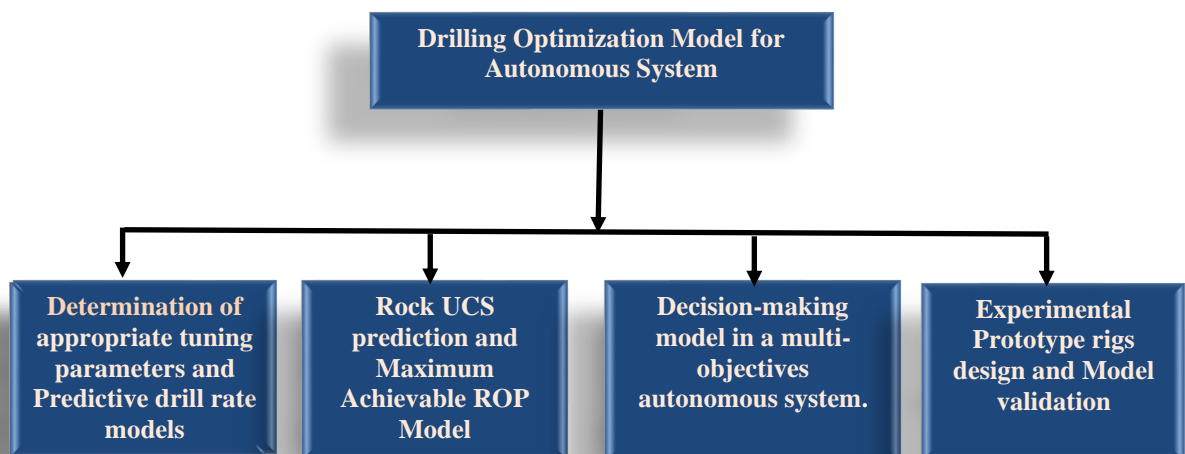


Figure 3.1: Generalized workflow for developing an autonomous self-optimizing drilling system.

3.1 Determination of appropriate tuning parameters and Predictive drill rate models

This section evaluates appropriate drilling parameters to be used in a high fidelity autonomous downhole drilling system that is self-optimized using real-time drilling data and able to precisely predict the optimal rate of penetration. Prior to determination of the appropriate drilling parameters a comparative study of the Physics Based model and the Machine learning model was evaluated and the model with higher accuracy recommended was selected for predictive ROP modelling.

3.1.1 Methodology for comparative assessment between Physics Based Model and the Artificial Neural Model (ANN)

Established Physics Based Models (PBM) were used to predict ROP. PBM used includes Maurer Model, Bingham model and B&Y model. Similarly, ANN model was used to predict ROP and both results compared. The analysis required using drilling input (WOB, RPM) to predict the output product (ROP). **Figure 3.2** shows the general workflow used in the study.

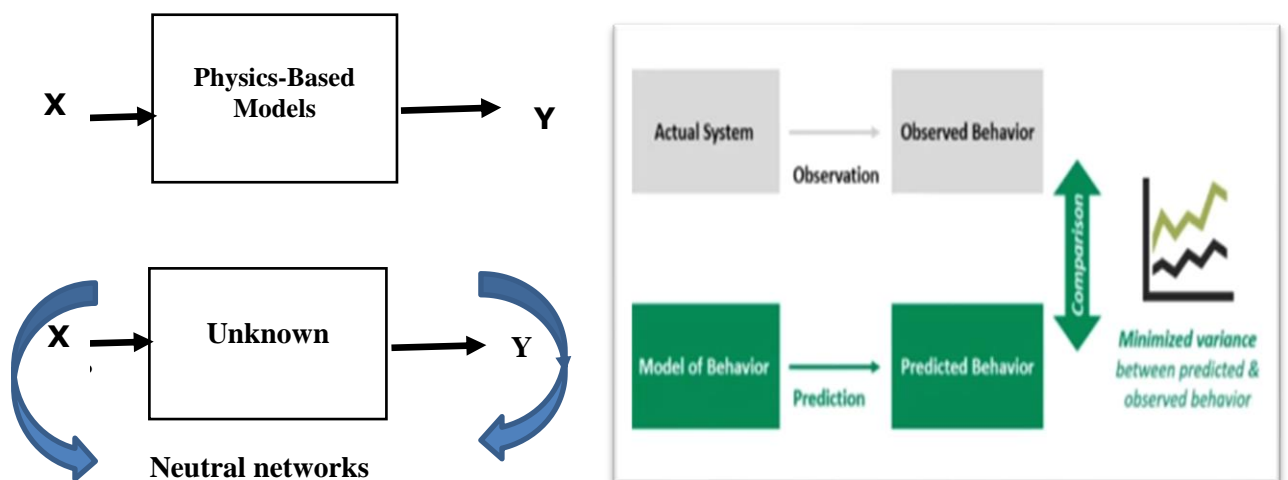


Figure 3.2: Generalized workflow for comparative study between PBM and ANN.

3.1 Determination of appropriate tuning parameters and Predictive drill rate models

The most accurate model where the predicted values are closed to the actual values was selected for further studies. The best model was selected based on assessment criteria (R^2) and root mean square error (RMSE). ANN further investigation was performed to establish the set of input parameters that will yield ROP close to recorded in actual drilling operation.

3.1.2 Methodology for determination of appropriate tuning parameters between Actual Surface Parameter (ASP) and Derived Controllable Parameters (DCP)

The rotary drilling operation uses surface parameters Weight on bit (WOB) and rotary speed (RPM) to facilitate rock breaking process. Therefore, these two parameters are used as the input variables whilst ROP is the output variables with ANN configuration. Alternative a new derived energy parameters of Drilling mechanical specific energy (DMSE) and Feed thrust (FET), which were derived from WOB and RPM and used as input variable to predict ROP using the same ANN configured. **Figure 3.3** shows the workflow for evaluating appropriate tuning parameters for an autonomous system.

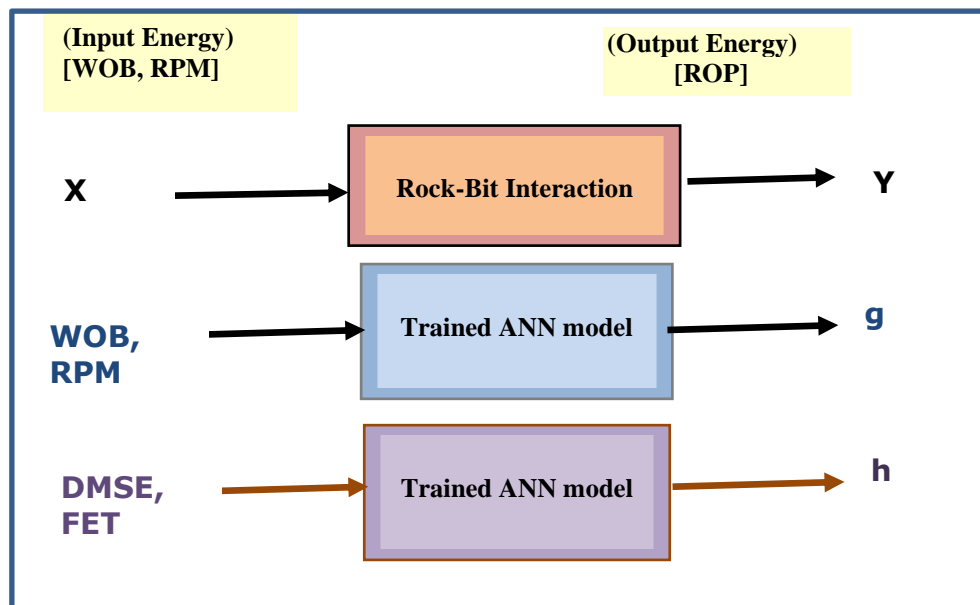


Figure 3.3: Schematic of showing the workflow for determination of appropriate tuning parameters.

3.2 Rock UCS prediction and Maximum Achievable ROP Model

The drilling mechanical specific energy (DMSE) and Feed thrust (FET) are expressed as equation (3.1) and equation (3.2) respectively. Details of the concept have been discussed in section (4.2.3)

$$DMSE = \left(\frac{480 * TOR * RPM}{Dia^2 * ROP_{(i-1)}} + \frac{4 * WOB}{\pi * Dia^2} \right) \times \text{bit factor} \quad (3.1)$$

$$FET = \frac{1.5 * Tor}{Dia} \frac{\varphi - 2v}{\sqrt{(\varphi v - v^2)}} \quad (3.2)$$

Where TOR is the surface torque in (Kpsi)

RPM is rotary speed in r(rev/min)

WOB is the wight on bit in (Klbs)

Diameter of the wellbore diameter (inch)

ROP_(i-1) is last previous update of drill rate in (ft/hr)

φ is the), φ is Cutter radius (in)

v^2 is the penetration rate per revolution (ft/rev),

The set of input variables used in conventional drilling (WOB, RPM) and output variable of ROP was used to train the ANN model. The model was trained to simulate the rock-bit interaction using the input-output relation. Once the training of the model was completed, a new set of input variables were used to predict ROP and compared with measured ROP. Similarly derived variable from the input variable (DMS, FET) was also used train and subsequent predict ROP and both predictions compared.

3.2 Rock UCS prediction and Maximum Achievable ROP Model

Rotary drilling operation involves bit-rock interaction, with rock failure occurring when the resultant stress from the drill bit is more than the rock strength. The UCS of rocks is the maximum compressive stress that the rock can endure before breaking down when uniaxial load is applied. Therefore, the rate of destruction of the rock

3.2 Rock UCS prediction and Maximum Achievable ROP Model

(ROP) depends on the strength of the rock material. If the law of energy conservation holds true in this case, normal drilling parameters such as WOB, RPM, TOR and ROP can be used to predict the rock strength. **Figure 3.4** shows the generalized workflow for predicting rock UCS and estimating of maximum achievable ROP across the rock formation. In the study the performance assessment criteria were measured using the correlation coefficient (R^2) and the root mean square error (RMSE). The summary of the procedural steps are as follows.

1. Literature review on proven empirical model for the estimation of formation UCS using Sonic and neutron porosity data. The model was selected due to its improved accuracy in documented in 1
2. Use Sonic or porosity data to predict UCS prediction as per current practice.
3. With basic drilling data as input, WOB, RPM, ROP and TOR and resultant UCS result from empirical model develop and train ANN model.
4. Using a different dataset using the input variables; WOB, RPM, ROP, TOR predict UCS from five machine learning model including, Support vector regression, Decision tress, Randon Forest, catboost and ANN models. There are different ways of selecting the best predictors if a large number of predictors are available. One common method used in this study is a detailed search in which all possible regressions are tried, and one is selected based on the most appropriate predictor according to statistical performance criteria (R^2) and (RMSE) (Neter et al. 1996).
5. Finally compare results from the model with empirical calculated UCS with the dataset. Define similarity in terms of correlation coefficient (R^2), The coefficient of determination is a measure of how well a regression curve fits a data set. It

6. ranges from 0 to 1, with zero showing no relationship and one being a perfect correlation. Root mean square error (RMSE), Mean absolute error (MAE). The details of the analysis steps, discussion and results and summary of finding are presented in chapter 5

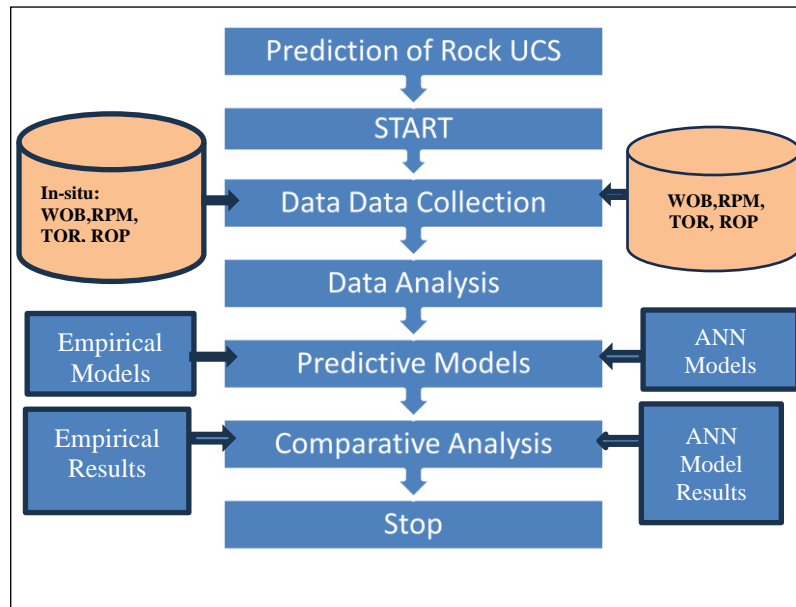


Figure 3.4 Workflow for the prediction of rock UCS

3.3 Decision-making in multi-objectives autonomous system.

In the development of autonomous downhole drilling system, sequential decision-making has become one of the main technical challenges. Traditional manual drilling method lack adaptive capability when dealing with complex interactions and changing downhole drilling environment. However, data driven control system with machine learning shows the potential to solve sequential decision problems and determine the most influential parameters in a drilling process. In this study an independent decision-making method based on reinforcement Q-learning is proposed, **Figure 3.5** shows the workflow of multi-objective decision-making mechanism of an intelligent agent.

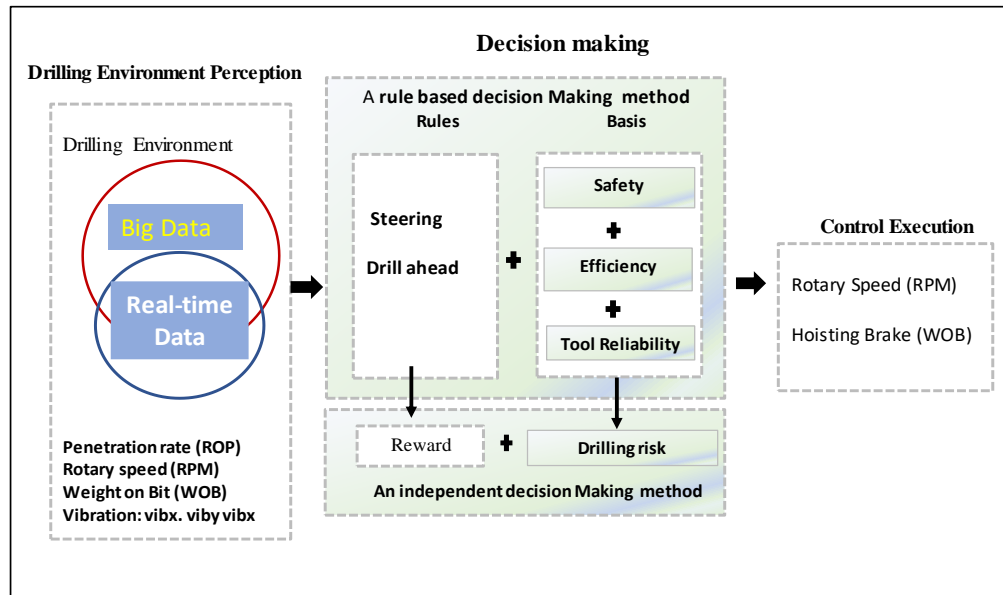


Figure 3.5. Formulation of Autonomous Systems as an MDP problem

First, a Markov decision process (MDP) is established by analysis of agent exploration and exploitation of possible actions taken in an environment. Second, the state set and action set are designed by the synthesized consideration of surface operating parameters from the published data within the range of operational limit. Then, sequentially, at each timestep, the agent takes an action (e.g., changing rotary speed or changing axial force) that makes the environment (formation) transition from one state to another. consequently, the agent receives a reward (e.g., distance drilled) before taking the next action. Furthermore, a recursive reinforcement Q-learning algorithm is developed mainly based on the reward function and update function. The generalized flowchart for the Q-learning algorithm is shown in Figure 3.6. The detailed process for the formulation of Markov Decision Process (MDP) and value function as well as detailed explanation of the process steps in the flow diagram is presented in Chapter

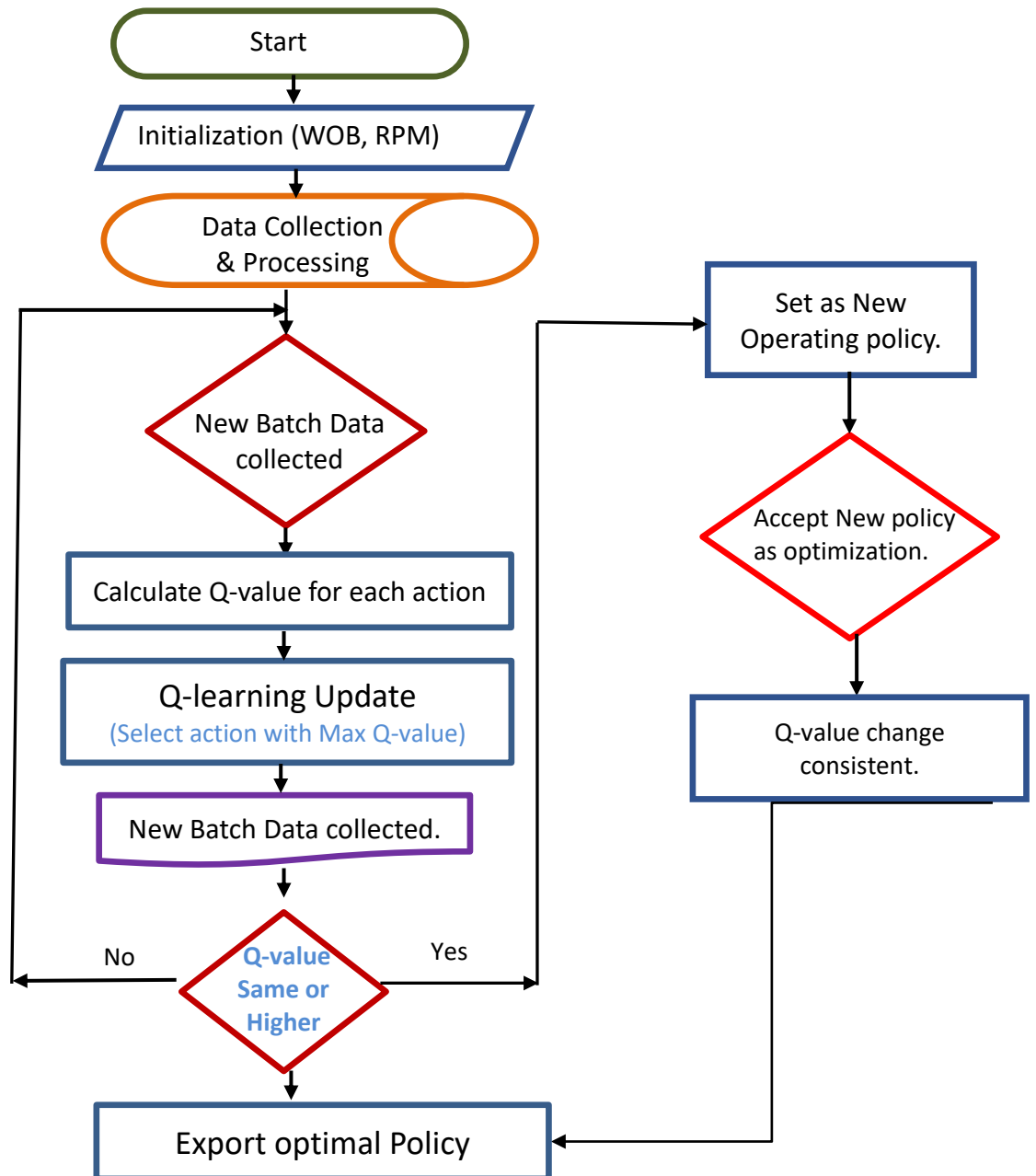


Figure 3.6: The flow chart for Modeling MDP based on the Q-learning algorithm

3.4 ANNs. Model Performance Assessment Criteria

The criteria applied for assessing performance of the two cases are the three commonly used in engineering analysis benchmark to align with the best practice. The predicted performances of neural network models were assessed by; correlation coefficient (R2) and root mean square error (RMSE) and absolute average percentage error (AAPE)

Correlation coefficient (R^2) is a measure of the similarity between the actual and the predicted values. The range of value of (R^2) varies between 0 and 1. Whilst the value of 0 suggests no similarity and 1 signifies an excellent correlation between the model output and the actual predicted values. It is mathematical expressed using equation (3.1):

$$R^2 = 1 - \frac{\sum_{i=1}^n (f(x_i) - y_i)^2}{\sum_{i=1}^n f(x_i)^2 - \sum_{i=1}^n f \frac{(y_i)^2}{n}} \quad (3.1)$$

Where y_i presents actual data

x_i are the input parameters, and

n is the total number of records.

The higher R^2 shows a close approximation between the actual and predicted values.

Root means square error (RMSE) - The root means square error (RMSE) is a measure of error between the actual and the predicted values. It is used as an error function for the quality evaluation of the model. It is mathematically expressed in equation (3.2).

$$RMSE = \sqrt{\frac{1}{n} \sum_{i=1}^n (f(x_i) - y_i)^2} \quad (3.2)$$

The Average absolute percentage error (AAPE) is a statistical measure of the relative accuracy of the model prediction expressed in percentage. It can be calculated as the ratio of the mean of the absolute error as shown in equation (3,3)

$$AAPE = \frac{1}{n} \sum_{i=1}^n \left[\frac{|x_i - y_i|}{x_i} \right] * 100 \quad (3.3)$$

Chapter 4

Tuning Parameters and Predictive ROP model with Drilling Data

4.1 Introduction

In the design of an automatic system, an important component of the system is the controller variables also referred to as the tuning parameters. Autonomous self-optimizing downhole system have four essential components: (i) Data management system (ii) Model and simulation tools for performance prediction and (iii) module to communicate decision to the actuator (iv) Feedback and control system. The tuning variables forms part of the second category used in the simulation of the system performance. This section will discuss part (i) and (ii). The steps used in the data management include the collation of offset drilling data, calculating derived variables from the dataset, and using industry recognized model to predict the drilling performance and then compare with actual measured result. Different modeling procedures for predicting ROP both the Physics based models and the ANN model were evaluated. In addition, the evaluation of different tuning variables as input parameters on model and their accuracy will be presented. To answer the research question how to determine the optimal drill rate of an autonomous self-optimizing rotary drilling system in heterogenous drilling environment? To estimate optimized operating procedure, a comparative study of surface operating parameters using weight on bit (WOB), and rotary speed (RPM) versus drilling mechanical specific energy (DMSE), and fee

(FET) was performed. The study used a data-driven approach, that uses offset drilling data with machine learning models in finding a pair of input operating variables that serves as best tuning parameter for the topdrive and drawwork system. The aim of the analysis was to establish the best tuning parameters for the autonomous system and to test its effectiveness accurately in replicating the result of a measured outcome. The model was tested with a different set of datasets from previously drilled wells.

4.2 Data gathering and preparation.

The steps involve collation of offset drilling data, cleaning of the dataset and calculating derived variables from dataset input parameters.

4.2.1 Data Collection.

Data collection and quality check is the most challenging and time-consuming process in this study. Actual field drilling mechanics data was taken from two wells: Well, W1 and Well P05. Well, W1 was resampled at 10ft intervals whilst Well P05 was resampled at 30ft interval to reduce the data density. The following drilling surface parameters were collated: Hole depth, weight on bit (WOB), rotary speed (RPM), torque (τ) and penetration rate (ROP).

Table 4.1: Sample of the Drilling data collected for analysis.

Field measured drilling parameters				
DEPT (ft)	ROP5	RPM	TQA	WOB
MD (ft)	(ft/hr)	(rev/min)	(Kft-lb)	(Klbs)
7400	10.86	125.32	16610.76	18.79
7430	9.91	120.47	18018.95	20.49
7460	22.83	113.58	18435.46	25
7490	16.13	106.36	16420.58	230.69
7520	17.86	106	15600	237.01
7550	50.92	124.75	20218.43	35.27
7580	104.18	136.04	23887.9	50.97
7610	89.42	139	22760.78	62.44

4.2.2 Data filtration and quality check

Data filtration and quality check are performed to remove dull values, check for data consistency, especially if data are from two independent sources, ensure unit consistency and depth alignment. quality checks also help to identify gaps, spot peaks and data points that are too high or outside the parameter range.

4.2.3 Calculation of derived functions

Calculation of derived variables from the drilling parameter was performed using established empirical relationship that relates the penetration rate with the derived variables. A brief description of the derived variables is presented.

Depth of Cut (DOC): DOC is defined as ROP per unit revolution as in (4.1)

$$\text{DOC} = \text{ROP/RPM} \quad (4.1)$$

Where DOC is depth of cut (ft/rev), ROP is in ft/hr, and RPM is in rev/min.

Feed Thrust (FET): The force applied on a surface in the direction perpendicular or normal to the surface is referred to as thrust. The speed or rate of the application of the force is known as the feed thrust. The equation of feed thrust of a rotating system is derived from earlier work of [Lindqvist \(1982\)](#) and [Clark \(1982\)](#) on the indentation force of hemispherical carbide buttons in rock as defined in equation (4.2)

$$\text{FET} = \frac{1.5 * \text{Tor}}{\text{Dia}} \frac{\varphi - 2v}{\sqrt{(\varphi v - v^2)}} \quad (4.2)$$

Where, FET is Feed rate (inches/sec),

Tor is Surface torque (Kft.lbs),

φ is Cutter radius (in),

v is Penetration rate per revolution (ft/rev)

Dia is drill bit or hole diameter (in)

Drilling Mechanical Specific Energy (DMSE); The concept of mechanical specific energy was first introduced by Teale (1965), defined as the amount of energy required to destroy a unit volume of rock. For optimal drilling efficiency, the objective is to minimize the DMSE and to maximize the rate of penetration (ROP). Equation (4.3) is the mathematical relationship for DMSE in oilfield units.

$$DMSE = \left(\frac{480 * TOR * RPM}{Dia^2 * ROP_{i-1}} + \frac{4 * WOB}{\pi * Dia^2} \right) \times \text{bit factor} \quad (4.3)$$

Where MSE is Mechanical Specific Energy (Kpsi),

Tor is Surface Torque (Kft.lbs)

RPM is revolution per minute,

Bit Factor is 0.125 for PDC bit ,

WOB is weight on bit (klbs),

ROP_(i-1) is rate of penetration (ft/hr) of the previous update

Dia = Hole diameter (in).

4.3 Statistical and graphical Analysis:

The influence of the input surface drilling parameters on ROP (output product) in the drilling system were studied by performing statistical analysis of the dataset. The statistical analysis was useful in identifying outliers (data outside the acceptable limits) which were subsequently deleted from the datasets. Tables 4.2 and 4.3 show the range of input parameters for W1 and P05.

4.5 Modeling Results

Table 4.2 : Range of input data and statistic (W1)

Parameters	Min	Max	Mean
Database counts	4185	4185	-
Depth (ft)	5577	11647	1040
ROP (ft/hr)	4.30	307.67	48.98
Torque (Kft-lb)	5.03	16.33	11.42
SWOB (Klbs)	1	50	23.32
RPM (rev/min)	20	190	174
Stick-slip(rev/min)	15	360	167

Table 4.3 : Range of input data and statistic (P05)

Parameters	Min	Max	Mean	Median
Database counts	246	246	-	-
Depth (ft)	7400	10630	9308	9345
ROP (ft/hr)	1.03	163.39	26.42	17.06
Torque (Kft-lb)	0	28	21.4	3.7
SWOB (Klbs)	1	70	38.0	38.7
RPM (rev/min)	1	150	119	120
Stick-slip(rev/min)	36	174	76	69

Dataset-W1 consists of 4185 datapoints from borehole measured depth of 5577 to 11647ft taken at 10ft interval. While Dataset-P05 consists of 246 datapoints from measured depth of 7400ft to 10630ft at an interval of 30ft. Figure 4.1 shows the graphical analysis of the dataset of W1 and P05 respectively. In the graphical analysis, investigation was performed to see the trend and relationship between the drilling surface input parameter with output variables (ROP, stick-slip) at increasing depth. The relationship between rotary speed, Weight on bit (WOB), rate of penetration. (ROP) and stick-slip were plotted as in **Figure 4.1**.

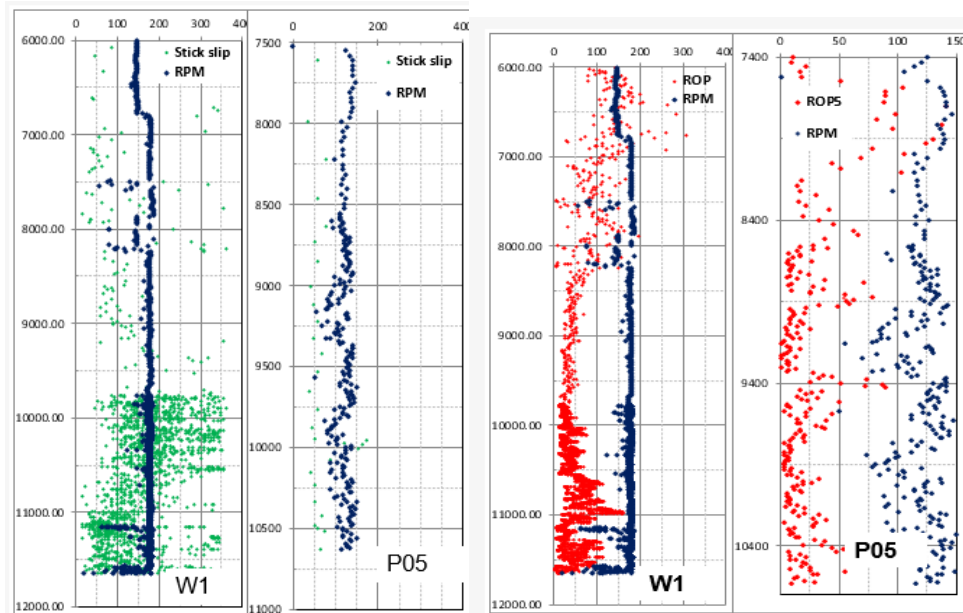


Figure 4.1: Plot of Stick-slip vs RPM and ROP vs RPM for W1 and P05

Similarly, the plots Derived variables calculated in section 4.3.2 of ROP vs DMS.

From the charts (**Figure 4.2**), the derived variables show a strong relationship with the output variables (ROP, stick-slip) as the plot showed an inverse relationship between the ROP and DMSE and a direct relationship between DMSE and stick-slip.

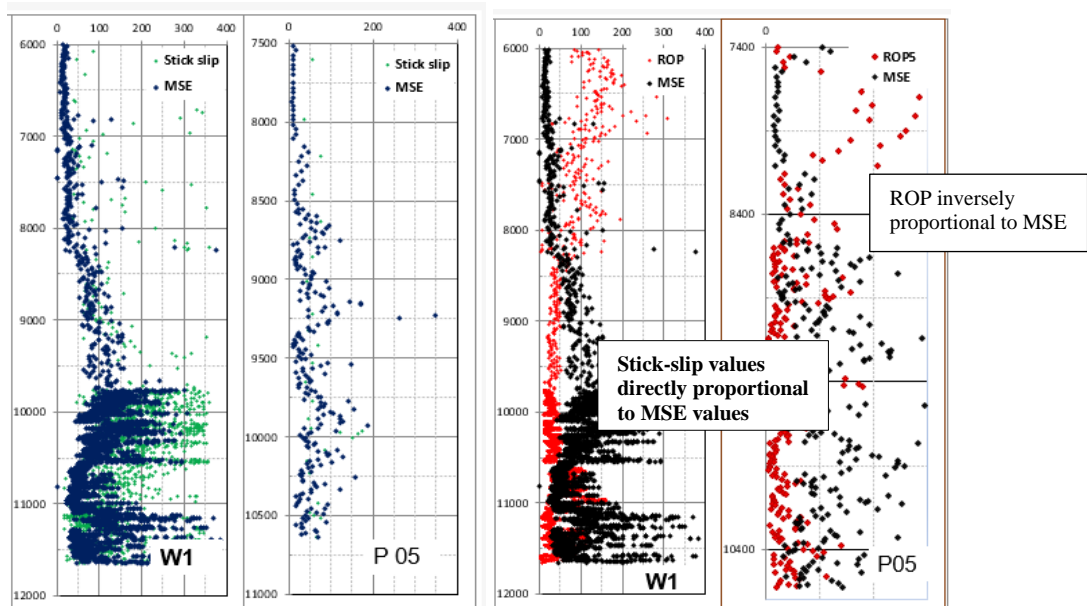


Figure 4.2: Plot of Stick-slip vs DMSE and ROP vs DMSE for W1 and P05 well

The strategy adopted was to use the two most influencing parameters in the prediction as adding more input parameters than necessary will result in large network size and subsequently decrease learning rate and efficiency. Since the drilling process has many effective parameters, it is essential to find the best set of variables that are related to ROP. The most influential parameters are RPM and WOB as reported in (Ahmed et.al 2019).

4.4 Modeling techniques

This section discussed the model for rate of penetration prediction. In order to decide the most suitable model for the autonomous system, a comparative evaluation was performed between the physics-based model and the data driven system. Once the most accurate prediction model was selected, further investigation was carried out to

determine the best tuning parameters for the selected model for the automatic system were determined.

4.4.1 Comparative parameter evaluation

To select the best ROP model for the prediction, comparative study was performed by comparing the performance of industry proven physics-based models and the ANN model. The analysis setup for both models is shown in **Figure 4.3**.

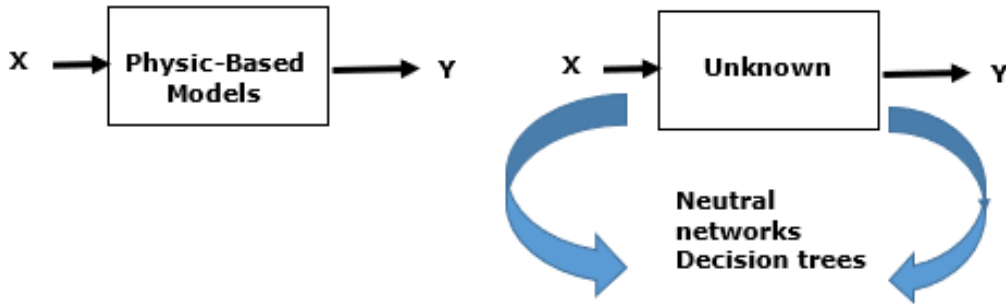


Figure 4.3 : Simulation workflow for Physic based Model and ANN model

The empirical model developed by Maurer in equation 2.3, Bingham in equation 2.4 and Bourgoigne and Young in equation (2.8) were used to predict penetration rate of already drilled wells using the recorded drilling parameters used during the drilling operation. For the Maurer model in equation (2.3) the best fit was achieved iteratively with the drillability constant of 4.4. The Bingham model of formation drillability constant (0.03) gave the best fit for the dataset. Details of the result and discussed are in section 4.3.2 For the Bourgoigne and Young model, the determination of the coefficient (a1-a8) using multivariable regression was performed in Microsoft excel (GRG) solver and the value of the coefficient estimated for the field data is given in table 4.4

$$\frac{df}{dt} = Exp \left[a_1 + a_2(10000 - D) + a_3 D^{0.69} (g_p - 9.0) + a_4 D (g_p - \rho_c) + a_5 \left\{ \ln \frac{\left(\frac{w}{d}\right) - \left(\frac{w}{d}\right)t}{4 - \left(\frac{w}{d}\right)t} \right\} + a_6 \ln \left[\frac{N}{100} \right] + a_7 (-h) + a_8 \left(\frac{Fj}{1000} \right) \right] \quad (4.4)$$

Table 4.4: Bourgogne and Young model coefficient for the field

Variable	Constant	Value
Drillability	a1	-57.63
Normal Compaction	a2	0.00448
Under Compaction	a3	0.0195
Differential Pressure	a4	0
Weight on bit	a5	0.52
Rotary speed	a6	2
Tooth wear	a7	0
Jet impact force	a8	0.18

ROP is obtained using the equation (3.4) below;

$$f(x) = \text{Exp} [-57.63] + 0.00448(10,000 - D) + 0.0195 D^{0.69}(g_p - 9.0) + 0.52 \ln \frac{\left(\frac{w}{d}\right) - \left(\frac{w}{d}\right)t}{4 - \left(\frac{w}{d}\right)t} + 2.0 \ln \left[\frac{N}{100} \right] + 0.18 \left(\frac{F_j}{1000} \right) \quad (4.5)$$

4.4.2 Artificial Neural Networks configuration

Artificial Neural Networks (ANNs) are interconnected in multilayer network topology that comprises of three layers: (1) input layer, (2) one or more hidden layers, and (3) an output layer as show in Figure 4.4. The hidden layer(s) are the coefficients that provide the relationship between the input and output layers. The most common types of ANNs are feed-forward networks, which are the most efficient ones (Abbas et'al (2018).

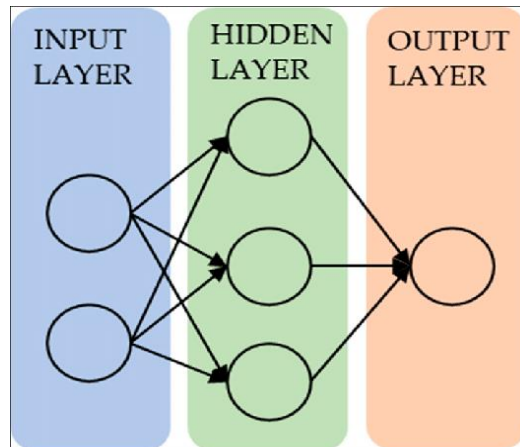


Figure 4.4: ANNs Structure with one hidden layer (Ganasan et'al (2021)

4.3 Statistical and graphical Analysis

During this analysis, the model was built using ANNs with 2 neurons in the input layer and only 1 neuron in the output layer (ROP). The optimum number of neurons and layers was selected based on an iterative process by performing sensitivity analysis on the number of neurons that provides the highest accuracy correction coefficient (R^2). **Figure 4.5** shows the flowchart for the ANN modeling. In the modeling process, the database is randomly divided into two parts: A training dataset is applied to develop and adjust the weights in a network and a testing dataset is applied to examine the final performance of the ANNs. A total of 4185 datasets and 246 datasets points were used in W1 and P05, respectively. the ratio of 70:30 was utilized for training and testing the developed ANNs model, respectively.

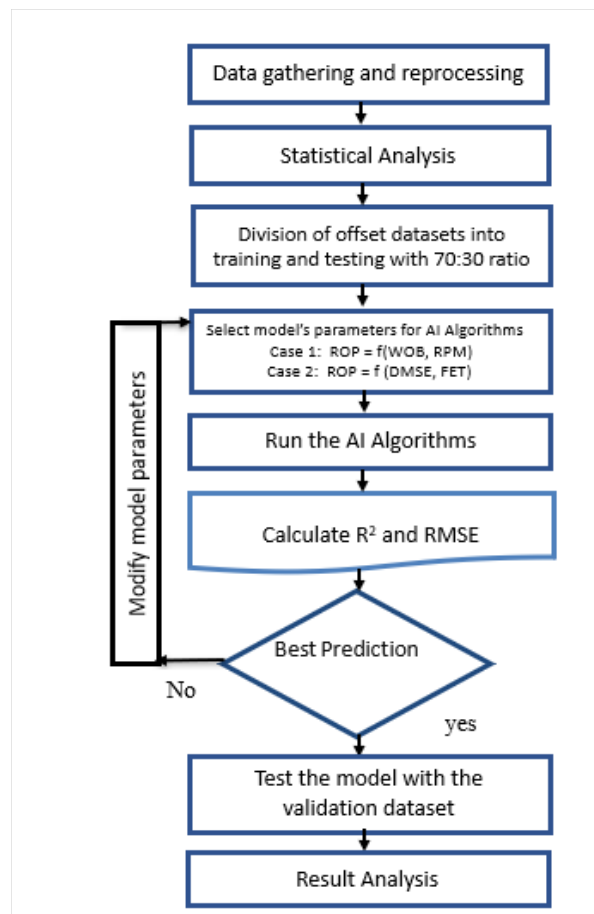


Figure 4.5: Flowchart for ROP Modeling using ANNs Modeling

4.4.3 ANNs Simulation cases.

Two simulation cases were studied; “Case 1”, the two input parameters used in this case were DMSE and FET with ROP as the output variable. However, in the second case (Case 2) the input data (WOB and RPM) were used and the ROP as the output parameter. Upon simulation the number of neutrons were iteratively changed whilst monitoring the improvement on R^2 .until no further improvement was recorded. To effectively compare the performance of the input variables in ROP prediction same ANNs network configuration, number of hidden layers and transfer function were used for both cases.

4.5 Modeling Results

In this section, summary of the results of the analytical and modeling procedures are provided, including discussion of the result of dynamic relationship between input variables and output variables, modeling and predicting of ROP for drilling system.

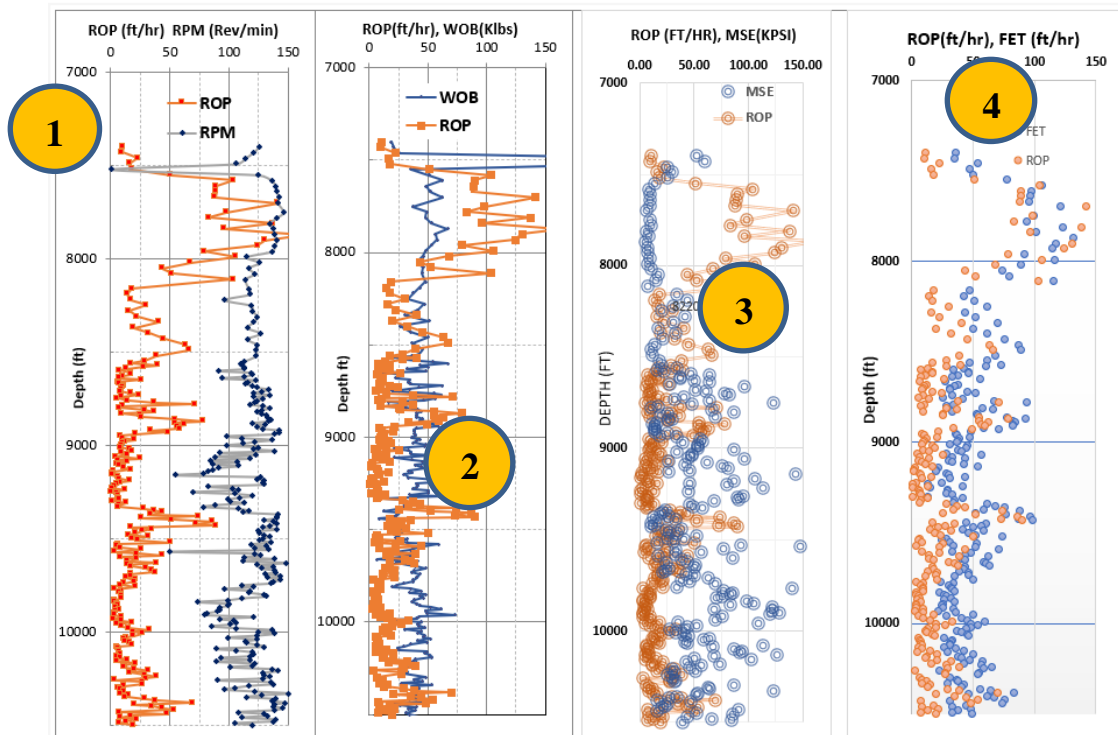
4.5.1 Establish relationship between input and output data (ROP)

Table 4.5 : First 15 datapoints sample of Calculated derived variables.

Field measured drilling parameters					Derived parameters		
DEPT (ft)	ROP5	RPM	TQA	WOB	DMSE	DOC	FET
MD (ft)	(ft/hr)	(rev/min)	(Kft-lb)	(Klbs)	(Kpsi)	(inch/rev)	(Inch/sec)
7400	10.86	125.32	16610.76	18.79	52.77	0.02	0.12
7430	9.91	120.47	18018.95	20.49	60.30	0.02	0.12
7460	22.83	113.58	18435.46	25	25.26	0.04	0.18
7490	16.13	106.36	16420.58	230.69	29.97	0.03	0.16
7520	17.86	106	15600	237.01	25.66	0.03	0.17
7550	50.92	124.75	20218.43	35.27	13.66	0.08	0.26
7580	104.18	136.04	23887.9	50.97	8.62	0.15	0.35
7610	89.42	139	22760.78	62.44	9.78	0.13	0.32
7640	89.25	140.23	22356.96	48.64	9.70	0.13	0.32
7670	88.22	141.94	21980.66	52.08	9.77	0.12	0.32
7700	141.8	141.28	23837.69	62.51	6.58	0.20	0.40
7750	98.04	145.95	22319.75	36.76	9.17	0.13	0.33
7780	82.96	139.93	22771.51	48.75	10.61	0.12	0.31
7810	137.87	134.24	23836.32	47.89	6.42	0.21	0.41
7840	96.18	137.06	22912.25	52.95	9.03	0.14	0.34

4.4 Modeling techniques

The dataset for Well- P05 consist of 246 datapoints ranging from 7400ft to 10630ft measured Depth (MD). Presented a sample of Fifteen (15) datapoints in table 4.5. The entire dataset is plotted as shown in **Figure 4.6**. In calculating the DMSE, the bit size of 14.25in and bit factor of 0.125 for polycrystalline diamond compact (PDC) bit. The dynamic relationship between the drilling input parameters (WOB, RPM) with ROP and these derived parameters (DMSE, DOC and FET) were investigated by graphical representation as shown in **Figure 4.6**. The plot tracks are defined with the orange color circle from 1 to 4. The input energy used in a drilling system comes from WOB and RPM, which results in output energy in the form of ROP. Evaluating the input and output relationship using the plot of RPM vs ROP in track 1 and the plot of



Note : Both variables are plotted on the same scale

Figure 4.6 Relationship between input variable and output variable (Penetration rate)

WOB vs ROP in track 2. There is no explicit relationship as the correlation are fuzzy as significant changes in drill rate occurred with no respective changes in WOB and RPM.

However, the dynamic non-linear relationship between drill rate and drilling specific mechanical energy (DMSE) in track-3 shows an explicit indirect relationship irrespective of the occurrence of other downhole conditions and reliable tuning parameter for an autonomous drilling system. The finding supports the work of (Amadi and Iyalla 2012), (Hegde, Soares and Gray 2018) which stated that minimization of DMSE was the best approach of single objective functions as this option provides the best trade-off between optimum ROP and drilling efficiency. Similarly, the dynamic non-linear relationship between the drill rate and feed thrust (FET) in track-4 indicate a direct relationship, which also support research of (Tlegenov, San and Soon 2015). Based on the data trend from Figure 4.6 it is evident that DMSE and FET show a clear relationship with ROP and would be a better parameter for predicting rate of penetration (ROP). Furthermore, DMSE and FET are couple parameters derived using other input parameters such as TOR and previous update $ROP_{(i-1)}$

4.5.2 Comparative study of Physics based model versus ANN model

Penetration rate model performance of the different models tested using Fig 4.3 workflow are presented in **Table 4.6**. The criteria applied in the performance assessment are the two commonly used in engineering analysis benchmark; correction coefficient (R^2), and the root mean square error (RMSE) to align with the best practice.

Table 4.6: Physic Based model and ANN model performance results

ROP Model	Classification	Performance Indexes
Maurer model	Physic Based Model	$R^2 = 0.50$, RMSE = 30.23
Bingham model	Physic Based Model	$R^2 = 0.51$, RMSE = 37.89
Bourgogne and Young (B&Y)	Physic Based Model	$R^2 = 0.70$, RMSE = 27.34
Artificial Neutral Network (ANN)	Data Driven Model	$R^2 = 0.985$, RMSE = 5.80

Although all the tested models performed above average, the best model performance was from the artificial neutral network (ANN) with R^2 value of 0.985, followed by the

4.5 Modeling Results

Bourgogne & Young model with R^2 value of 0.70 whilst Bingham model and the Maurer model have R^2 values of 0.51 and 0.50 respectively. The scatter plots is in (Fig 4.7)

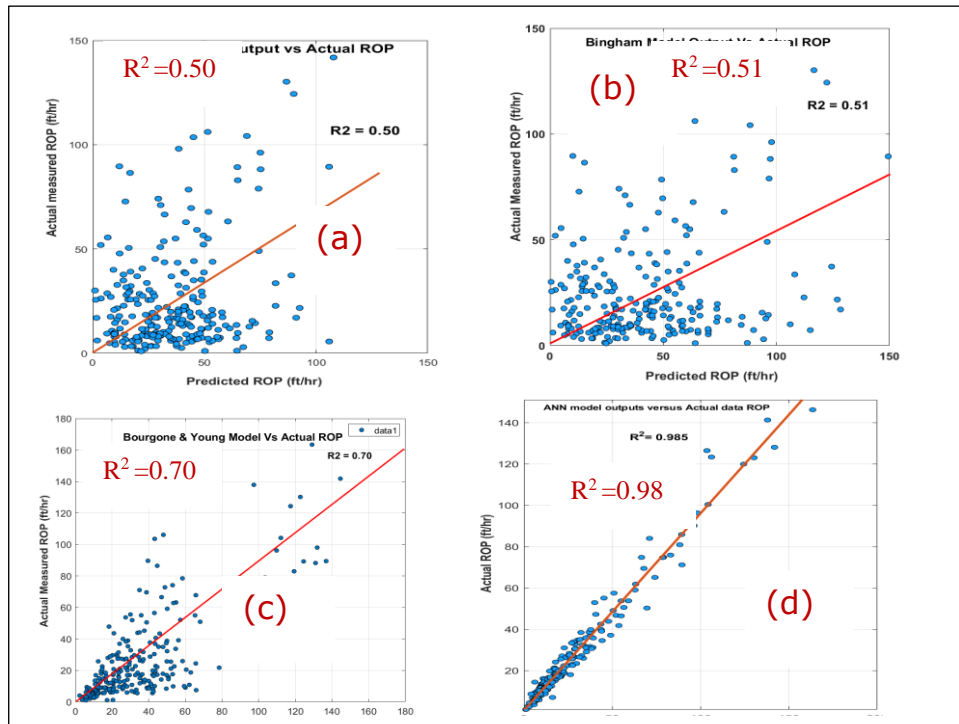


Figure 4.7 : Predicted ROP Vs Actual ROP; (a) Maurer Model (b) Bingham model (c) B&Y model (d) ANN model

Similarly, Fig 4.8 shows plot of predicted ROP vs Actual ROP along hole depth.

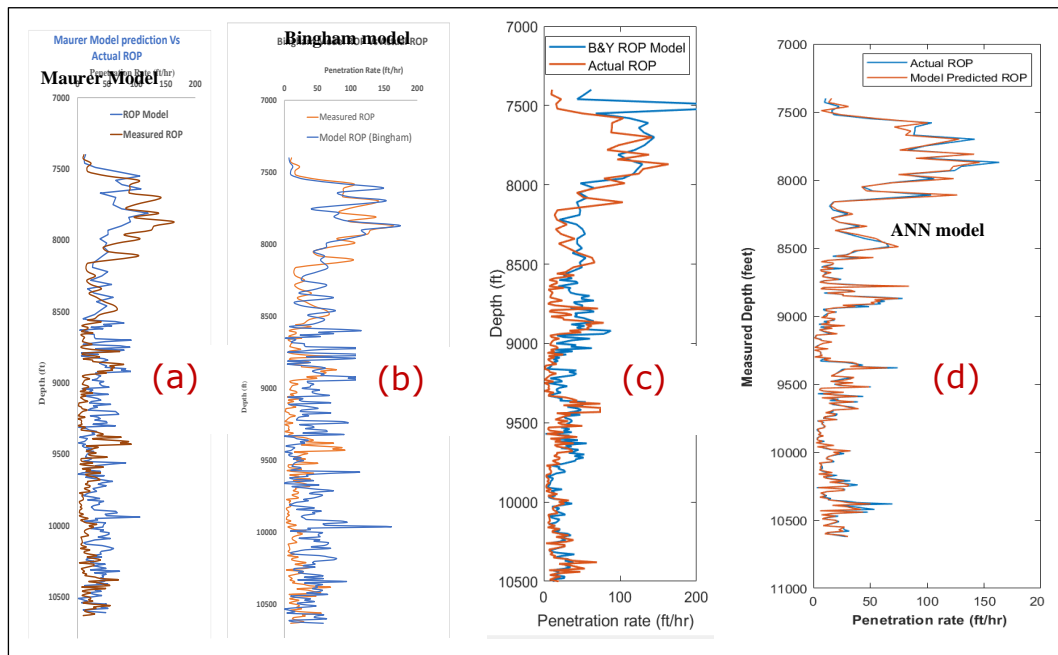


Figure 4.8 : Comparison plot of Model Predicted ROP Vs Actual ROP; (a) Maurer Model (b) Bingham model (c) Bourgogne and Young model (d) ANN model

4.5.3 Derived controllable variable versus Actual surface parameters

The summary of results of the evaluation of the most suitable variables for turning the automatic system using ANN model using the workflow in Figure 4.5 is presented in table 4.7. The analysis was performed with two set of offset datasets: Well-P05 and well-W1 to test for the repeatability of the result.

Table 4.7: Summary of Model result for selection of Tuning parameters

Dataset	Input variables in ANN	Performance Indexes
Well – P05	Case 1 – [DMSE, FET]	$R^2 = 0.985$, RMSE = 7.6
	Case 2 - [WOB, RPM]	$R^2 = 0.74$, RMSE = 28.0
Well – W1	Case 1 – [DMSE, FET]	$R^2 = 0.98$, RMSE = 5.8
	Case 2 – [WOB, RPM]	$R^2 = 0.65$, RMSE = 34.7

The evaluation examined the accuracy of using derived variables calculated from drilling parameters (DMSE, FET) referred as Case-1 and compared with using WOB and RPM expressed as (Case–2).

Dataset-W1 - Case 1 – The derivative variable (DMSE, FET) from dataset W1.

In case-1 the input data used to predict ROP includes DMSE and FET and the influence of these input parameters in the prediction of the penetration was evaluated and compared. The correlation coefficient (R^2)of predictions 0.98 and RMSE of 5.8. The plot of the actual ROP and predicted ROP shown in figure 4.9. The result shows an excellent prediction.

4.5 Modeling Results

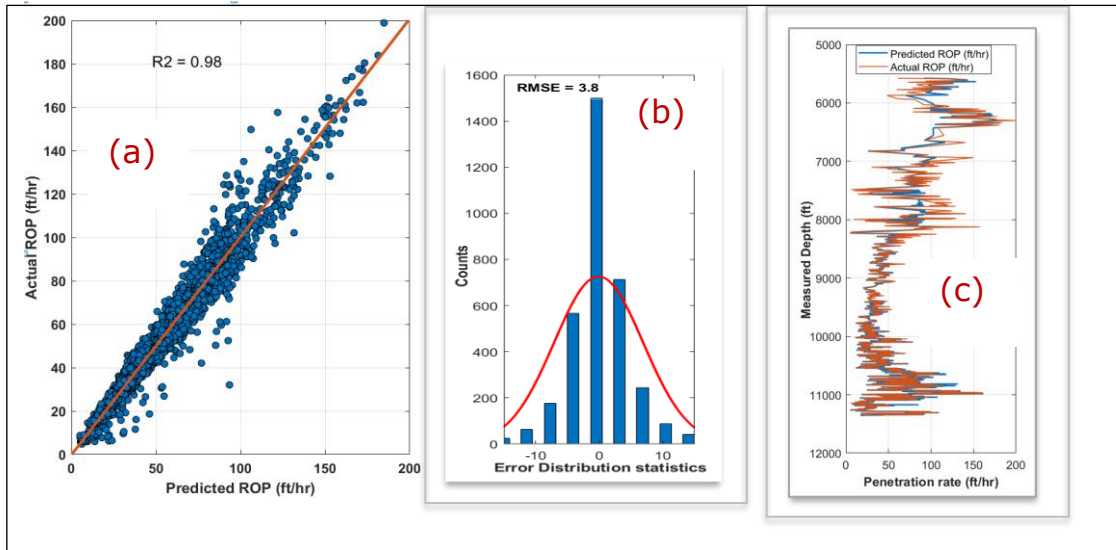


Figure 4.9 Model outputs Vs Actual data: for Case 1 (a) Crossplot Actual vs Predicted ROP (b) Error distribution curve (c) ROP Comparison Plot along hole depth

Dataset-W1 Case 2

Similarly, analysis was performed using Actual surface parameter (WOB, RPM) from the dataset W1 to predict ROP whilst keeping the model configuration and parameters the same. Figure 4.10 shows the model Crossplot, error distribution curve and the comparison plot along hole depth. The correlation coefficient (R^2) of 0.28 and RMSE of 25.36. The results show a very poor prediction accuracy as presented in Figure 4.10

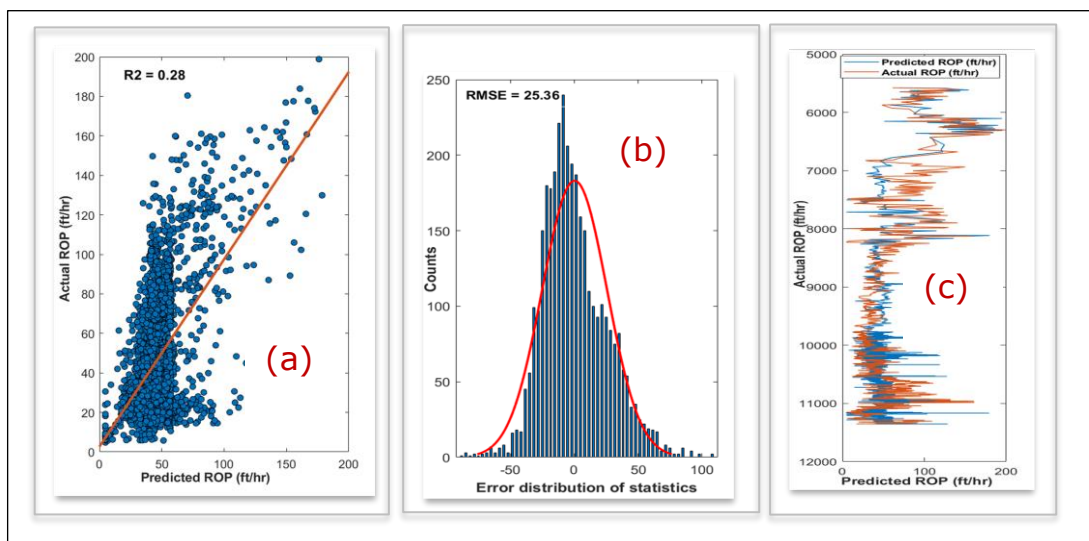


Figure 4.10 Model outputs vs Actual data: for Case 2 (a) Crossplot actual vs predicted ROP (b) Error distribution curve (c) ROP Comparison plot along hole depth for Dataset-W1

Dataset-P05 - Case 1

Further analysis was performed using a new dataset -P05 of 246 datapoints to test the repeatability of the observed trend by using DMSE and FET as input data as shown in figure 4.11 with Correlation coefficient (R^2) of 0.985 and RMSE of 7.6. The model predicted values and the measured ROP values are presented in Table 4.8

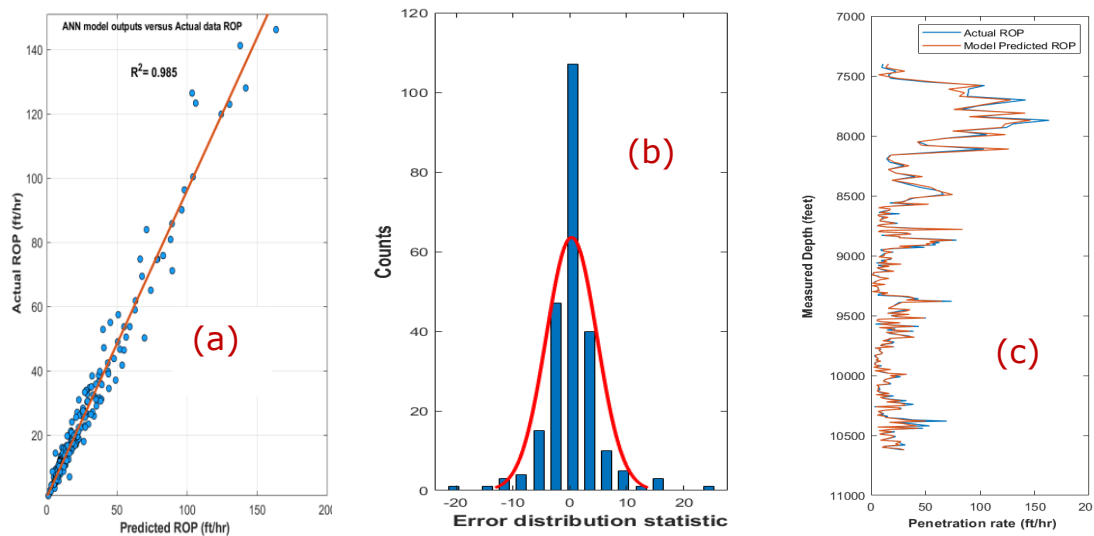


Figure 4.11: Model outputs Vs Actual data: for Case 1 (a) Crossplot Actual vs Predicted ROP (b) Error distribution curve (c) ROP Comparison Plot along hole depth Case 1 Using Dataset-P05.

Table 4.8 : Sample of predicted Vs Actual ROP using [FET, DMSE]

Depth interval (ft)	FET (Klbs)	MSE (Psi)	Actual Measured (ROP) (ft/hr)	ANN Predicted ROP (ft/hr)	Prediction quality
7460	0.308	25.85	22.83	31.82	Average
7550	0.42	14.7	50.92	59.10	Average
7780	0.48	12.23	82.96	80.15	Very good
8160	0.18	35.58	17.91	19.15	Very good
8550	0.26	22	28.70	29.40	Excellent
8670	0.13	87.60	7.73	7.21	Excellent
8790	0.12	67.78	10.06	9.05	Excellent
9000	0.15	54.66	9.24	11.20	Very good
9400	1.63	16.85	51.94	52.00	Excellent
9800	0.22	75.48	9.85	10.38	Very good
10310	0.14	32.67	25.78	28.64	Very good
10630	0.13	71.22	9.50	9.21	Excellent

Dataset-P05 - Case 2

In the same vein, using dataset-P05, surface parameters (WOB, RPM) were also used to predict ROP and the model results as shown in figure 4.12. which returned performance similar to the earlier investigation with a poor prediction value with Correlation coefficient (R^2) of 0.74 and RMSE of 28 respectively. The model predicted ROP and the actual measured ROP are presented in Table 4.9

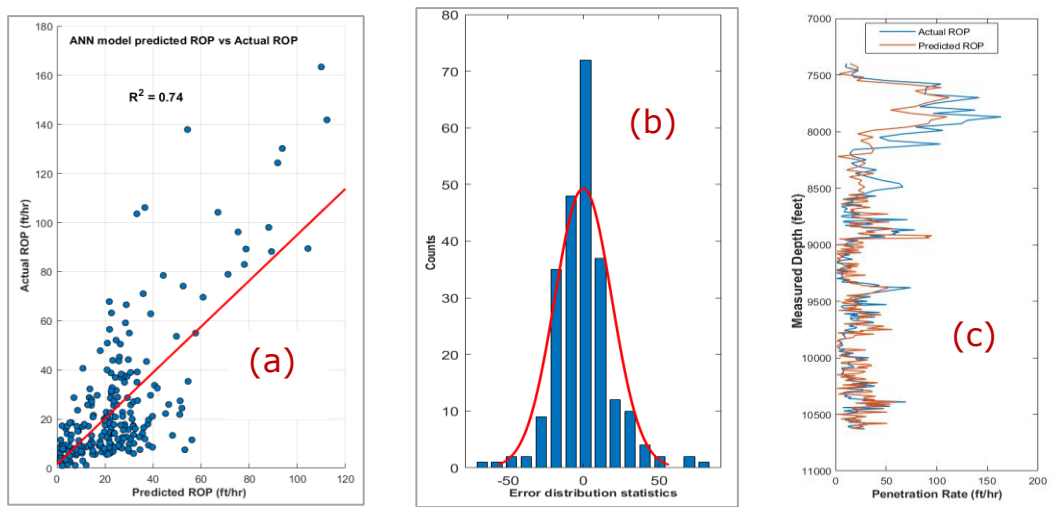


Figure 4.12 Model outputs vs Actual data: for Case 2 (a) Crossplot actual vs predicted ROP (b) Error distribution curve (c) ROP Comparison plot along hole depth for Dataset-W1

Table 4.9 Sample of predicted Vs Actual ROP data using [WOB, RPM]

Depth (ft)	WOB (Klbs)	(RPM)	Actual Measured (ROP) (ft/hr)	ANN Predicted ROP (ft/hr)	Prediction quality
7460	25	115	22.83	11.6	Poor
7550	35	125	50.92	22.92	Poor
7780	48	140	82.96	139.54	Poor
8160	48	115	17.91	23.02	Average
8550	42	115	28.70	15.05	Poor
8670	40	115	7.73	1.05	Poor
8790	36	130	10.06	22.8	Poor
9000	36	100	9.24	18.76	Poor
9400	12	130	51.94	25.23	Poor
9800	20	130	9.85	22.76	Poor
10310	37	100	25.78	21.62	Average
10630	46	115	9.50	11.80	Average

4.6 Sensitivity Analysis

Sensitivity Analysis was performed in the selection of optimum number of neurons for the hidden layers to improve the result accuracy. Results Showed that the optimum number of

4.7 Discussion Of Results

neutrons that gave the highest accuracy, which cannot be further improved was 30 neutrons. The results of the sensitivity analysis with number of neutrons at 1000 iterations performed using the derived controllable variable (DCV) at 10,20,30 and 40 neutrons respectively.

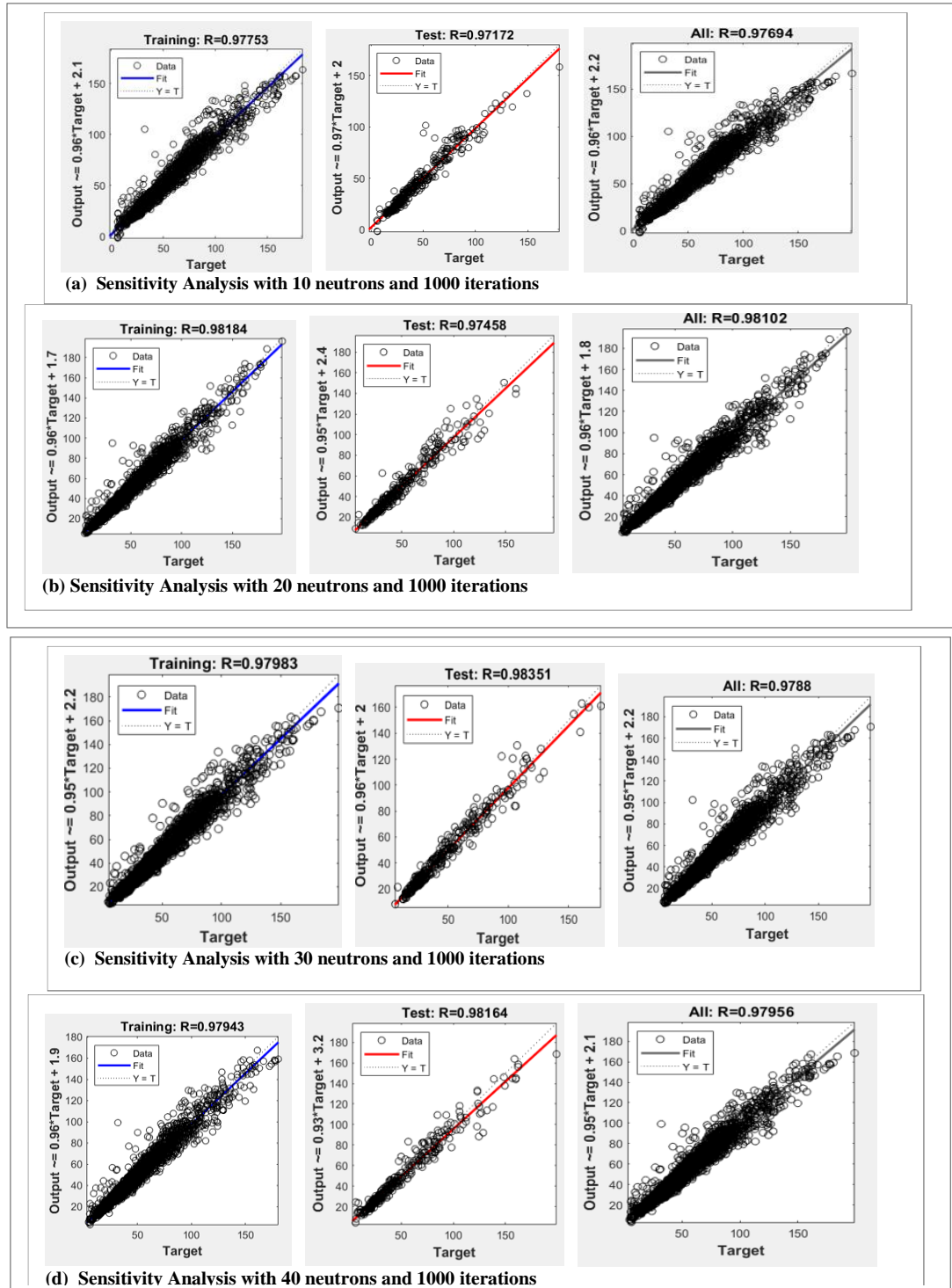


Figure 4.13 Sensitivity Analysis for the selection of optimal number of neutrons. (a) 10 neutrons (b) 20 neutrons (c) 30 neutrons (d) 40 neutrons

4.7 Discussion of Results

This study evaluated the suitability of various predictive ROP models for autonomous rotary system by comparing empirical models with data driven ANN model by using the same set of input parameters to predict output variable (ROP) using an already drilled well data. The result showed that the data driven model-artificial neural network model gave the highest prediction accuracy when compared with the physics based empirical model. This is because ANN can simulate the input and output relationship with adaptive information processing systems, establishing a functional feature vector based on learning from the past events. Thereby adjusting the weights and bias based on features learned from the data. But, In the physics Based empirical model the functional relationship of input parameters and output data is constant hence requiring tuning empirical constants to fit the output data, the empirical model are likening to a data fitting model which tries to fit a constant coefficient data through a heterogenous formation. Based on the result, the ANN are able to build associations and mappings between data, resulting in high predictive capability, it has proven its capability to be used in autonomous self-optimizing predictive ROP model.

The study further investigated the suitability of tuning parameters by determining appropriate combination of tuning parameters for controlling the topdrive and hoisting system in an autonomous rotary drilling system. The adaptive self-optimizing ability of the system was investigated by evaluating the effect of the tuning parameters with changes in penetration rate across the heterogeneous rock. The ANN model was designed for two input parameters each acting as a tuning parameter for the topdrive and the draw works hoisting system respectively. Similarly, a predictive optimization evaluation with two sets of tuning parameters; the actual surface operating parameter [WOB, RPM] and their derived energy variables of [DMSE, FET] and tested their effectiveness as a controller variable. The performance of the actual surface parameter (ASP) [WOB, RPM] in the prediction of ROP was very poor, even though these parameters were the input parameters used in the actual drilling operation. The poor

preformation is an indication that these variables do not maintain a direct linear relationship with ROP as the influence of downhole conditions such as wellbore tortuosity, borehole drag influence the performance of the input parameters. [Armentia \(2008\)](#) identified these conditions for inefficient drilling. Therefore, ASP are not effective as an adaptive input parameter in autonomous system . Nevertheless, the performance of the derived energy variable (DCV) played an important role in effectively prediction of ROP with a high level of accuracy with a well-established relationship with drill rate performance thus proven to be an effective adaptive input parameter in autonomous system. It was observed that the accuracy of the model depends on the quality and number of datapoints used in the training the model. Accuracy increases with the increasing number of datapoint available. The summary of the result is presented in Table 4.8

4.8 Summary of Results

This worked focused on modeling and predicting performance of ROP model The summary of the results are presented in Table 4.10

Table 4.10 : Summary of results for ROP modeling.

Research Objectives	Options	Variable / parameters	Current practice	Research Results & Contribution
Evaluation of dynamic relationship between drilling Input and output parameters	Evaluating dynamic relationship between WOB, RPM with ROP	WOB, RPM	Increase in WOB, RPM denotes, increase in energy in the drilling system which of	The non-linear relationship between WOB & RPM are susceptible to environmental factors such as vibration, formation change, flounder points.
	Evaluating dynamic relationship between DMSE, FET with ROP	Derivatives of WOB, RPM	Increase in WOB, RPM denotes, increase in energy in the drilling system which o	Decrease in DMSE and Increase in FET results in increase in drill rate. This is not affected by environmental factors and always holds true
Modeling and prediction of ROP of autonomous drilling system	Physics Based Models (PBM)	Maurer model Bingham model B&Y model	Physics Based Models are (Maurer, B&Y, Bingham). In use, intermittently halt drilling to perform drill-off test to estimate formation coefficient	Maurer [$R^2=0.50$, RMSE=30] Bingham [$R^2= 0.51$, RMSE=37] B&Y [$R^2= 0.70$, RMSE=28] PBMs are data fitting model as formation coefficient are required to fit the model as functional relationship of input & output is constant
	Data driven model	ANN Model	Recent and proven technology but low application in drilling operation. Suitable for drilling automation with the benefit of the big drilling data.	ANN [$R^2= 0.98$, RMSE=5.8] ANN models offer the best solution with dynamic functional association between input and output as the model learn by feature engineering from past events
Real-time drilling input variables vs derived variables in optimizing performance of an autonomous system	Tuning input for ANN[WOB, RPM]	WOB, RPM	Several models with 4 – 8 input drilling variables which is not suitable for autonomous system	Model performance result [$R^2= 0.74$, RMSE=28]
	Tuning input for ANN [DMSE, FET]	DMSE, FET	The concept first introduced in this research.	Model performance result [$R^2= 0.98$, RMSE=7.8] Better accuracy and low prediction error

4.9 Section Summary

This research aimed to identifying appropriate tuning parameters and its predictive performance for self-optimizing autonomous rotary drilling system using artificial neural network with actual surface drilling parameters and derived controllable energy parameters. The study used a drilling data from a previously drilled well to develop a model for an autonomous drilling system. Based on the results of this study the following conclusions are made as follows:

1. Derived controllable variables; DMSE and FET have been proven to be suitable tuning parameter for autonomous rotary drilling system as it showed more accurate and adaptive prediction of drilling rate of penetration with ANN.
2. The application of the energy variables is supported by the strong relationship that exists between the derived input variable (DMSE) and FET with drilling output ROP.
3. The accuracy of the machine learning models is a function of the data quality and the size of training dataset used in model training.
4. Understanding of feature engineering is vital to the accuracy of machine learning models since the number of input parameters used entirely determine the accuracy of the predicted outcome from the model.
5. The non-linear relationship between WOB & RPM are susceptible to environment factors such as hole cleaning, formation strength, wellbore tortuosity and inexplicit therefore inadequate to be used alone as a tuning parameter for a autonomous system.
6. Combination of both the physic-based model and machine learning techniques would improve the processing speed of the prediction by using the feature vector from the physic-based model in the machine learning modeling

Chapter 5

Real-time Prediction of Rock UCS and Maximum ROP Model

5.1 Introduction

Geomechanical properties of rock such as the unconfined compressive strength (UCS) plays a significant role in oil or gas well construction process, especially in wellbore stability analysis, bit selection and evaluating the performance of an autonomous rotary drilling system. The UCS of rocks is defined as the maximum compressive stress that the rock can endure before breaking down when uniaxial loading is applied Chau and Wong (1996). Rotary drilling operation involves bit-rock interaction, with failure of the rock occurring when the resultant bit stress is more than the rock strength. In current oilfield practice, UCS data is used for bit selection, real-time wellbore stability analysis, estimation of optimal time for roller cone bit trip, design of enhanced oil recovery (EOR) procedures and reservoir subsidence studies Nabael and Shahbazi (2012).

5.2 Direct Methods for the estimation of rock strength

There are direct and indirect methods for the estimation of rock strength along a drilled wellbore. The direct technique includes uniaxial, triaxial, point load test (PLT), Schmidt rebound hammer test, scratch test, indentation, and thick wall

5.1 Real-time Prediction of Rock UCS and Maximum ROP Model

cylinder (TWC) test. Although these methods are affected by the test condition and core sample preservation, they deliver an accurate and consistent result, where the triaxial test is considered to have the highest accuracy. The laboratory techniques have their limitations that restrict their application such as the high cost of coring operation and limited number of samples collected, which often results in a discontinuous measurement. In addition, these tests are only representative of the cored interval and cannot produce a continuous profile of the rock strength along the drilled wellbore Abdulraheem et al. (2009). Fig.5.1 shows the Schematic of the unconfined compression test set-up as illustrated in Gullu, and Hazirbaba (2010)

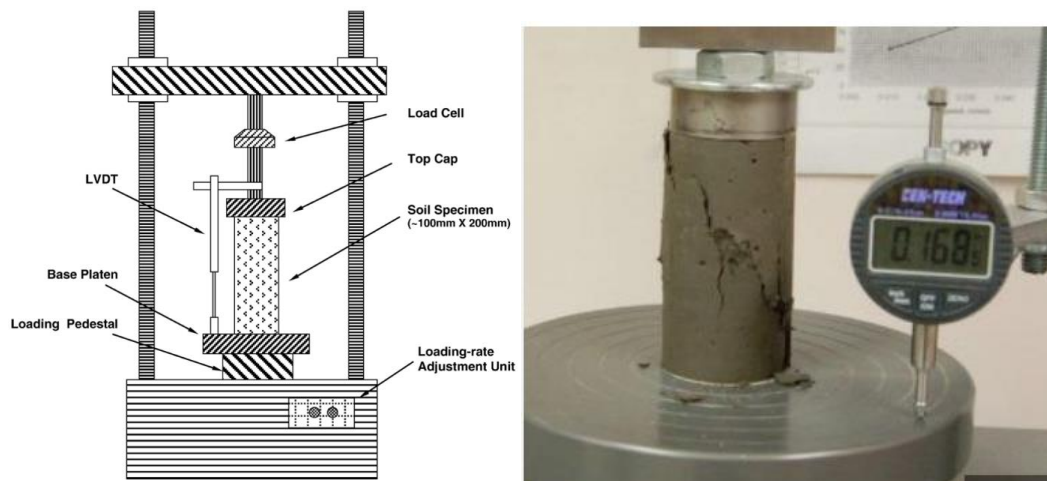


Fig. 5.1. Schematic of Unconfined Compression Test Setup. adopted from Gullu, and Hazirbaba (2010)

5.3 indirect Methods for the estimation of rock strength

Indirect methods of using derived correlations were developed to fill the missing gaps between the rock mechanical properties using petrophysical well-log data. The use of empirical correlation that interrelates UCS to rocks petrophysical properties that can be measured directly or indirectly from wire line logs can be used for estimation of UCS. Trixier et al. (1973) proposed a correlation for UCS using the rock strength

5.4 Proposed Model of UCS estimation using Drilling data

Most of these models in the literature utilizes sonic transit time (Δt) as seen from equations [2.15– 2.20]. Whilst other models were based on the porosity values (\emptyset) to predict UCS values. Ideally, each formation type responds in a different way to produce logging parameters. Therefore, formations are grouped into three main categories of sandstone, shale, and carbonates. For each grouping, specific correlations have been developed. However, there is no universal correlation that can predict UCS for all rock types (Mostofi et al. (2011))

5.4 Proposed Model of UCS estimation using Drilling data

Most models in literature used some logging data, which may not be available while drilling especially in the top-hole section as logging while drilling (LWD) is not usually logged on most top-hole section of wells. Even when the LWD is present in the bottom hole assembly (BHA), it is placed tens of feet above the bit and therefore does not reflect the instantaneous response of the rock-bit interaction that occurs when formation is been penetrated in real-time. This model explores the application of machine learning algorithms with basic real-time instantaneous drilling data in the prediction of rock UCS.

5.5 Research approach

In this study, new models were developed to estimate UCS values of the downhole formations while drilling using five ML tools including the artificial neural network (ANN), CatBoost (CB), Extra Tree (ET), Random Forest (RF) and Support Vector Machine (SVM). The developed models used the mechanical drilling parameters as feed inputs to predict the output, UCS values. The UCS is not one of the drilling parameters that can be measured during the drilling operation. However, the UCS

5.5 Research approach

value can be estimated using sonic log data and Neutron porosity log. Numerous correlations have been developed to predict the UCS of the rock as a function of sonic transit time (Δt) and formation porosity (\emptyset), as presented in **Table 2.4**. But often these logs (Sonic, NPHI) are ran only in the production section and rarely in the top-hole section of the well. Therefore, a model that can predict UCS using readily available drilling parameters has become essential. A general stepwise procedure used in the study is illustrated in **Fig.5.2**

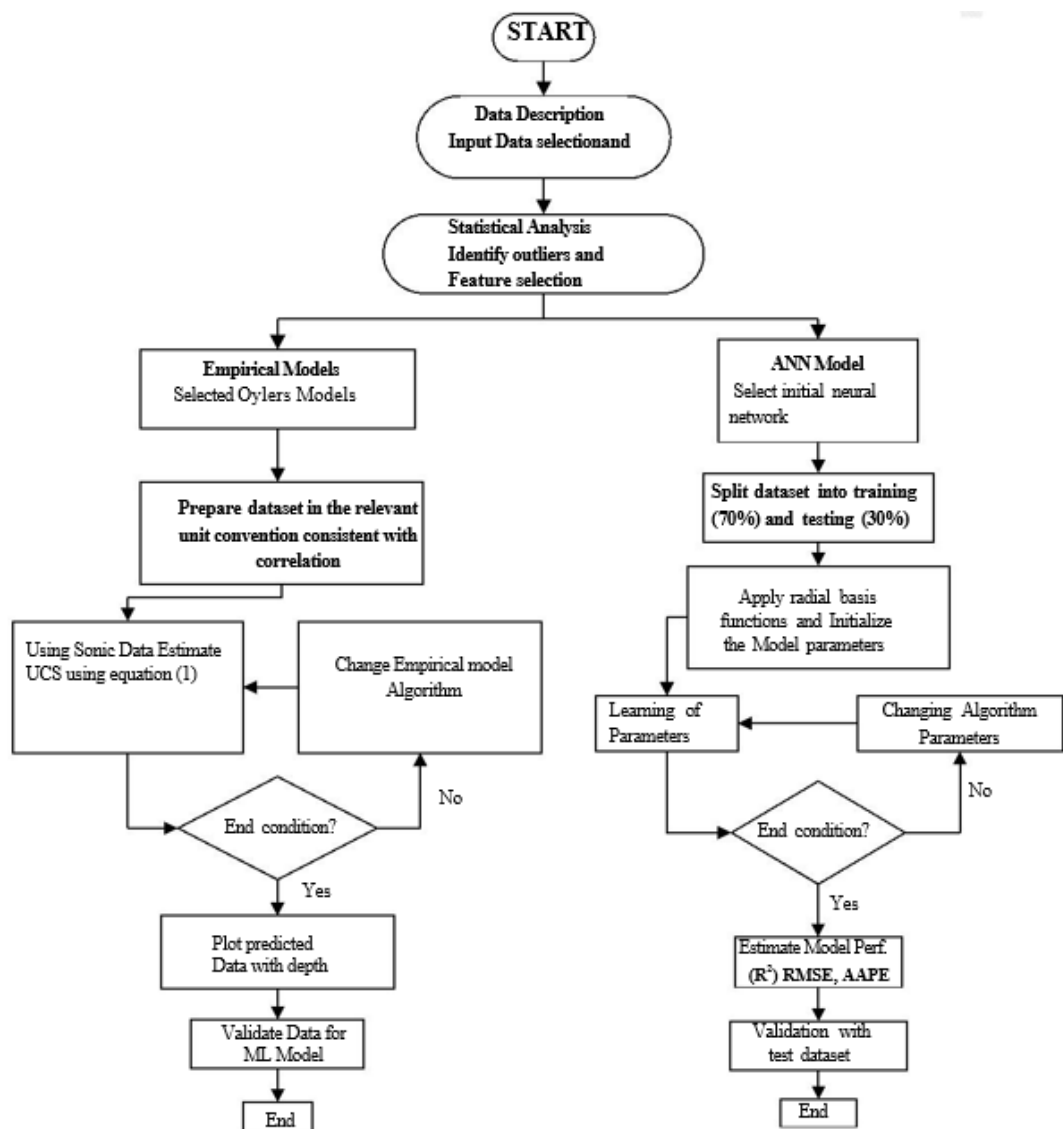


Fig.5.2: Research Flowchart showing the step-by-step approach

5.5 Research approach

Step 1: Data description and transition

The set of datasets including the drilling data, the formation pressure and depth from two wells were collected representing a composite rock formation. A dataset of 1157 points included GR, ROP, WOB, TOR, Rotat, DTS, RHOB, neutron porosity (NPHI) were cleaned by deleting the unrepresentative values such as -999 values, and NAN (not a number) removed. The drilling data were utilized as inputs to feed the model to predict unconfined compressive strength (UCS) of the rock as output. The data was further transformed to conform to the required unit required by the Physics based empirical model used to estimate the UCS from sonic data. The minimum data requirement includes WOB, Rotat, TOR, ROP and GR which are always readily available irrespective of the hole section.

Step 2: Statistics and graphical analysis was performed to identify and eliminate outliers from the dataset. Statistical analysis was performed on the field dataset, and it showed that the data covered a broad range of the inputs and the output as presented in Table 5.1.

Table 5.1: Statistical analysis describing the ranges and distribution of the used data

Statistical Parameter	WOB [Klbs]	RPM (Rotat) [rev/min]	TOB [Kft-lb]	ROP [ft/hr]
Minimum	1.17	49.6	4.57	12.81
Maximum	27.84	130.91	22.54	130.41
Range	26.67	81.30	17.97	117.60
Mean	16.17	129.31	18.33	74.4170

Step 3: Input and Output Relationship

To identify the strength of the relationship between the output (UCS) and the input parameters, the relative feature importance analysis was performed. This section of the study is devoted to investigating the influence of the input features of real-time drilling parameters on the predicted target variable (UCS)

5.5 Research approach

The most commonly accessible drilling parameters including weight on bit (WOB); Gamma ray (GR); pump pressure (Pp); rotary speed (Rotat); rate of penetration (ROP); equivalent circulating density (ECD); and mud flow rate (MF) Down hole pressure (DownP), are considered in this study. In the analysis, the relative feature importance analysis tool offered by CatBoost is utilized. The outcomes provided by this tool is presented in **Fig.5.3**. As shown in the figure, the three most impactful input parameters are: down hole pressure, weight on bit, and gamma ray.

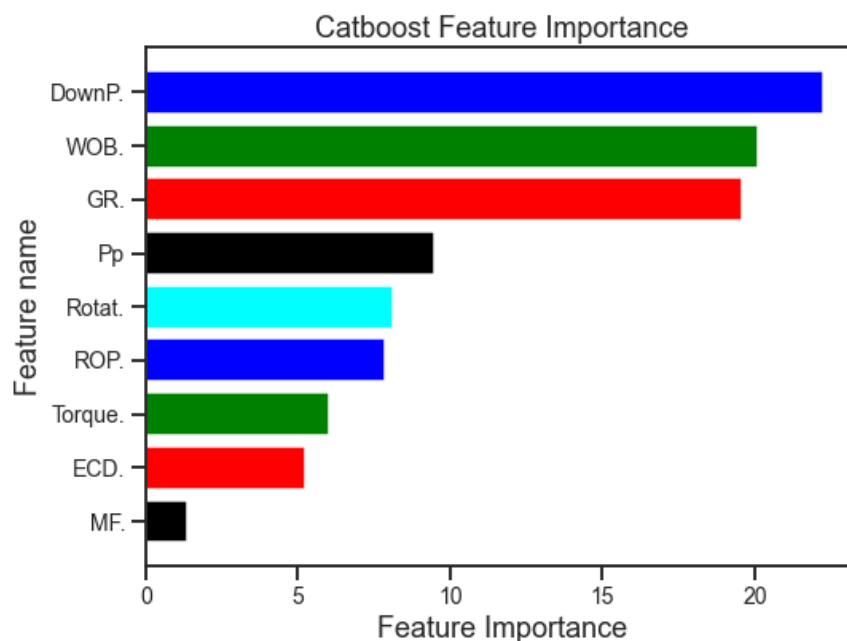


Fig.5.3 — Relative Feature Importance Plot Generated by CatBoost Model

The study also revealed that mud flow rate has minor and insignificant impact on the UCS prediction. Overall, CatBoost algorithm uses the significance of the selected drilling parameters in calculating uniaxial compressive strength (UCS). In a similar vein, the scatter matrix of selected features in the experimental database from python experimental database is presented in **Fig. 5.4**. The feature importance from the matrix shows that ROP, WOB, Torque, rotary speed are the most influential parameters.

5.5 Research approach

This observation was found to be consistent with the finding from previous study Gowida et al. (2021), where the rate of penetration (ROP) showed the highest influence on UCS prediction. Based on the feature importance revealed from these two studies, Four input parameters were selected for the ANN model including WOB, ROP, Torque and rotary speed (Rotat). Downhole pressure was neglected since this parameter is not always available unless an annular pressure measuring tool was ran in the bottomhole assembly (BHA).

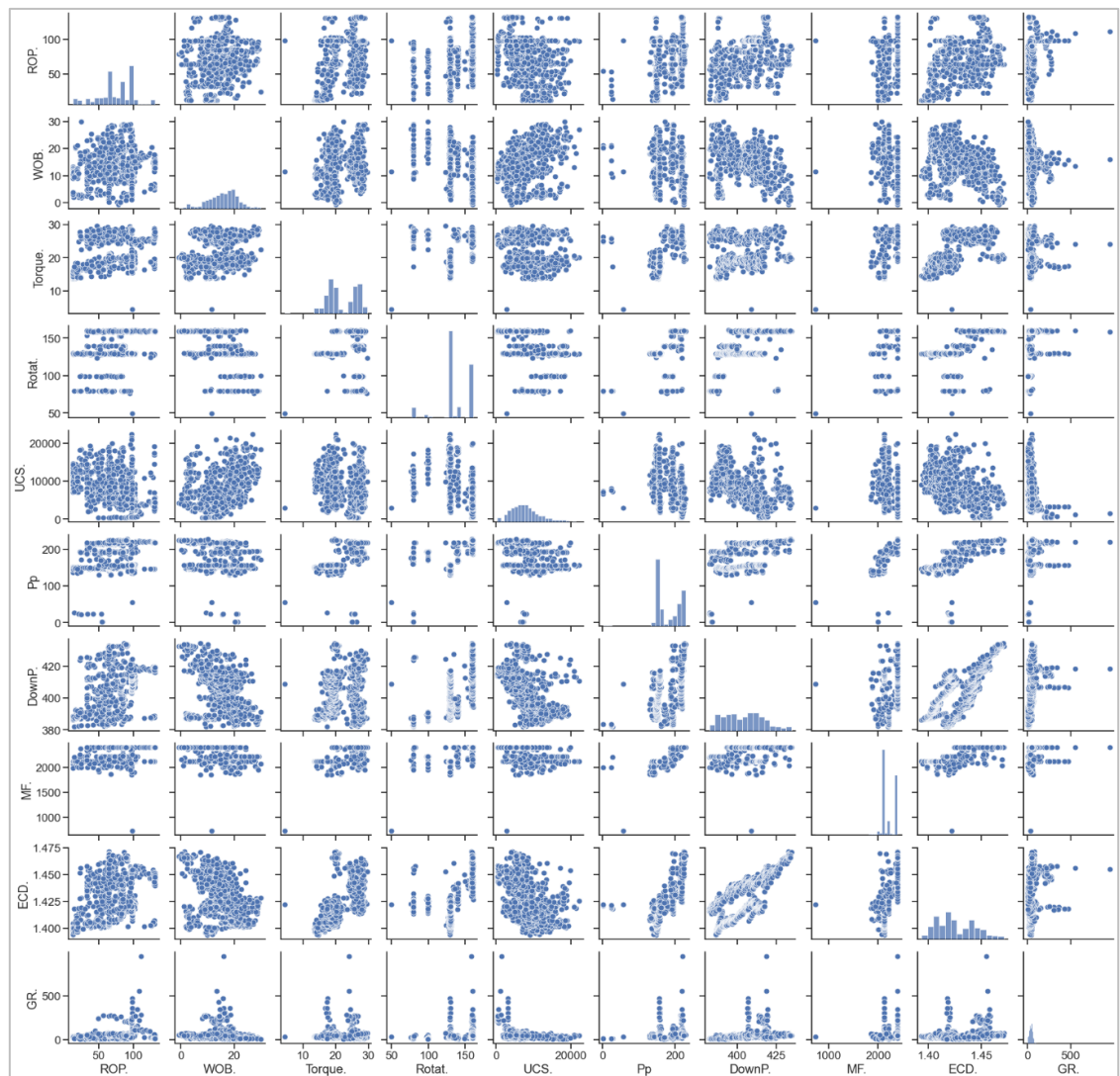


Fig. 5.4— Scatter Matrix of Selected Features in the Experimental Database

Step 3: Estimate UCS from established empirical physics Based model.

As mentioned earlier, UCS is not a measured parameter, estimated values of UCS were obtained from three established models as shown in **Fig.5.6**. In this study, the prediction of UCS value were obtained using three different correlations (Oyler et al. 2010) Mostofi et al. (2011) and Nabaei and Shahbazi (2012). The comparison of UCS predictions is shown in **Fig. 5.6**. The (Oyler et al. 2010) UCS prediction has a greater spread and fairly agreed with the other correlations and therefore consequently chosen for ML output target variable.

Step 4: ANN model configuration.

The study investigated a new ANN model developed using basic drilling parameters to predict UCS. The model was developed in MATLAB using feedforward network with the input parameters to estimate UCS. The ANN model was constructed with input layer, one hidden layer and an output layer. **Fig.5.5** shows a schematic diagram for the developed network architecture. The model development involved three key stages: the training process, the testing process, and the validation process. First, the collated dataset was randomly split into two sets; training and testing set for building the model. **Table 5.2** shows the ANN configuration and tuning parameters.

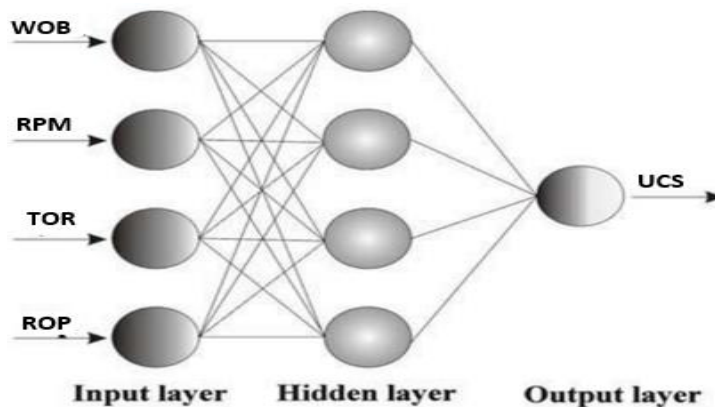


Fig. 5.5 — Schematic of ANN network Architecture

5.5 Research approach

Table 5.2: ANN algorithm configuration and tuning parameters

ANN Parameters	Range of values	Optimal Value
Number of hidden layers	1	1
Number of neurons	1-20	10
Type of network function	FEED FORWARD	FEED FORWARD
Type of transfer function	PURELIN	PURELIN
Maximum no. of iterations	1000	1000
Training Function	Levenberg	Levenberg
performance gradient	15.4	15.4
Maximum value for Mu	0.00100	0.00100

Step 5: The dataset for ANN modeling was divided in the ratio of 70:30 for training and testing. A total of 1150 datapoints were used for well-1. The unseen dataset from Well-2 (560 points) was used in the model validation. The input data includes WOB, rotary speed, torque, and rate of penetration.

Step 6: Estimate model performance.

The quality of the model was measured using different performance assessment indicators to evaluate the goodness of fit between the actual and the predicted values using the coefficient of determination (R^2) expressed as equation (5.9), The root mean squared error (RMSE) between the actual and the predicted values and the Mean average error (MAE).

5.6 Results and Discussion

The stepwise procedure shown in **Fig 5.2** was applied to the obtained results for physics based empirical model and the ML algorithms for training and testing of the proposed algorithms. A concise presentation of the results is presented below.

5.6.1 Result of estimation of UCS from established empirical physics Based model

The prediction of UCS using the empirical models proposed by Oyler et al. (2010), Mostofi et al. (2011) and Nabaei and Shahbazi (2012) are shown in **Fig.5.6**. All the three models showed sensitivity to changes in the formation hardness.

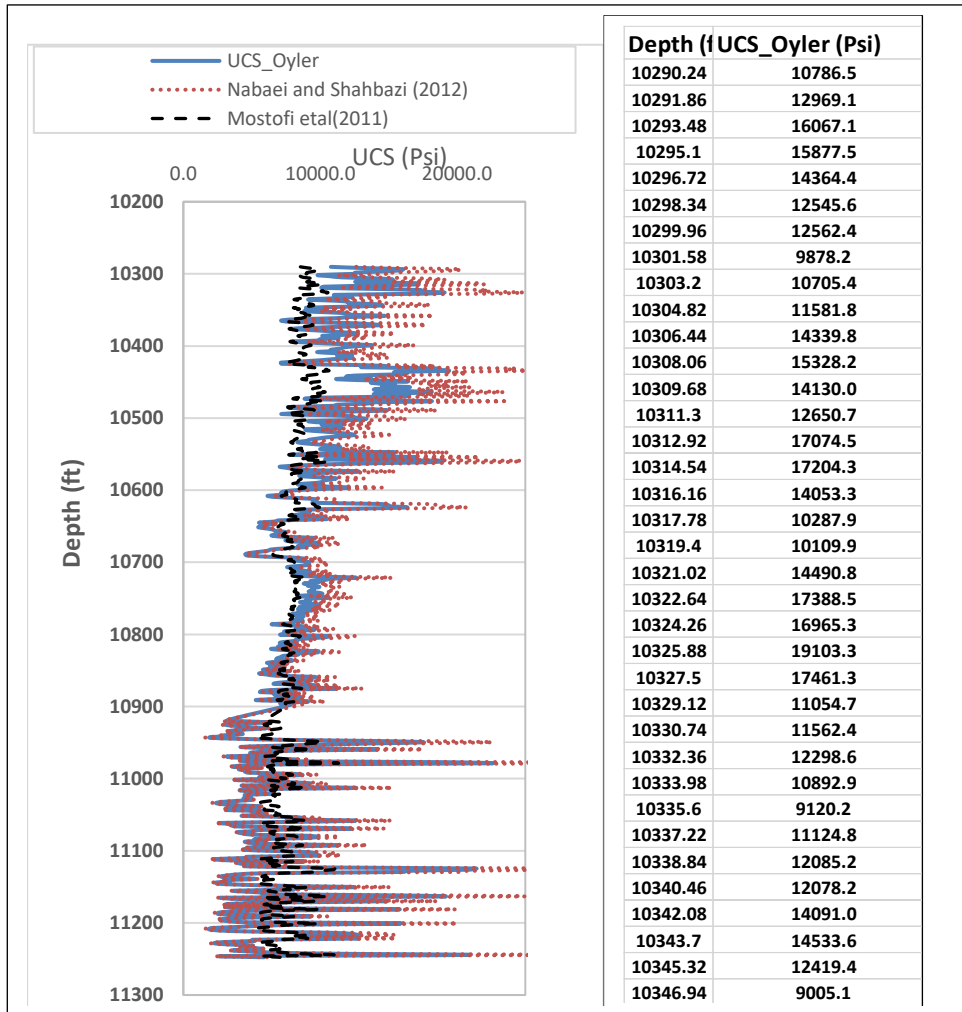


Figure 5.6 : Plot of estimation of UCS from established empirical based model

Whilst the Mostofi et.al (2011) model gave conservative prediction, Nabaei and Shahbazi (2012) showed a highest prediction value with intermittent peak values. However, the prediction of the Oyler et.al (2010) provided an average and good spread prediction therefore was selected for the ML prediction.

5.6.2 Results of UCS prediction from Machine Learning Algorithms

The prediction performance of the five ML models was evaluated by comparing their predictions to the measurement derived from the target dataset. The assessment metrics consist of R^2 for training and test data sets, Mean Squared Error (MSE), Mean Absolute Error (MAE), and Root Mean Square Error (RMSE). These metrics were utilized to compare the ML models selected as the best-performing model. Moreover, correlation coefficient R^2 was calculated for the training data set to assess the training efficiency and check the generalization capability of the proposed model. The performance summary of the five algorithms is presented in **Table 5.3**

Table 5.3: The Performance Assessment of six ML Algorithms on Training and Test Data

Model	Training Accuracy (R^2)	Test Accuracy (R^2)	MAE	MSE	RMSE
SVM-R	0.7473	0.6331	0.08	0.0111	0.1053
Random Forest	0.8528	0.6754	0.06	0.0098	0.099
Extra Tree	0.8638	0.5994	0.08	0.0121	0.110
CatBoost	0.9741	0.7012	0.06	0.009	0.095
ANN	0.85	0.77	0.035	0.303	0.0420

As presented in the table, most of the ML algorithms (SRM-R, Random Forest, CatBoost, and Extra Tree) attained relatively good accuracy during the training process. However, the algorithms (SRM-R, Random Forest, and Extra Tree) failed in predicting UCS values by providing an average R^2 of 0.63 on independent test dataset. A possible explanation for this average prediction accuracy is that the nature of the models' formulation necessitates sufficient data as input features to create a generalized model. Catboost model, algorithm gave high accuracy on the training data with R^2 of 0.97 while an acceptable accuracy ($R^2 = 0.70$) was achieved on the test dataset. Similarly, the ANN model provided a high accuracy on the training data with

R^2 of 0.84 while an acceptable accuracy of R^2 of 0.77 on the test dataset. As a result, the CatBoost and ANN models are considered as the best-performing models compared to the other ML algorithms in forecasting the unconfined compressive strength of the rock (UCS). The disparity in accuracy between the training and testing model assessment occurs due to the provided data for training process being insufficient for developing a generalized model. Moreover, the nature of the relationship between the input features and predicted variable is non-linear correlation. A linear fitting plot is created between the predicted and the actual UCS values for both training and test dataset. The cross-validation plot for CatBoost is presented in **Fig.5.7**. Furthermore, the measured versus predicted values along the wellbore depth is plotted with sample points as shown in **Fig.5.8**. In the same vein, linear fitting plot created between the ANN predicted and the actual UCS values for training and test dataset is presented in **Fig.5.9**. Likewise, the measured versus predicted values along the wellbore depth plot with sample values from the ANN model is shown in **Fig.5.10**. It is important to mention that the accuracy of both models can be greatly improved by the addition of logging datapoints such as logs (Sonic, NPHI, RBOH) when available, especially in the lower productive section of the well as per the logging program of the section. When these additional data points are added the model would need to be re-trained with all the input datapoints prior to using the model for prediction which greatly improves the accuracy of the model. In order to appreciate the prediction accuracy, a snapshot of the prediction at some depths.

5.6.3 Model result of UCS from CATBoost Algorithm

Summary results of the catboost model is presented in Fig.7 and Fig.8 below.

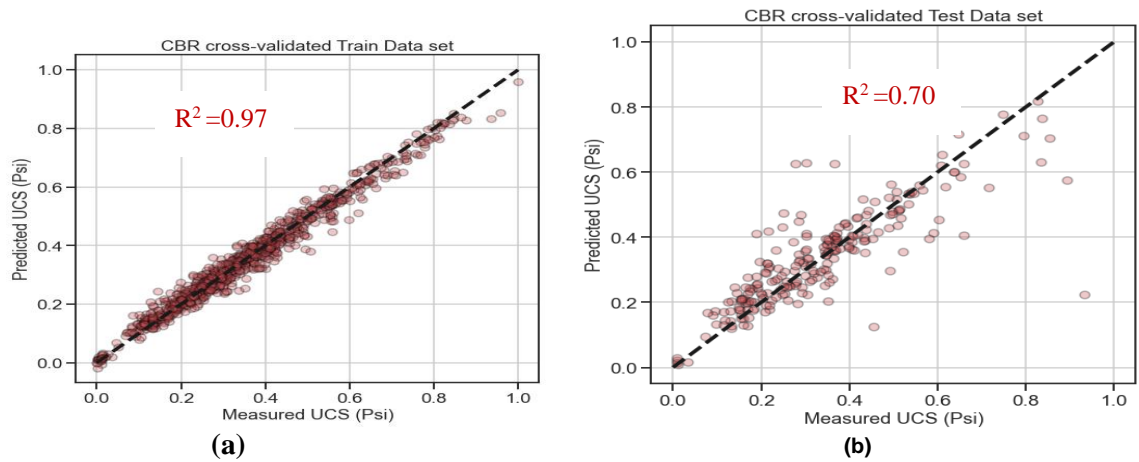
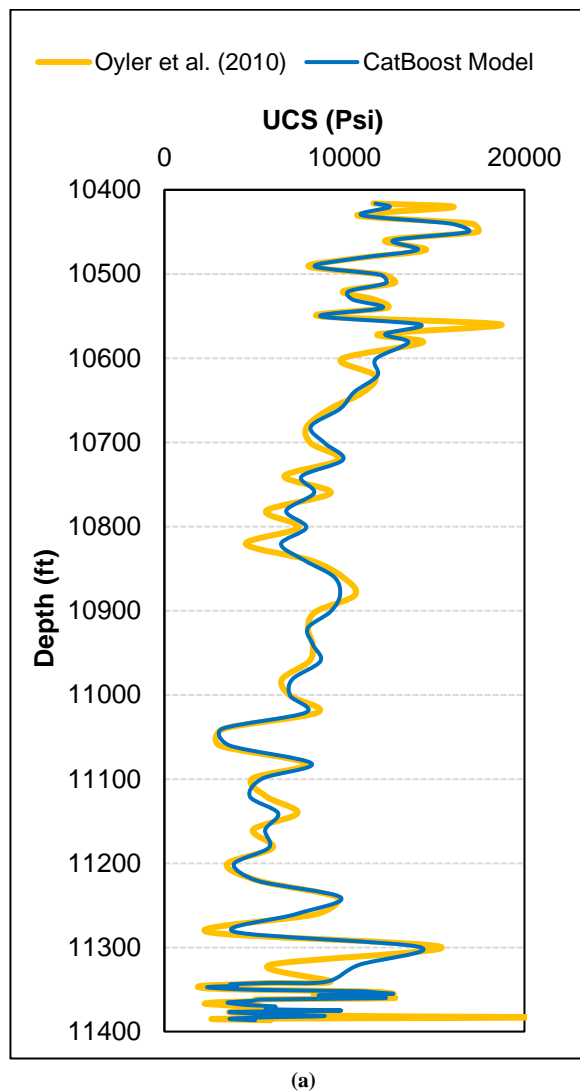


Fig.5.7— cross-validation plot between measured and predicted UCS value using Catboost Model: a) training, and b) testing dataset.



Depth (ft)	Oyler (2010) UCS (psi)	CatBoost UCS (Psi)
10416	11607	11727
10430	10705	10998
10450	17388	16884
10460	12299	12723
10471	14534	14061
10481	10737	10730
10491	8016	8357
10501	12157	11996
10521	9913	10237
10530	11681	10462
10540	12356	12119
10550	8577	8668
10571	11920	12263
10621	11694	11833
10640	11052	10542
10660	9216	9768
10681	7914	8133
10701	8137	8910
10721	9690	9923
10740	6664	7620
10781	5655	6765
10801	7476	7884
10840	8137	7798
10860	9908	9435
10881	10591	9754
10921	7968	7962
10940	8237	8254
10960	8038	8661
11001	6993	6989

Fig. 5.8— Measured and predicted UCS value with depth using Catboost Model: a) plot and b) sample values

5.6.4 Model result of UCS from ANN Algorithm

Summary of results of the ANN model is presented in Fig.9 and Fig.10 below.

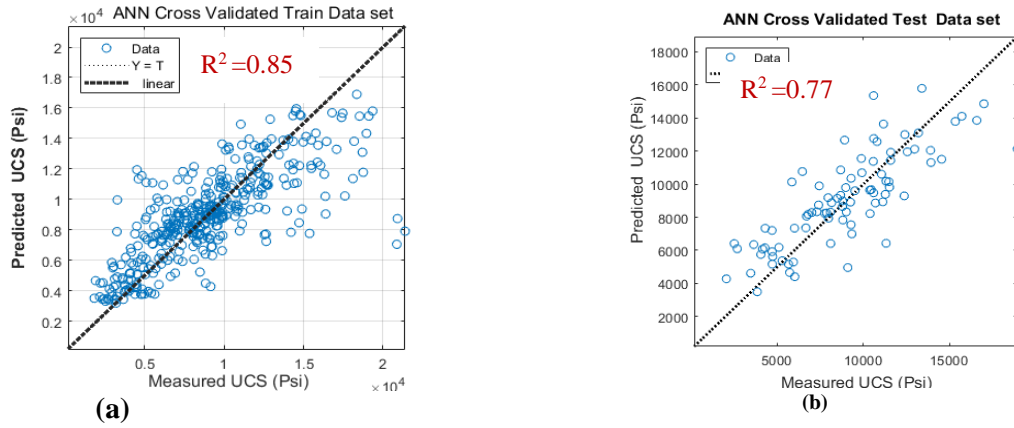


Fig5.9— cross-validation plot between measured and predicted UCS using ANN Model: a) training, and b) testing dataset

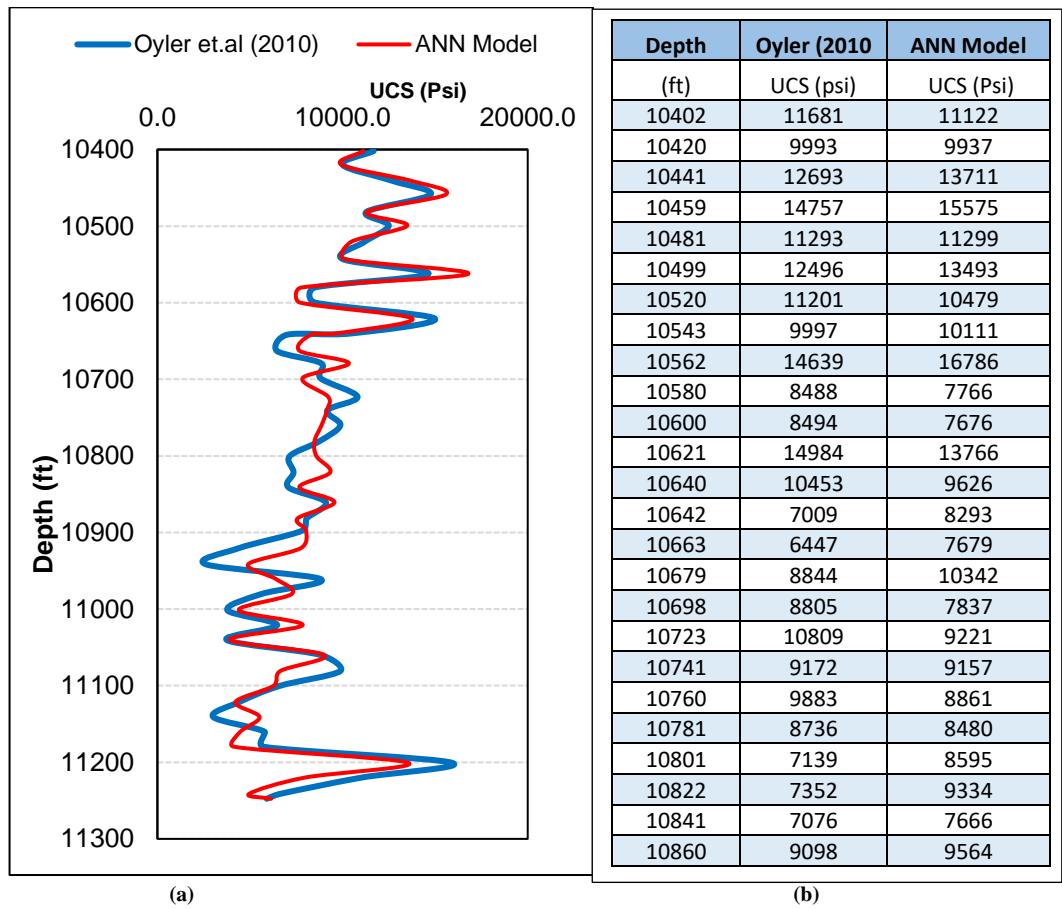


Fig. 5.10— Measured and predicted UCS value along wellbore depth with ANN Model: a) plot of values, and b) sample values.

5.7 Application of instantaneous UCS estimation in maximum Achievable ROP Model

Drilling operations are performed without knowledge of expected ROP across the various lithologic zones and therefore rarely performed at an optimum level. This is mainly due to lack of knowledge of what is the expected optimum value, across the different lithologic zone. In addition, the industry philosophy of setting performance benchmark by using the first drilled wells in the field have several setbacks; in a newly developed field there are not enough offset wells for healthy comparison, even when it exists, the drilling practices may not represent the good engineering practices and the technology used may not be the optimal solution to the application. Therefore, this developed model for estimation of instantaneous apparent unconfined compressive strength (UCS) of the rock at the bit, will remove the much uncertainty and subjectivity regarding rock strength and drillability. The new method enables improved decision whilst drilling in many areas including determination of formation tops, early detection of formation change and adjusted parameters and formation stratigraphic sequence. The model further provides an estimated maximum achievable ROP across the different heterogenous formation, enabling a comparable benchmark between the autonomous system performance and the maximum achievable limit.

5.7.1 Determination of Optimum ROP Baseline

An embodiment that relates to the Quality of Experience (QoE) at assessing the quality perceived by a user, while experiencing a service from a new technology, is the availability information of the technical limit in comparison to the actual performance of the model. The possibility of a proposed model for UCS estimation using drilling data. The application of the instantaneous UCS in the determination of the optimum

5.7 Application of instantaneous UCS estimation in maximum Achievable ROP Model

achievable ROP is based on the principles which state that the amount of energy required to drill a given formation depends on the unconfined compressive strength of the rock. Earlier work of Teale (1965), Amadi and Iyalla (2012) showed that DMSE is close to UCS at maximum efficiency. Therefore, optimum ROP could be derived from DMSE equation (5.1)

$$ROP_{opt} = \frac{2538 * W}{Dia^2 * DMSE} \quad (5.1)$$

The instantaneous penetration rate (ROP) in ft./hr, DMSE in Kpsi, the bit diameter in inches (Dia) and the power input to the drilling process in horsepower (W) is define by equation (5.2)

$$W = (T * RPM) / 5252 \quad (5.2)$$

where T is in ft-lb and the RPM in rev/min. Recent work has defined that UCS can be expressed in terms of DMSE as in equation (5.3) Loeken et'al(2018)

$$UCS = 0.35 * DMSE \quad (5.3)$$

Subsequently optimum penetration can be expressed as

$$ROP_{opt} = \frac{1.05 * Tor * RPM}{Dia^2 * UCS} \quad (5.4)$$

The optimum penetration rate that can be reasonably be expected from the drilling system, in other words the ROP that would be achieved with best operating practices optimum equipment, operating and right operating parameters, if no significant drilling problems occurred. Using the dataset W-1 used in the UCS prediction. The optimum ROP curve was defined with the actual measured ROP compared as shown in Figure 5.11. The baseline ROP performance curve shows the disparity of the actual performance compared to estimated technical limit. This will aid the operator to

5.7 *Application of instantaneous UCS estimation in maximum Achievable ROP Model*

evaluate the performance of the autonomous drilling system. It is expected to stay as close as possible to either the upper (green) or lower (red) optimum baseline across the different lithologies. Estimation of the expected performance improvement can be performed by comparing the average of the actual measured ROP with the Lower Baseline as shown below.

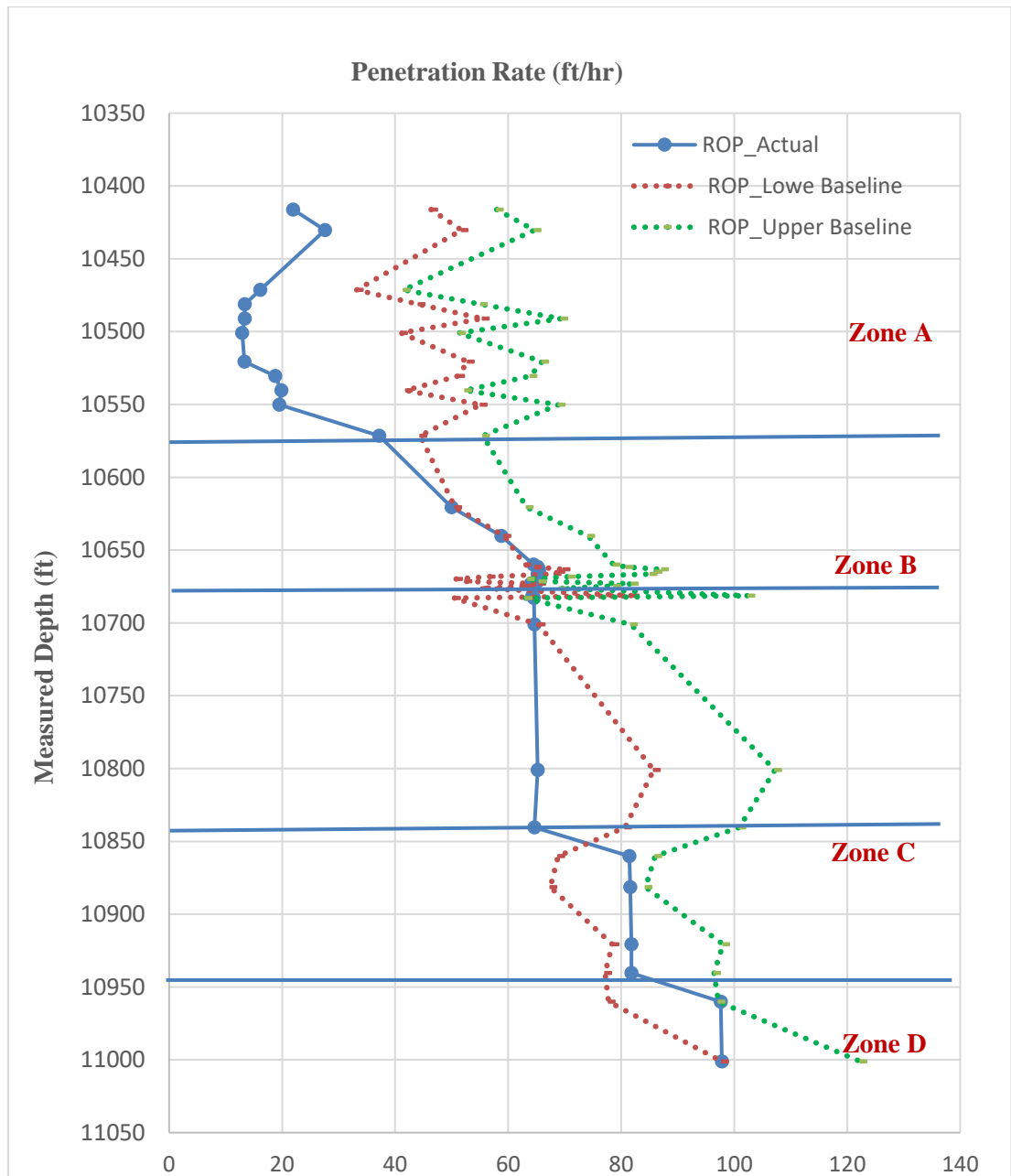


Fig. 5.11— Complot of Optimum ROP performance curve and the actual measured ROP.

5.7.2 Performance Benchmark evaluation

The main challenge addressed was to develop an index of comparison between the actual drilling performance and the expected performance based on engineering technical limit. It is essential to validate this novelty, with the concept of DMSE as maximum efficiency occurs when the ratio of DMSE to UCS equals to 1. (Hamrick 2011) and Amadi and Iyalla (2012) . **Fig. 5.12** shows the plot of DMSE versus UCS.

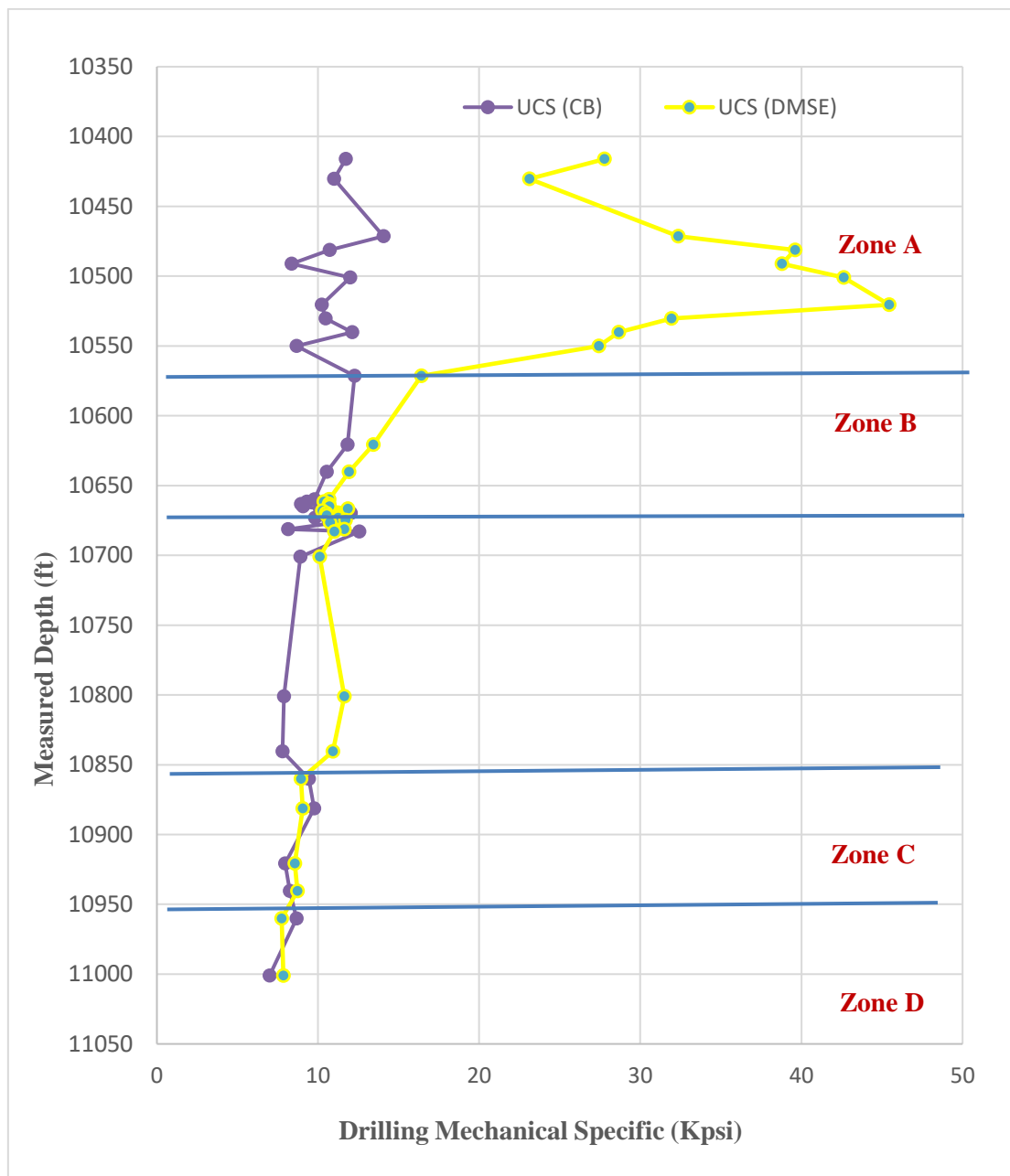


Fig. 5.12 — Comparison of CatBoost Predicted UCS versus DMSE Derived UCS measured ROP

5.7 Application of instantaneous UCS estimation in maximum Achievable ROP Model

It is observed from **Fig.5.12** that drilling operation at Zone A was inefficient, this is evident with the high values of the DMSE and comparison with the technical ROP benchmark shows that efficiency was st 40%- of the technical limit. Review of the drilling parameters shows that this is due to low WOB operating parameter (2-5 Klbs). However, the drilling efficiency with subsequent increase in the WOB (10-15Klb) with efficiency increased to 70% efficiency. At Zone C and Zone D drilling was performed at an optimum rate as shown in **Fig. 5.11**. This is confirmed by the DMSE derived UCS. At this zone the UCS predicted by CatBoost matches the UCS calculated using the DMSE empirical relation which further confirms that the benchmark for the ROP model is accurate and reliable.

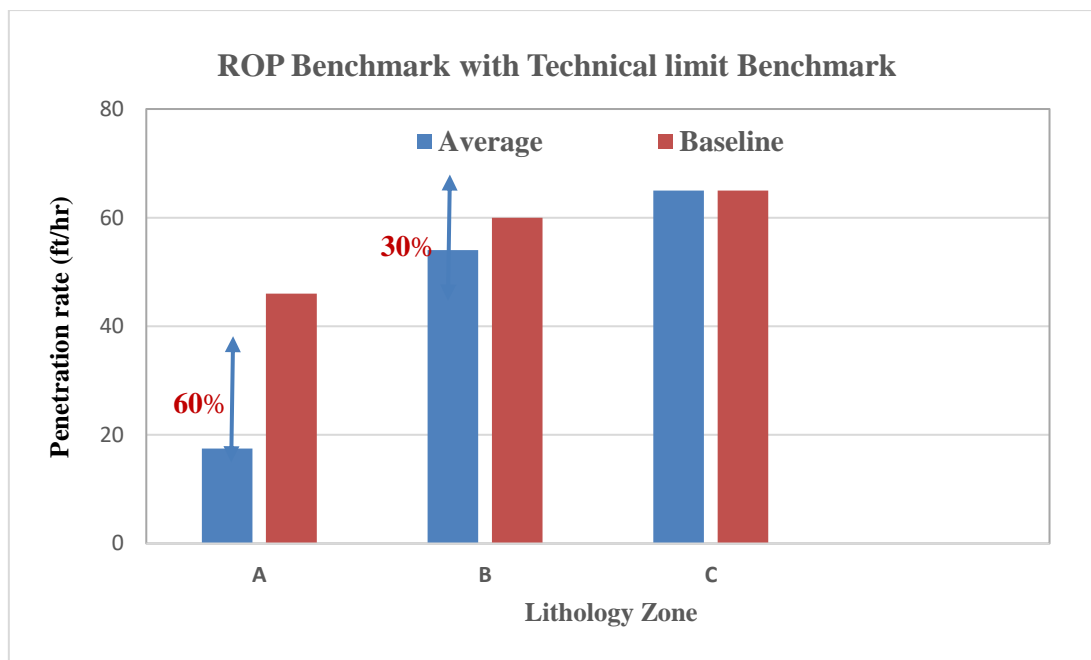


Fig. 5.13 — ROP performance Benchmark Actual measured ROP vs ROP Baseline

Since rock strength has significant influence on instantaneous ROP and represent the inherent difficulty in drilling, it is used in the determination of expected ROP. In **Figure 5.11**, it was observed that due to control drilling with lower operating

5.7 Application of instantaneous UCS estimation in maximum Achievable ROP Model

parameters the drilling performance was at 40% of expected technical performance. In Zone B, following further optimization in the drilling performance the drilling performance improved operating at 70% of the technical rate. However, at Zone C and Zone D the drilling was performed at a technical limit as shown in **Fig. 5.12**. The performance measures discussed above is useful for both conventional and autonomous drilling in comparing new drilled well with “performance benchmark” at technical limit of specific energy, and not nearby offset well. This reveals whether the drilling performance was close or departs substantially from the expectation of the well. The step change in drilling performance monitoring with this output is that the benchmark could be determined in real-time on the fly during the drilling operation and decision could be taken immediately to enhance the drilling performance.

5.7.3 DMSE and Drilling Efficiency

Drilling more efficiently with less hidden time (HT) is the main enabler that reduces field development cost. To achieve a more efficient and secure drilling using automatic real-time drilling optimization models that is tuned by drilling mechanical specific energy (DMSE) and Field thrust (FET). The algorithm’s performance is demonstrated to successfully finds and maintains the optimal WOB and RPM. The application of calculate DMSE values that reflect the actual energy spent in the rock braking process, the use of downhole torque is highly recommended. This is due to BHA friction loss along the borehole wall would increase the surface torque reading which is usually higher than on bottom bit torque. Figure 5.14 demonstrates how the DMSE varies with WOB at constant operating rotary speed of 130rpm. From the plot it was observed that the optimal operating WOB which happens at the Minimum DMSE occurs at a value of approximately 18Klb

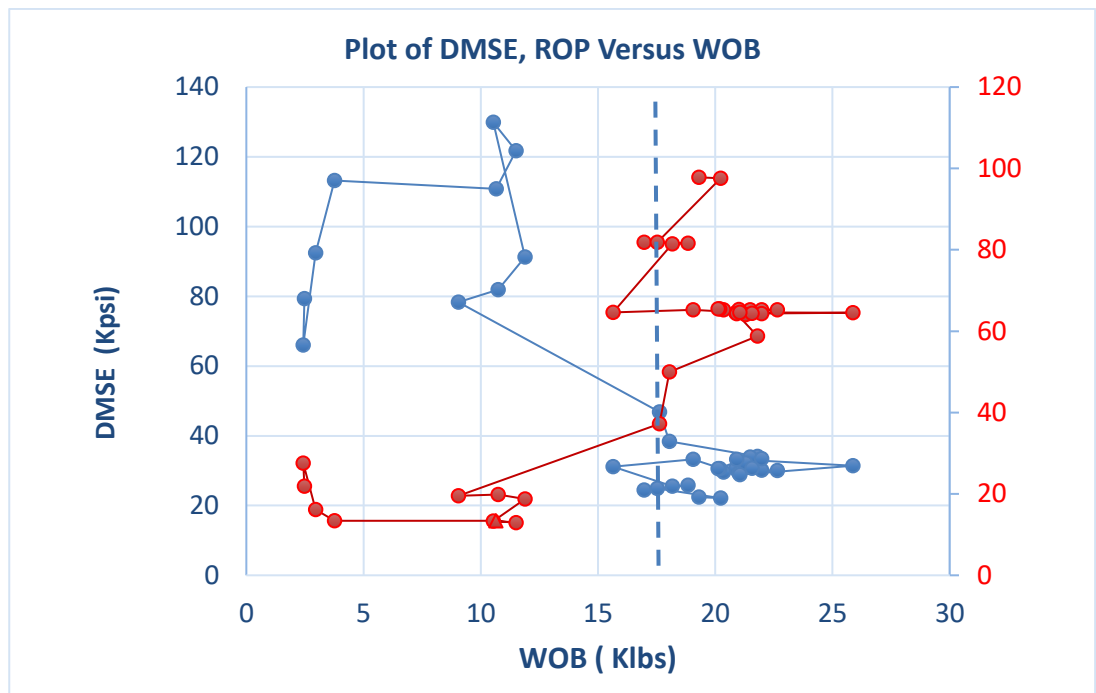


Fig. 5.14 — DMSE and ROP as functions of WOB, illustrated for a constant RPM value of 130rpm.

.Beyond this point ROP starts deviating from straight-line which present phase II according to work of Detournay et al. (2008). Drilling at higher values of Penetration rate can be achieved by increasing the WOB past the founder point, but this increase the risk of wear and tear of drilling equipment and can result in premature downhole tool failure. The minimum DMSE therefore correspond to the maximal “good ROP” that can be achieved without deleterious side-effects (Koederitz and Weis (2005).

When DMSE is used as a trend monitoring tool for ROP optimization, the MSE calculated from the surface torque may still be used if the downhole torque is not available to identify more efficient drilling, but there is a risk of possible inaccuracies due to higher surface torque especially caused by fluctuations in the drillstring torque fluctuation due to tight hole. Furthermore, the downhole torque measurement can be estimated from the topside torque with a torque and drag model if the DMSE shows an increasing trend in regions I and III the most efficient drilling can be identified by

seeking out the highest WOB that does not make the MSE increase as illustrated in Figure 5.14

5.8 Section Summary

This section investigated the possibility of predicting the formation unconfined Compressive strength (UCS) using basic drilling parameters such as weight on bit, rotary speed, drilling torque, and penetration rate which is readily available in all drilling operation. It further established ROP performance benchmark for the various heterogenous lithology based on rock-bit interaction. The study used five Machine Learning models in predicting UCS using basic drilling parameters: WOB, ROP, RPM, and torque. The following conclusions were observed from the study.

1. The procedure was developed for the calculation of instantaneous apparent unconfined compressive strength (UCS) of the rock to the bit. This method will remove the much uncertainty and subjectivity regarding rock strength and drillability.
2. The ML method is globally applicable, based on fundamental and/or first principles, and requires little initial calibration. Which improved the existing physics based empirical methods that requires calibration of the empirical model estimation with experimental core data or fracture pressure test on every formation stratum.
3. The model performance of both ANN and Catboost algorithm showed sufficient accuracy for a qualitative UCS prediction within acceptable margin of errors. The overall performance can be further improved by the addition of other datapoints(e.g Sonic, NPHI, RBOH) whenever available as per section logging requirement.
4. Improve current practice of bit selection and bit performance prediction especially for cases involving significant overbalance and at deeper depth. This new system has

been proven invaluable, with the potential of improving drilling performance and reducing well cost by improving bit performance prediction.

5. The available of predicted UCS and be further used to estimate the ROP technical limit performance benchmark for the drilled well. ANN can be recommended for predicting UCS from offset drilling data before drilling using legacy well data. This would assist in eliminating drilling surprise and assist in fit for purpose well planning and equipment selection at no additional cost but by drilling from data.

6. The new method enables improved decision whilst drilling in many areas including determination of formation tops, early detection of reservoir core points and formation stratigraphic sequence.

7. The unconfined compressive strength of the formation predicted can be used to set optimum penetration rate across the different lithologic enabling a prompt comparison between the actual versus technical limit performance of drilling operation.

8. Drilling efficiency occurs at the region of lowest drilling mechanical specific energy (DMSE) unconfined compressive strength of the formation predicted can be used to set optimum penetration rate across the different lithologic enabling a prompt comparison between the actual versus technical limit performance of drilling operation.

9. The minimum DMSE will therefore correspond to the maximum “good ROP” that can be achieved at highest WOB, without resulting in an increase in DMSE value or any deleterious side-effects on the drilling system.

10. Resulting information will improve adequate pre-job planning in terms of number of Approval for Expenditure (AFE) day and cost, which will improve the well delivery process.

Chapter 6

Decision-making model for autonomous drilling system

6.1 Introduction

In the development of autonomous downhole drilling systems, decision-making and selection of optimized operating parameters has become one of the technical difficulties. Traditionally, the driller performs a trial-and-error approach in search of optimal parameters often referred to as drill-off test. Which is now less effective and non-sustainable to the changing drilling environment, therefore, requiring an intelligent system. An intelligent agent is anything that can be viewed as perceiving its environment through sensors and acting upon that environment through actuators. The increasing need for an autonomous system that exhibit effective decision-making in an unpredictable drilling environment is the focus of the model of decision-making of autonomous systems that presents significant challenges, especially when it is has a content of multi-variant optimization component like in the rotary drilling system that must achieve its goals within a dynamic environment. This section investigates an intelligent drilling Optimisation application that performs an adaptive auto-driller using machine learning (ANN) algorithms to improve on-bottom drilling performance. **Figure 6.1** shows the schematic of feedback loop control method for an autonomous

system. The drilling control system performs predictive data-driven analysis (PDA) using machine learning to determine the force applied to the rock by the drillbit from received downhole drilling data. Based on the analysis of the data estimation of the descend velocity of the drillstring referred as feed thrust (FET) is computed and then communicated to the actuator (draw work). Similarly, the drilling control system set an angular velocity (ω) in response to the rotary force applied based on the rock-bit interaction which determines the outcome of the drilling process. **Figure 6.1** shows the schematic and flow process of the decision control of autonomous drilling system (ADS)

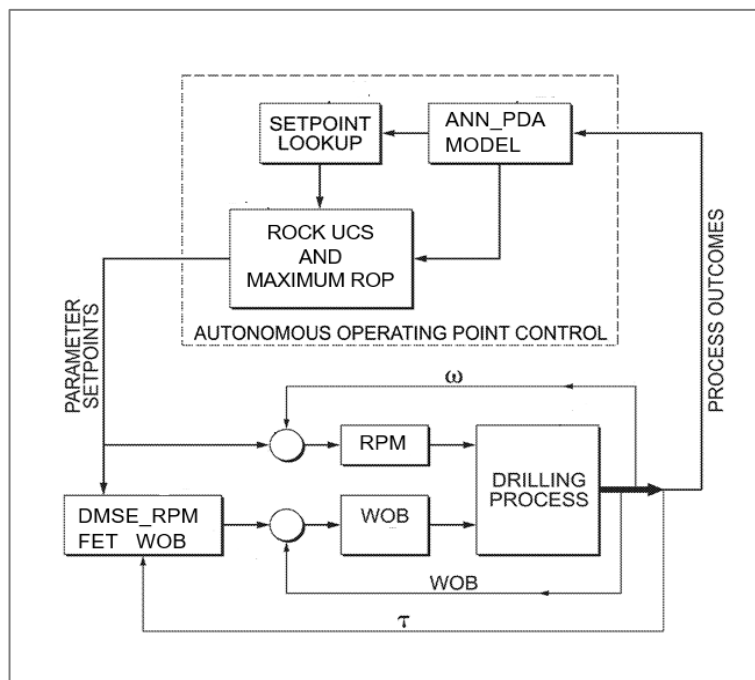


Figure 6.1: Schematic of a Decision control for Autonomous drilling system

The torque generated between the drill bit and rock and the rate of penetration, and the tuning metrics computed from directly measurable parameters such as

DMSE and FET are used to generate the desired setpoints in terms of RPM and WOB based on the input and output relationship of the drilling process parameters.

6.2 Reinforcement Learning: Concept of Markov Decision Processes (MDP) Modeling for Autonomous

Reinforcement Learning (RL) is an aspect of machine learning in which an agent learns its behaviour by the feedback it receives from its environment in the form of rewards. The RL framework is a stochastic dynamic programming, with varying estimation techniques towards a goal-directed sequential learning from interaction paradigms. RL can be set up as an actor-critic method, which utilizes artificial neural networks to evaluate both the parameterized policy and value function Sjøvold (2021). The algorithm uses feedback received from interactions with the environment to learn its optimal behavior that gains its maximum reward. Most times the RL algorithm is formulated as Markov decision Process.

6.2.1 Concept of Markov Decision Processes (MDP)

The Markov Decision Process (MDP) is a mathematical model framework used in solving sequential decisions making problems and a dynamic optimization method. The application of reinforcement learning in predictive decision making in an autonomous drilling system is presented. This work presents decision making process for selecting an optimal feed rate policy for rotary drilling system using Markov decision process (MDP) using experimental published data. The proposed optimization model was computed using value iteration, enabling an intermittent systematic stepwise process of changing surface drilling parameters to maximize the penetration rate and determine the founder point. It is crucial to

understand some of the terms used in RL algorithms.

State (S) – The concept of state is fundamental to RL, it describes the present situation or environment of the agent. The agent must be able to take an action that affects the state to move from that state to another state. The State (**S**) space consists of all valid state (S) defined as the finite set $\{s_1, \dots, s_N\}$ where the size of the state space is N, i.e. $|S| = N$.

Action (A) – Decision that changes the state of the agent. Action is used to control the state of the system. The set of actions that can be applied in some states $\in S$, is denoted $A(s)$ and defined as the finite set $\{a_1, \dots, a_K\}$. Actions produces result (**Rewards**)

Reward (R)– The reward function define the feedback positive (gain) or negative (loss) rewards received for doing an action in a given state. The state reward function is denoted as $R : S \rightarrow \mathbb{R}$, and it defines the reward obtained in states. Therefore $R : S \times A \rightarrow \mathbb{R}$, is defined as reward for an action (A) in state (s).

Transition Probability Function (P_{sa}) – When an action (A) is taken in each state, the system makes a transition from the initial state S to a new state S'. Applying action, $a \in A$ in a state $s \in S$, the system makes a transition by moving from s to a new state s' based on possible probability distribution.

Discount factor (γ) - is a discounted factor that quantifies the desirability of immediate reward of states compared to long term reward of states. $\gamma \in [0, 1]$

The system been controlled is described as Markovian system if decision process in that state S_1 only depends on the previous state S_0 and action a_0 .

6.2.2 Model formulation

The decision-making problem can be formulated as a Markov decision process (MDP), which can be written in terms of five-tuple (S, A, P, R, γ) (Engbroks et al. 2018), where S is the state space, A is the action set, P is the state-transition probability model, R is the instantaneous reward set and γ is the discount factor corresponding to the weight of the future rewards when compared with immediate reward. Table 6.1 shows the MDP element and symbols, and Figure 6.2 shows the basic components of the MDP.

Table 6.1: MDP elements.

Element	Symbol
State set	S
Action set	A
State transition probability	P_{sa}
Discounted factor	$\gamma \in [0,1]$
Reward function	R

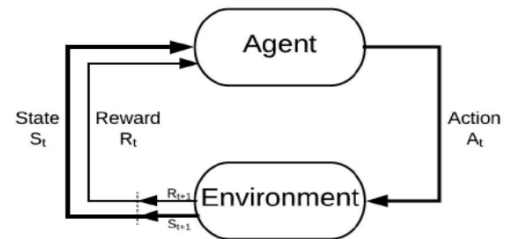


Figure 6.2: Basic component of MDP (Sutton and Barto 2018)

Figure 6.1 illustrates the computer agent that takes an action A_t (set of WOB, RPM) and observe the state (S_t the (rock-bit interaction). This action causes a change in the environment moving it to a new state S_{t+1} , and the agent receives the reward R_{t+1} (distance drilled) for its action A_t . The reward received is only connected to the performing action A_t in the current state of the system and is unconnected to its history and future state. The agent receives the feedback of the reward before taking subsequent actions. Similarly, the next state is only related to the current state and action. Since the agent gets feedback from the action it take in the environment, before the next action, the agent can learn and modify its action to improve its reward. An optimal decision is the set of action that yields the maximum reward which cannot be

Improved upon.

6.3 Return

The goal of the RL agent is to maximize reward over the course of the decision process Sutton and Barto (2020). In MDPs, there are three core concepts used to evaluate the quality of decisions (1) policy, (2) reward, and (3) value function (Gao, Sun and Xiao 2019).

6.3.1 Policy

The policy (π) is a mapping from states to actions and represents the way the agent strategically selects an action to maximize its reward. The reward is the instantaneous assessment of the outcome from the selected action (A_t) in current state (S_t)

6.3.2 Reward

In RL agent is seeking to maximize the reward over the episodic period, which is formalized using the return G_t . An episode is a finite period in which the goal is achieved. This can be expressed in the form of equation (3). Where G_t is the reward in the time t . Actions that yield large rewards are encouraged, while less reward are considered a punishment and therefore discouraged.

$$G_t = R_{t+1} + R_{t+2} + R_{t+3} + \dots + R_{t \text{ final}} \quad (6.1)$$

6.3.3 Value Function

The value function is the accumulation of immediate rewards over the duration. Action

is selected based on the largest value function. Therefore, we reflect on a series of actions reward under policy (π), as shown in equation (6.2):

$$V^\pi(s) = r_t + \gamma r_{t+1} + \gamma^2 r_{t+2} + \dots = \sum_{t=0}^{\infty} \gamma^i r_{t+i} \quad (6.2)$$

Where γ is the discount factor. The objective is to find an optimal policy, i.e., π^* , that maximizes the value of each state. An important role in many RL algorithms are action-value functions, which assign values to admissible state-action pairs as shown in equation (6.3):

$$V_t(s_t) = r(s_t, a_t) + \max_a \gamma \{V_{t+1}(s_{t+1}) | s_t\} \quad (6.3)$$

Where $r(s_t, a_t)$ is the immediate reward for taking the action (a_t) in state (S_t) and $\gamma \{V_{t+1}(s_{t+1}) | s_t\}$ is the sum of discounted value of future reward from the decision. When $V^\pi(s)$ is at its maximum, policy π becomes an optimal policy “ π^* ” as shown in equation (6.5). Next, there is the action value function that considers the state and action. The agent uses the Q-function as a criterion for selecting the action. The Q-function is defined as follows:

$$Q(s, a) = r(s, a) + \gamma V^* \{ \delta(s, a) \} \quad (6.4)$$

$$\pi^*(s) = \arg_a \max Q(s, a) \quad (6.5)$$

6.3.4 Exploration and the Exploitation trade-off

A common challenge with RL is the trade-off between exploration and exploitation. Since the only way the agent receives a reward is to take action. In exploration the RL agent interacts with the environment by performing actions by trial and error and perceiving the reward to learn a correct policy. In a drilling system this can be applied in intermittent drill-off test where the agent varies the rotary speed and perceive the reward in the form of footage drilled which represent the penetration rate. In

exploitation the RL agent continues with the known or assumed best action in the given state although without exploration the agent may not know if there are a better action is a sub-optimal action. Therefore, there is a need to balance the exploration and exploitation to maximize the expected return.

6.4 RL Solution methods

The section briefly discuss the estimation method for a Reinforcement Learning problem, although some of the solutions were discussed for completeness, but not utilized any part of this work, while others were used in the subsequent modeling section of this research. There are two commonly used estimation methods in RL for value function algorithms. The temporal difference method and Monte Carlo method.

6.4.1 Temporal Difference Method

Temporal difference (TD) learning method allow for the computation of the cumulative reward by direct interaction with the environment. is a combination of MC methods and dynamic programming. An optimization technique that relies on recurring problem TD can learn directly from experience like MC methods. Unlike MC methods, TD methods update the estimates without knowing the actual return value. TD methods update the estimated value functions using the estimates from successor states structures [Sutton and Barto \(2020\)](#). This is called bootstrapping. The fact that TD methods bootstrap gives a more frequent update rate

6.4.2 Monte Carlo Method (MC)

This is a technique for estimating the value function of a agent performing an action in a reinforcement learning environment. MC involves learning through sampling reward from the environment and average over In this method, the agent generated experienced sample and then based on average return the value function of the state action pair. In MC there is no defined model and agent does not know the MDP transition probabilities., the value of the value function is known only after the complete episodic state and there is no bootstrapping

6.5 Q-learning algorithm

After the formulation of the MDP model, the next step will be to solve the model through an algorithm. Dynamic Programming (DP) is a recursive algorithmic approach for solving sequential decision problems, which was first proposed by Richard (Bellman, 1957). DP algorithm uses the value function to search for a good policy, which requires all accurate dynamic information of the external environment, and the value iteration calculation, which often becomes very large and complex. Formally, the Q-value for state and action pair is defined as the sum of expected reward for that state and action pair plus the discount factor times the best expected Q-value in the next state as shown in equation 6.5. Equation can be expressed in a compact form as shown in equation (6.6)

$$Q\pi(s, a) = E \{r_{t+1} + \gamma r_{t+2} + \gamma^2 r_{t+3} + \dots | s_t = s, \pi\} \quad (6.5)$$

Where γ is the discount factor and r 's are the reward obtained from an action and t the step count.

$$Q(s, a) = r(s, a) + \gamma V^* \{ \delta(s, a) \} \quad (6.6)$$

Which means that Q-function predicts the future reward based on state and action pair. The agent aims at performing optimally by choosing the state and action pair that yields the highest Q-function (Q^*) value amongst possible actions at the current time step (t). The optimal policy (π^*) indicates the state action pair that returns the greatest value of Q-function commonly referred as Q-max.

$$\pi^*(s) = \arg_a \max Q(s, a) \quad (6.7)$$

The Q^* -function can be expressed in the form of Bellman optimality equation in a recurrent form, where the s' and a' are the next state and next action:

$$Q^*(s, a) = E \left(r + \gamma \max_a Q^*(s', a') \middle| s, a \right) \quad (6.8)$$

The corresponding actions are selected in accordance with the maximum Q-value, and the current state is executed and updated, as shown in Figure 4. The value successively updated,

the initial value iteratively using an operator called the Bellman backup to create successively better approximations for each state per iteration which stops when the value function converges. Therefore, it is attempted to transform value function $V(s)$ into an evaluation function $Q(s,a)$ associated with action when addressing the MDP problem as shown in equations (6.6) and (6.7)

6.6 Model Application (Case study Analysis)

In the drilling environment, rock-bit interaction is in a certain state “s” of state set S and continuously computes the cumulative return corresponding to all actions in action set A on the basis of a greedy strategy. Using experimental data on rotary drilling taken from published literature, having different axial force parameters (WOB) as well as various feed rate with length of a hole drilled as reward the algorithm was implemented (Tlegenov et al. 2015a). The next section discusses the steps and workflow used to obtain the results.

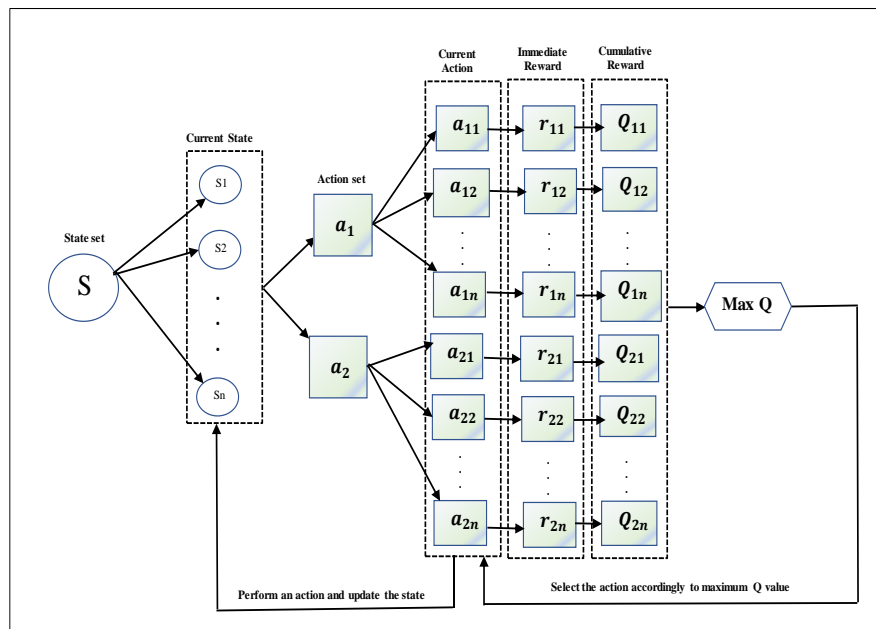


Figure 6.3: Q-Learning flowcharts showing the State, actions, and reward profile

6.6.1 Data and Method

This section presents the description modeling data and the workflow used in the analysis. The modeling was performed in Matlab®. Manual calculation was performed using the first episodic set to verify the result from the simulation. The data set used, initialization procedure and the pseudo code are successively discussed

6.6.2 Data collection and processing

The data needed for the MDP model was taken from published experimental results for spiral drilling using a number of different tryouts taken from (Tlegenov et al. 2015b). For each set of the axial force values, there are five sets of different feed rates along with final length of the hole being drilled for each of these chosen parameters. Axial force values are set as conditions for given problem, so there are five conditions for description of the axial drilling parameters (Table 6.2).

Table 6.2: Published Experimental Data for MDP model adapted from (Tlegenov et al. 2015b)

State (Si)	Axial Force (Fx) (N)	Iteration (ki)	Rotary Speed (rpm)	Feed Rate (mm/rev)	Transitional Probabilities							Reward-Dist. drill L(mm)
					P1	P2	P3	P4	P5	P6	P7	
1	51	1	1370	0.05	0.75	0.15	0.1	0	0	0	0	72
		2	1270	0.06	0.65	0.2	0.15	0	0	0	0	74
		3	760	0.07	0.5	0.5	0	0	0	0	0	50
		4	280	0.07	0.2	0.65	0.15	0	0	0	0	21
		5	60	0.08	0.15	0.75	0.1	0	0	0	0	5
2	84	1	995	0.08	0	0.75	0.15	0.1	0	0	0	83
		2	910	0.09	0	0.65	0.2	0.15	0	0	0	85
		3	570	0.11	0	0.5	0.5	0	0	0	0	60
		4	240	0.12	0	0.2	0.65	0.15	0	0	0	28
		5	65	0.13	0	0.15	0.75	0.1	0	0	0	9
3	112	1	760	0.10	0	0	0.75	0.15	0.1	0	0	78
		2	810	0.12	0	0	0.65	0.2	0.15	0	0	95
		3	560	0.13	0	0	0.5	0.5	0	0	0	75
		4	230	0.15	0	0	0.2	0.65	0.15	0	0	36
		5	60	0.17	0	0	0.15	0.75	0.1	0	0	10
4	147	1	735	0.13	0	0	0	0.75	0.15	0.1	0	92
		2	615	0.15	0	0	0	0.65	0.2	0.15	0	91
		3	270	0.18	0	0	0	0.5	0.5	0	0	47
		4	60	0.20	0	0	0	0.2	0.65	0.15	0	12
		5	6	0.23	0	0	0	0.15	0.75	0.1	0	2
5	160	1	615	0.13	0	0	0	0	0.75	0.15	0.1	81
		2	675	0.15	0	0	0	0	0.65	0.2	0.15	102
		3	445	0.18	0	0	0	0	0.5	0.5	0	79
		4	160	0.21	0	0	0	0	0.2	0.65	0.15	33
		5	35	0.24	0	0	0	0	0.15	0.75	0.1	8

In each state, five (5) iterations of varying the rotary speed (RPM) (1/min), at fixed thrust force (WOB) with the probability distribution forming an episodic set. The experiment was repeated for five different episodic sets as shown in **Table 6.2**.

Q-learning was aligned to match the batch dataset framework, with discrete samples of states, actions, and rewards, while interacting with the environment. The traditional reinforcement learning algorithms of Temporal Difference (TD) or the Monte Carlo (MC) are used for evaluation. The key difference between MC and TD is that the update rule of the latter is based on bootstrapping while the former does not. Bootstrapping occurs when the update of a state-value function is based on the value difference between the current and the previous state value as shown in equation (6.9):

$$Q(s, a) = Q(s, a) + \alpha (r + \gamma \max_a Q(s, a) - Q(s, a)) \quad (6.9)$$

Therefore, the result reflects the trend of the policy, and the final decision, whereas non-bootstrapping only considers state-action values independently from each other.

6.6.3 Q-Learning Pseudo Code

The algorithm estimates all the Q values of the state space based on a number of data sets fed offline. The data sets are in the form of episodes and for every episode the Q values are updated. At the end of every episode, a policy is extracted and updated by finding those actions that generated the biggest Q values. **Figure 6.6** shows the pseudo code for Q-learning algorithm.

Algorithm 1: Algorithm for Calculating Q-value program

```

0  Initialize :  $V_{T+1}(S_{T+1}) = 0$  for  $S_{T+1} = 0, 1, \dots, 10$ 
1  Step backward  $t=T, T-1, T-2, \dots$ 
2      Loop over  $a_t = 0, 1, \dots, 10$ 
3          Loop for step of episode,  $t=T, T-1, T-2 \dots 0$ 
4              Take the expectation over the distance drilled
5                  Compute  $Q(S_t, a_t) = r(S_t, a_t) + \gamma r(S_{t+1}, a_{t+1})$ 
6              End step 4
7          end step 3
8          Find  $V_t(S_t) = \text{Max}_{a_t} Q(S_t, a_t)$ 
9          Store  $\pi^*(S_t) = \text{arg}_a \text{Max} Q(S_t, a_t)$ 
10     end step 2
11 end step 1

```

Figure 6.4: Pseudo-code for Matlab Q-value programming

6.7 Results and Discussion

The summary of the result is presented in **Table 6.3**. Which shows the results obtained after applying the Q-Learning algorithm using the input data in Table 6.2 and the pseudo-code.

Table 6.3: Summary of results

State (Si)	Axial Force (Fx) Newton	Iterations (ki)	Vi(n)	V*	Decision	Action
			Distance Drilled (mm)	Arg.Max		Rotary speed
1	51	1	882	892	2	1270 RPM
		2	892			
		3	862			
		4	862			
		5	847			
2	84	1	940	947	2	910 RPM
		2	947			
		3	927			
		4	910			
		5	892			
3	112	1	973	992	2	810 RPM
		2	992			
		3	969			
		4	939			
		5	912			
4	147	1	1002	1005	2	615 RPM
		2	1005			
		3	965			
		4	942			
		5	933			
5	160	1	1020	1043	2	675 RPM
		2	1043			
		3	1019			
		4	978			
		5	952			

6.7.1 Effect of axial force (WOB) on feedrate

The modeling result showed that in each episodic state of axial force (WOB), there is a specific feed rate which would lead to highest reward compared to any other feed rate, this is contrary to the common notion that believes that Feed rate increases with increase in axial force (WOB). This evidence is a confirmation of the work of Dunlop et al. (2011) and Detonnray et al. (2008) illustrated in Figure 3. In addition, comparing the optimum reward in each state with fixed thrust force, it can be observed that the best decisions are neither the highest nor the lowest rotary speed but those at the middle range, which illustrate the trade-off of the optimization. Figure 6.7 shows the feedrate versus reward at different states optimization.

Figure 6.7 shows the feedrate versus reward at different states.

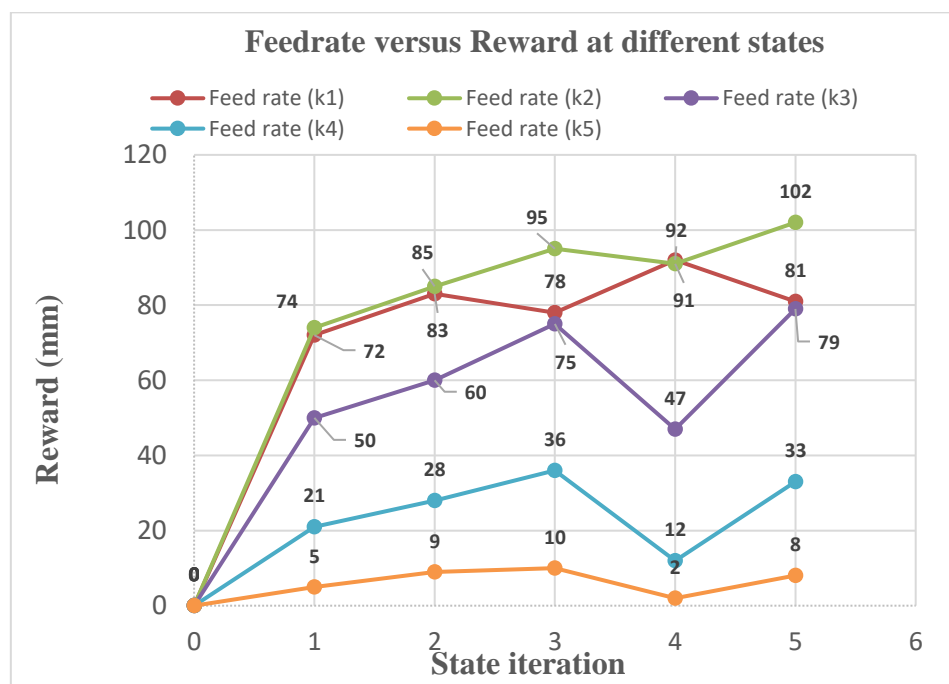


Figure 6.5: Plot of the Feedrate versus Reward at different states

The result also showed that the traditional practice of using different combination of thrust force (WOB) from low to high limit on a single rotary speed during most of the drilling operation is inefficient practice that leads to tool failure or increase in the drilling time and cost

6.7.2 Effect of rotary speed (RPM) on feedrate

Though at high rotary speed, increase the feed rate and the rate of penetration (ROP) which increases the current reward, but inefficient in the future reward as higher rotary speed increases the wear of the drill bit which could result in decrease in feed rate respective of the higher rotary speed. **Figure 6.8** shows the plot of the rewards (Distance drilled) with the different rotary speed of [1370, 1270, 760, 280 60] in state 1 and for the second episodic state 2 with the fixed thrust force of 81 N the rotary speed decrease of [995, 910, 570, 240 65], the third state (state 3) with the thrust force of 112 N, rotary speed [760, 810, 560, 230, 60] and the fourth state (state4) with thrust force of 147 N the range of rotary speed [735, 615, 270, 60, 6] while the fifth state of 160N used the range of rotary speed [615, 675, 445, 160, 35]. In all the states, it was observed that an increase in the thrust force (WOB) results in the slight decrease on the range of the operating rotary speed. This demonstrates a good operating procedure that with increasing thrust force (WOB), the rotary speed reduces as the optimum point usually shifts to a reduced rotary speed for the same material strength, which also help to reduce the wear and preserve the tool longevity.

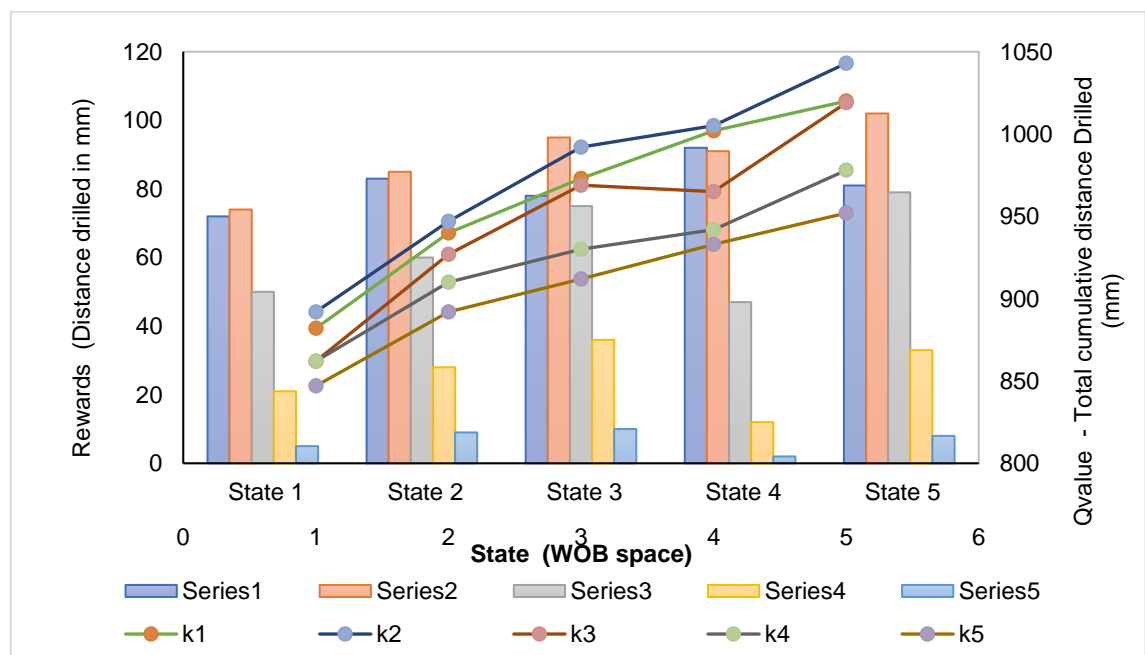


Figure 6.6 : Plot of the Rewards of various RPM (Distance drilled) Versus Episodic state (WO

The Q-value estimates represent the cumulative distance drilled (represented with a line charts) The analysis results revealed that the optimal value function was reached irrespective of the initial state conditions. The agent's objective is to learn policy mapping from states to actions such that the agent's cumulative reward (footage drilled) is maximized. Although the agent's initial action may not be optimum, if the agent's subsequent decisions are right, the Q-value function on further iterations converges which represent optimum performance.

6.8 Section Summary

In this paper, dynamic drill-off test whilst drilling using data driven decision making process that combines data-efficiency and the reinforcement learning was discussed. It analyzed how the RL agent chooses its action in the drilling environment with an off-policy search using the Q-learning algorithm which uses the value function to search for a good policy by successively calculating the cumulative return. It is demonstrated that drill-off testing can be formulated as an MDP which intermittently analyzes a batch real-time data using Q-value algorithm to select the pair of surface operating parameters (WOB, RPM) that yield the maximum value on the episodic set. Modeling of published experiment data showed that the proposed approach can improve decision process and realize the optimal value function irrespective of the initial state conditions. This research could be used as a decision-making tool in drilling operations that could provide an engineered approach for optimal operating parameter selection and improvement in the efficiency of the drilling process in terms of cost and time.

The result confirmed the obvious fact that it is neither the maximum nor the minimum operating parameters that yield the optimum result. But the optimum operating lies within the limits and can be achieved by exploration. Interestingly this optimum operating condition changes with changing environmental conditions and must therefore be explored dynamically throughout the duration of the drilling process.

Chapter 7

Experimental rigs design and model validation

This chapter presents a description of experimental test rig utilized in the study. The instrumentation of the rig is required to provide the rig with the required WOB utilizing the WOB load cell and rotational speed and then record the dynamic WOB, TOB and ROP for respective rock drilled. The data is then to be post-processed using the excel spreadsheet to validate the model relations developed using field drilling data. Two experimental test rigs were utilized in the study; the uniaxial compressive test machine and the in-house Labscale prototype rig designed to study rock-bit interaction.

7.1 Uniaxial test machine

The uniaxial compressive strength machine shown in Figure 7.1 was utilized in the uniaxial compression test in this study. The machine allows for a fixed load rate to be applied to a material by moving the crosshead down by an electric motor which is placed inside the base. The frame panel has a jog button to adjust the crosshead manually until it in the right place as well as a switch button. The control console contains the manual controls for the machine used in zeroing load and displacement. The crosshead contains a positional transducer to record the displacement, whilst the Load is recorded by the load cell. This test was used to determine the unconfined compressive (UCS) strength of the core of the rock, used in testing the ML model of rock UCS prediction

7.1 *Experimental rigs design and model validation*

and the estimation of maximum achievable rate of penetration across the formation rock



Figure 7.1: Schematic of ADR1500 with its main components.

7.1.1 **Experimental procedure**

The experiment is performed following ASTM2938 where the material is cut to the suggested size with two flat-end surfaces and then the load is increased with either of constant strain or stress rate until the material fails at its peak load. The compressive strength of the material can be calculated by dividing the maximum load over the cross-sectional area of the specimen. Indentation tests follow the same method, and the only difference is that the indenter is placed on top of the sample as shown in Figure. 7.2



Figure 7.2: Experimental testing of Core UCS using ADR1500. Machine

7.2 Labscale Experimental rig

Lab-scale prototype rig is a bespoke research and testing device designed and built for laboratory testing and demonstration of key functionality of a new idea or piece of technology. As oil and gas drilling rigs are restricted to hazardous environments, the use of digitalized prototype rig to promotes learning and research in drilling engineering has become vital. During this research a Labscale prototype was designed and fabricated a fully functional and digitalized drilling rig for investigation of rock-bit interaction. The research studies with capability of simulating the functionality of the conventional drilling rig with models that control hoisting, rotary and circulating systems. Its components will include the Bottom Hole Assembly (BHA) comprising of drill bit, stabilizer, drill collar and drill pipe, acquisition system with sensors to measure weight on bit, rotary speed, and torque. . According to Agarwal (2019) system downscaling can be done using the law of similitude which would implies downscaling of both geometrical and mechanical parameters. On the basis for the selection of downscaling parameters; WOB, RPM, and TORQUE are three drilling parameters that are under human control and plays a crucial role in the optimization of the drilling system

Vimlesh et al (2017). Similar examples of design of miniature autonomous small-scale system designs were presented in Løken et al.(2018, 2019), Bilgesu et al. (2017) and Arnø et al. (2018). In the year 2015, The Society of Petroleum Engineers (SPE) launched the Drillbotic programs for university to enhance learning and innovation in drilling automation. Drillbotics® is an international university competition where teams from all around the world take part in the design and building of prototype version of automatic drilling rig loaded with sensors and control algorithm to autonomously perform drilling of given rock sample provided by SPE’s Drilling Systems Automation Technical Section (DSATS). The goal of the competition is to promote development of innovative techniques in drilling automation areas such as drilling machines and downhole tools, allowing participating teams to develop a deeper understanding of the drilling process Agarwal (2019). Table 1 shows the summary of the Drillbotics winning university from 2015 to 2018 and their essential design features. Figure 7.3 (a-d) shows the schematic of the prototype rig from the respective universities.

Table 7.1: Summary of Drillbotics winning teams to study drilling automation

Universities	Key Design features	Cons Discussion
University of Oklahoma 2015: Figure 7.3 (A)	<ul style="list-style-type: none"> ▪ Wheels for rig mobility ▪ Precise WOB control ▪ Optimization parameters used are high ROP and low MSE 	<ul style="list-style-type: none"> - WOB control allows electrical connection. - limited mobility - Precision parameter
West Virginia University (2016): Figure 7.3(B)	<ul style="list-style-type: none"> ▪ Attachable fluid circulation system ▪ Movable instruments for ease of mobility ▪ Hoisting lift with counterweight system ▪ Wireless conn. over Wi-Fi & Bluetooth ▪ Installed Speed and torque sensors 	<ul style="list-style-type: none"> - Limited rig mobility - Advance algorithm used to optimize drilling performance - Wireless connectivity improves data monitoring and ease setup.
Texas A&M University 2017: (Figure 7.3 (C))	<ul style="list-style-type: none"> ▪ Downhole sensors for vibrations and pressure. ▪ Wheels for ease rig mobility ▪ Optimization parameters; ROP and MSE 	<ul style="list-style-type: none"> - Basic optimization algorithm - Hoisting system is draw-works - Whirl causes uneven wellbore. - Easy mobility of the rig and extensive safety features.
2018: Norwegian University of Science and Technology (Figure 7.3 (D))	<ul style="list-style-type: none"> ▪ Wheels for rig mobility ▪ Downhole sensor for vibration and azimuth angle ▪ Ball screw hoisting system provides stable and precise hoisting 	<ul style="list-style-type: none"> - Experimental result-based optimization of ROP, WOB and RPM - Wired downhole sensor. - Ball screw based hoisting system provides precise and stable control over WOB.

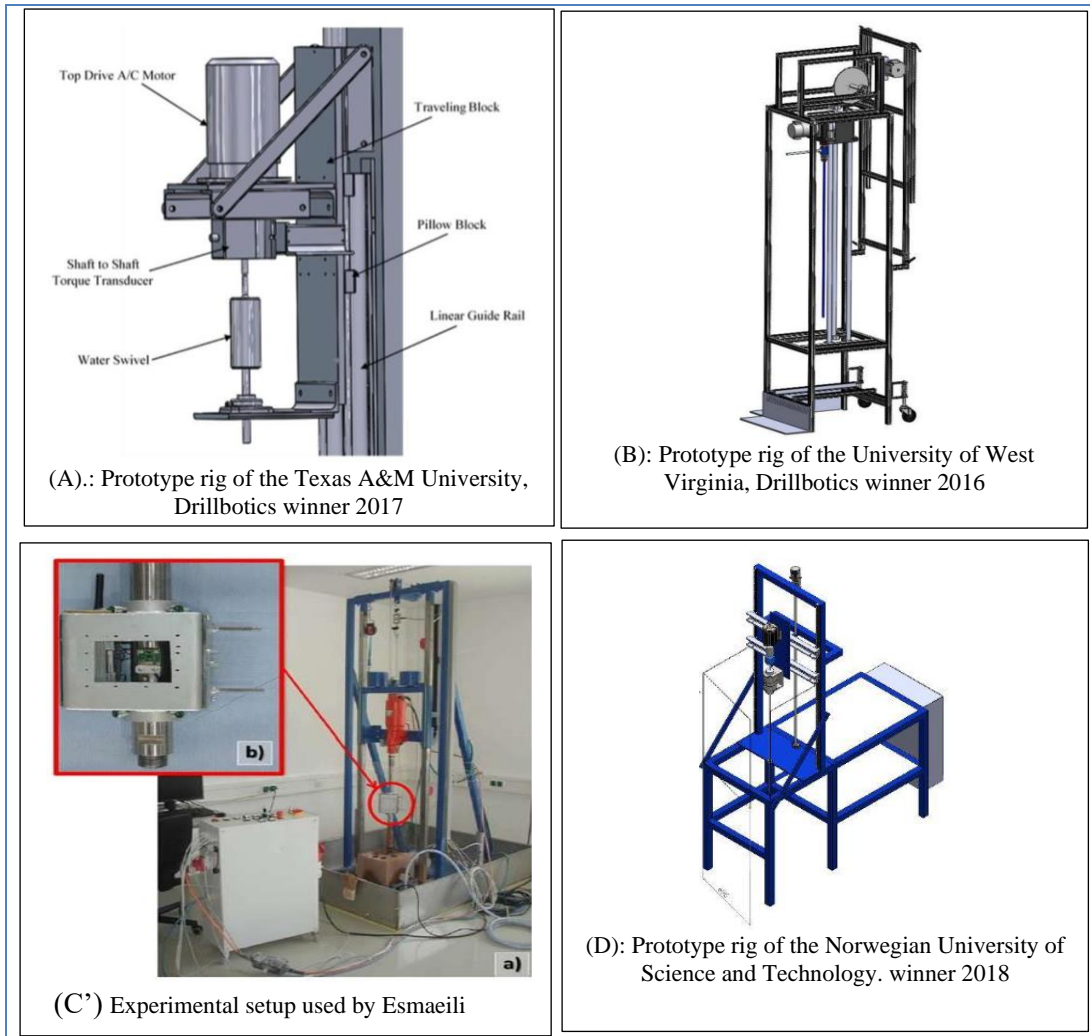


Figure 7.3: Schematic of prototype rig used in SPE Drillbotic (Agarwal 2019)

7.2.1 Discussion on previous Labscale experimental rig design

It is observed that all the discussed prototype rig setups have limited drilling depth potential. Which is logical since their idea was not to reproduce deep drilling well due to limited laboratory space constraint. A few setups such as University of Oklahoma and Norwegian University of Science and Technology have accurate WOB control of 50 grams. Precise WOB control has several benefits including minimizing vibrations and better penetration rate. A good number of the University setups use LabVIEW interface for visualization and programming and most of the setups have weight on bit sensor, displacement sensor, vibration sensor, torque sensor and the flowrate sensors

were used. The use of these sensors provide more data and information about the various aspects of drilling being investigated and supports in making a robust decision. It is also important that the sensors provide accurate information allowing accurate evaluation of the measurement. The DC motors was used in most of the control which was supported by PID controller to improve the accuracy of the decision. The application of Screw-slider based hoisting system proved robust and precise for control motion and effective application of steady weight on the drill-bit.

7.3 Current experimental In-House Prototype

The rig schematic was designed using solid works application software tool as shown in Fig.7.4. The rig framework was designed to integrate the two essential rig systems including the rotary and hoisting system. The base structure and the core holder was designed with embedded load cell weight on bit sensor. The framework divides the rig into two main compartments. First, a vertical 5cm x 5cm derrick to provide for the hoisting of the drillstring up and down providing weight on bit to the system. Second, the compartment underneath the rig floor are used for accommodating and keeping the rock sample whilst providing the retainer for the drilling fluid. This experimental rig, which is shown in Fig. 7.4, was designed with the features of an oil drilling rig to a large extent to operate with the rigid and flexible shafts to simulate comprehensive phenomena in rotary drilling operations. The main objective for the construction of the miniature prototype drilling system is for the testing of rock-bit interaction model in the research and to simulate comprehensive phenomena in rotary drilling operation and able to optimize the drilling performance. The system is designed to successfully drill through one foot of rock-samples given with constraint related to amount of electric

power and surface operating parameters based on the drill bit and drill string limitations.

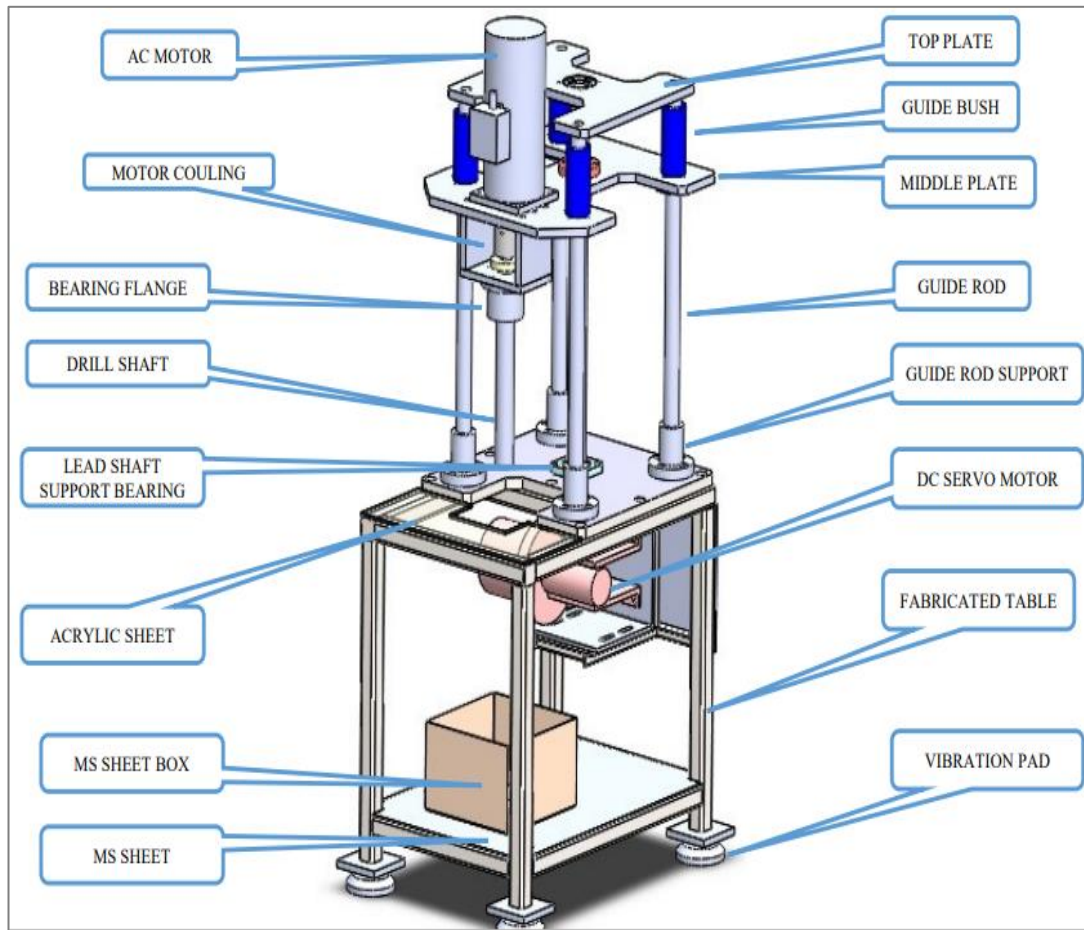


Figure 7.4: Schematic of the prototype rig setup. The system includes electric motor, Laser displacement sensor, load cell, ball screw assembly and rock holder

The goal is to link the surface operating conditions to downhole conditions through measurement of rock-bit interaction and using the measurement in validating models developed using field offset drilling data. The preceding section will discuss the system architecture and components of the prototype rig. Some of the design features of the prototype include application of higher weight on bit. Rig system stability which reduces the vibration. However, there are limitations to the current designs which includes it can only perform vertical drilling rig model, it is unable to measure drillstring vibration due to absence of accelerometers and magnetometer sensors.

7.3.1 Hoisting system

The hoisting system of a conventional oil and gas rig consist of the drawworks, derrick, crown block, traveling block and the drill lines in a block and tackle system. The functions of the hoisting system include providing mechanical support and power to raise and lower equipment into and out of hole. It also provides the thrust force to provide weight on the bit (WOB). The drill line is spooled on the drum of the drawwork and reeved through the crown block and the traveling block. The rotation of the drum causes the traveling block to move up and down based on the direction of motion. In the prototype rigs the hoisting system consist of Electric AC stepper, ball screw system, capable of precise speed and position control to make adjustment to optimize the thrust force to the drill bit and optimize the penetration rate. The rate of change in the speed of the hoisting system determines the hoisting system. Figure 7.5 shows prototype rig and the hoisting system.

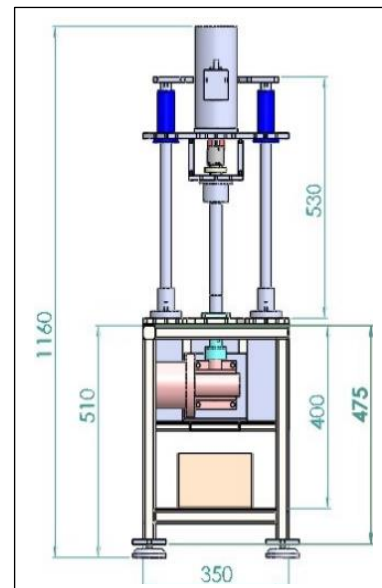
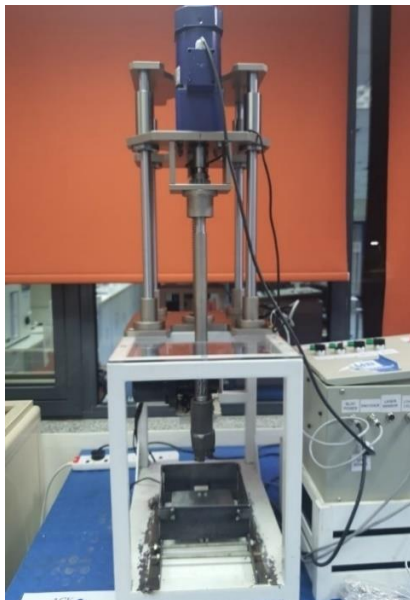


Figure 7.5: Schematic of the in-house prototype rig Hoisting system includes electric motor, LVDT sensor, load cell, ball screw assembly and rock holder.

7.3 Experimental in-house Prototype

The hoisting is designed to trail on tetra-pole using the 60V DC motor which drives the ball screw system by converting a rotational energy to a liner motion. This low torque and high-speed motor used is the Brushless DC Motor 1500W. To reduce friction each of the four legs is installed with ball bearings and provide stable vertical movement and accurate WOB measurement. Figure 7.6 shows the components of the hoisting system.

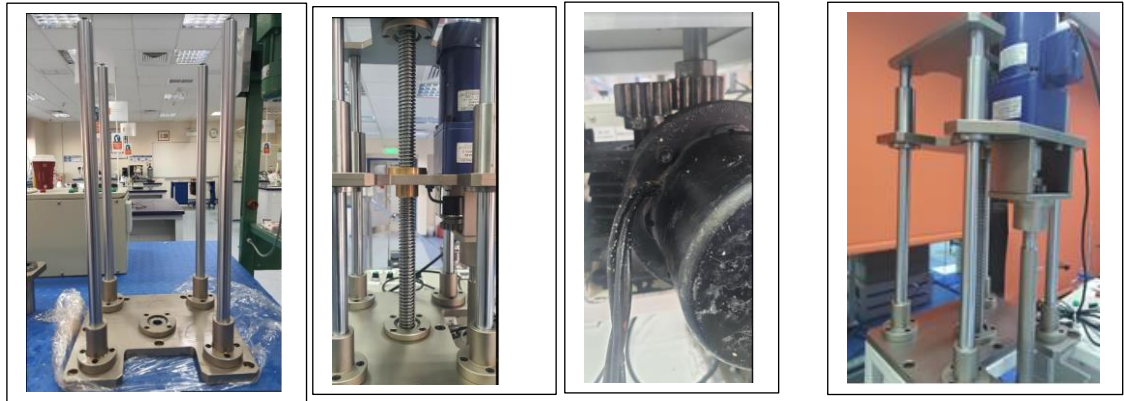


Figure 7.6 : Schematic of parts of the in-house prototype rig that make-up the Hoisting system including electric DC motor, ball screw assembly and topdrive variable speed motor. Unlike the traditional hoisting system, this system can push down the drillstring to apply weight on bit. The rotational speed of the motor which is translated to liner motion is used to change the applied weight on bit. Hence the slower the speed, the lower the weight on bit and the faster the speed the higher the weight on bit. The block and tackle system of the traditional drilling was considered but not used here due to the complexity and poor precision as well as the challenge of meeting the weight requirement to drill bit. The topdrive assembly is attached by a ball screw nut to the ball screw hoisting system. The hoisting motor power was calculated using equation (7.1) which was given in the motor specification.

$$T = \frac{F * l}{2\pi * \epsilon_{BS}} \quad (7.1)$$

Where F is the force acting on the ball screw (N)

l is the lead of the ball screw(m).

It is estimated that the total weight on the ball screw from the carriage and the weight of the rotary motor is 250N. The lead of the ball screw is 5mm with an efficiency of 0.9. Therefore, the torque on the hoisting motor is estimated at 0.22Nm.

7.3.2 Rotary system

The rotary system of the prototype design consist of an electric AC gear motor with variable speed used to rotate the drillstring at any desired RPM within the expected range. The rotary speed is provided with AC motor with the range of rpm [0-1500rpm]. Figure 7.7 shows the components of the rotary system including the rotary head, rotary encoder, and the rotary shaft and the drillstring. The topdrive transfer rotation directly to the drillstring.

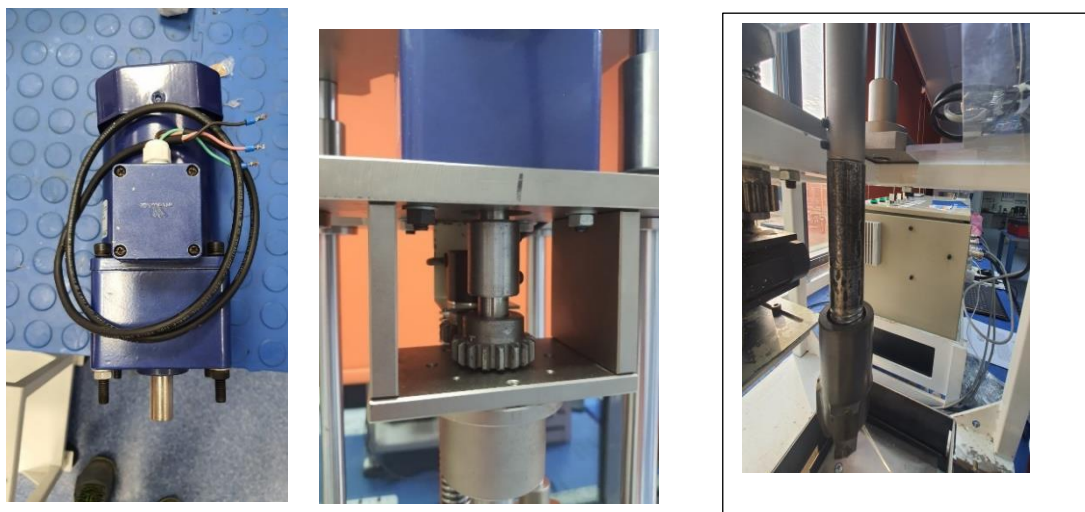


Figure 7.7: (a) Variable speed motor (b) Rotary encoder (c) Drillstring with the drill bit,

The rotary system of the prototype design consist of an electric motor with encoder. The main The function of the rotary system is to provide torque to the drill bit via the drillstring.

7.3 Experimental in-house Prototype

The rotary speed is measured is measured with a rotary encoder attached to the rotary shaft of the electric motor. Figure 7.8 shows the load cell installed between the Load core holder.



Figure 7.8: (a) Loadcell (b) Installed loadcell on core holder, (c) Position of rotary encoder.

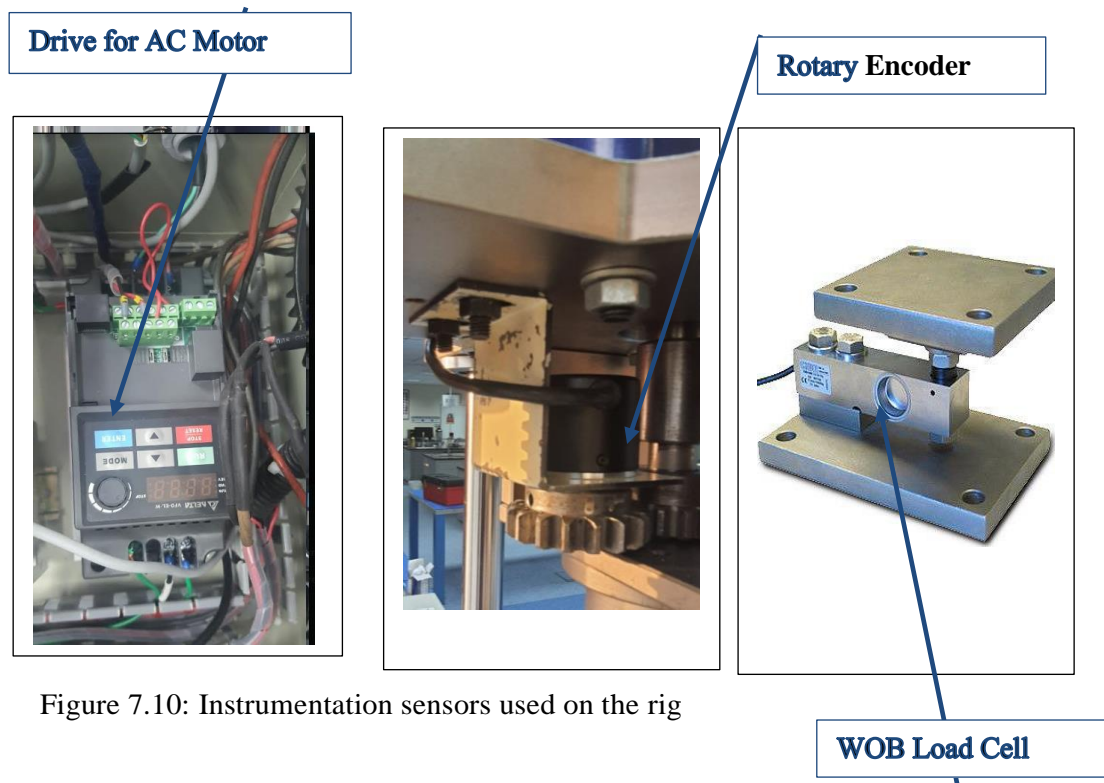
7.3.3 Circuit design architecture

The electronic circuit design architecture will be executed using the Arduino package with the virtual interface of the program compilation on the processor which aids the interfacing of circuit components. The processor will be interfaced with rotary encoder module. Figure 7.9 shows the instrumentation box and the sensor connection.



Figure 7.9: Instrumentation box and sensor connections.

With the aim task of simulating a drilling process data from the sensor are required in making decisions and understanding the rock-bit interaction and provide user with valuable information. The prototype rig is designed with five (5) key sensors including the load cell for weight on bit measurement, the rotary encoder for rotary speed, the energy meter torque estimation, Figure 7.10 shows the instrumentation sensors Drive for AC motor and brushless direct current motor (BLDC) for Motion up and down



7.3.4 Data Acquisition system

The data acquisition system (DAQ) is the process of measuring and communication physical and electrical phenomenon including pressure temperature, voltage and current with measurement sensors. The design of the DAQ setup involves sending analog signals to the DAQ device where the signal are converted into digital signals.

7.3 Experimental in-house Prototype

The signal are then sent to micro controllers (Arduino platform) using a data bus via a

USD comm port rig is designed to send sensor reading to a laptop PC for data analysis.

The data string are in the format: **## Displacement : RPM : Load : Torque\n**

representing the sequence of the number string received from the USB comm port.

Where the displacement is distance drilled in millimeters, rotary speed in rev/min, load

For weight on bit in Kg and torque estimated in NM

7.3.5 Bottom Hole Assembly (BHA)

The drillstring consist of the Drillbit, heavy walled drill collar, drill pipe as shown in Figure 7.11. The combined length of the drillstring is short compared to that used in actual oil and gas drilling operation. Rotation is transmitted from the topdrive motor to the drillstring using a rotary shaft. The torque delivered by the drillstring is estimated using equation (7.2)

$$\text{Torque} = 9.5488 \times \text{Power(kW)}/\text{Speed(RPM)} \quad (7.2)$$



Figure 7.11 : Bottom Hole Assembly Design

7.4 Miniature rig operating parameter

The essential drilling parameters used in drilling includes the WOB, RPM and the rotary torque. Whilst the WOB and RPM are controllable parameters, however torque is a resulting parameter. For the conventional full scale drilling system, weight on bit is applied from the suspend weight of the drillstring from a draw work system which is controlled via electronic brake. Due to the short length of drillstring in the miniature technically not possible to use the same system of the full-scale system based on the criterium that hookload should surpass the desired weight on bit required for drilling. To provide the desired weight on bit, a ball screw setup was desired that apply weight by pushing bit down by rotating a ball screw with an electric motor and corresponding weight measured using a load cell. Table 7.2 shows the summary of typical drilling parameters used in the miniature rig.

Table 7.2: Range of drilling variable data for experimental and full-scale rig

Items	Experimental rig	Full scale rig	Units
Bit size	3.25	6-36	inch
WOB	5-60	1000-20,000	kg
RPM	500-2000	50-250	rev/min
Torque	1-5	1000-15000	Nm
ROP	1-40	1-100	cm/min

7.4.1 Drilling Mechanical Specific Energy and Miniature rig setup

As discussed in section 4.2.3 Drilling mechanical specific energy is the ratio of input energy to the removed rock volume. Since there are principally two sources of energy the axial force from WOB and the rotational energy from RPM

$$DMSE = \frac{\text{Total Energy input}}{\text{Volume of rock removed}} \quad (7.1)$$

Decomposed into two forms, we have.

$$DMSE = \frac{\text{Vertical Energy input}}{\text{Volume of rock removed}} + \frac{\text{Rotational Energy input}}{\text{Volume of rock removed}} \quad (7.2)$$

Where vertical and rotational energy are respectively delivered through

$$DMSE = \frac{F \cdot \Delta h}{A \cdot \Delta h} + \frac{2\pi \cdot T \cdot n}{A \cdot \Delta h} \quad (7.3)$$

Where T is the drilling torque and n is the number of revolutions from the bit. The second fraction can be expanded

$$DMSE = \frac{F}{A} + \frac{2\pi \cdot T \cdot \frac{n}{s}}{A \cdot \frac{\Delta h}{s}} \quad (7.4)$$

$$DMSE = \frac{F}{A} + \frac{2\pi \cdot T \cdot RPM}{A \cdot ROP} \quad (7.5)$$

Therefore, the key tuning variable is the ($\Delta h/s$) which represent the speed of descend of the drillstring which is a function of ROP and the energy in the drilling system. The speed of descend will affect the weight on bit, the faster the speed of descend the higher the weight on bit and the slower the speed on descend the lower the weigh on bit. The combination of both the speed of descend and the rotary speed will affect the drilling torque and the penetration rate

To ensure accurate values of weigh on bit the load cell was calibrated with dumb iron of know weight , but the rotary speed record of the encoder was calibrated by measuring the time it takes for a complete revolution using a stopwatch.

7.4.2 Optimizing drilling efficiency using FET and DMSE

The concept of FET and DMSE are energy derivatives based on the basic drilling parameter (WOB, RPM) based on equation (7.5). Therefore, regardless of the size of the rig, similar DMSE values when drilling through the same rock. Accordingly, to Teale (1965) DMSE should be numerically equivalent to unconfined compressive strength (UCS)

7.4.3 Experimental study of the rock-bit interaction

Experimental tests were performed at various WOB and rotational speed. For rotational speed, tests were performed for 900rpm, 700rpm, 300rpm, 100rpm. However, it was observed at higher values of rotational speed the amount of applied WOB becomes limited due to rig design limitations.

7.4.4 Investigation on the Effect of change in Weight on bit on rock-bit interaction

The test was performed for varying values of WOB and rotational speed. However, at higher RPM the limit of WOB became smaller due to energy in the drillstring. The rate of penetration versus WOB are shown in Figure 7.12. The plot shows the relationship between measured ROP at different WOB at various rotational speeds. It can be observed at lower values of WOB alters the linear relationship that exist between ROP and higher WOB. At lower values of WOB a transition zone exist between the frictional dominant mode to the rock cutting mode which is separated by the blue arrows as shown in the plot. At 70RPM the increase values of weight on bit from 50N to 150N does not translate to any appreciable increase in the ROP

as the rotational speed is within the friction dominant zone. The rotational speed was just sufficient to overcome the frictional force due to the rock bit interaction. However, with the increase of to 300 RPM a much better response of ROP was observed with corresponding increase in WOB from 50-150N

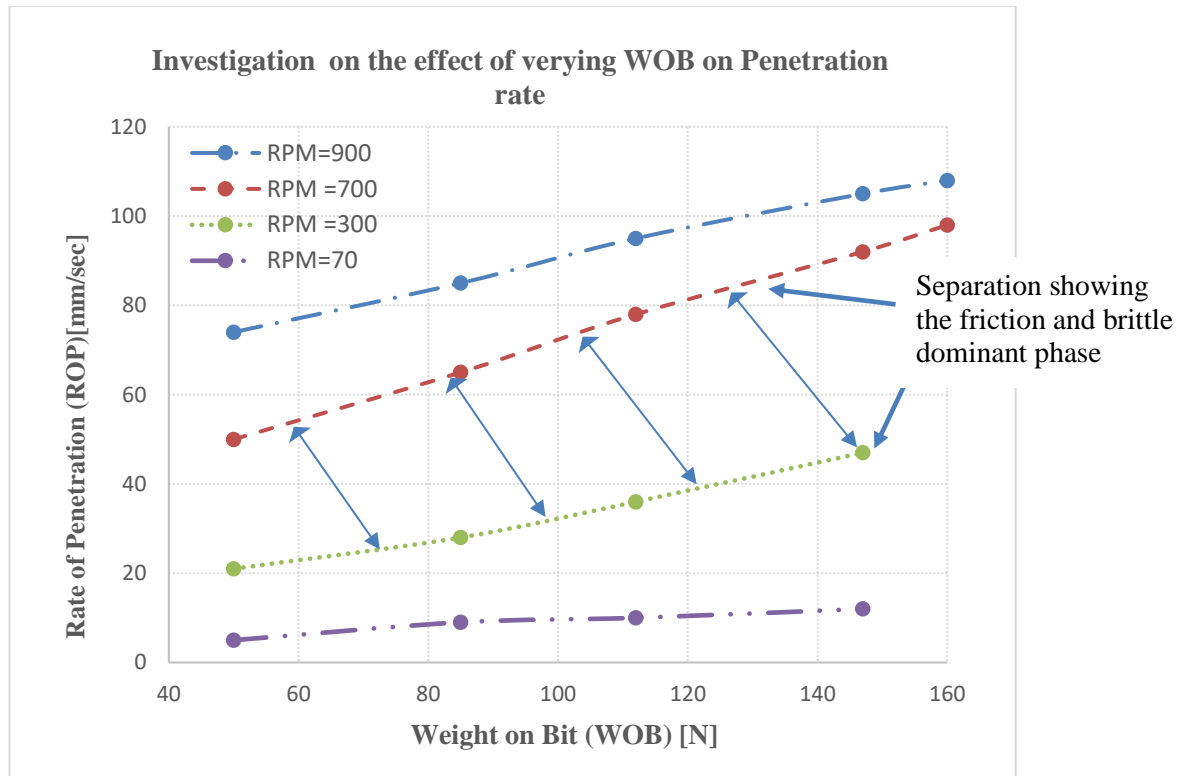


Figure 7.12: Plot of ROP versus WOB at different rotational speed

However, at 300rpm shows a much greater departure from the friction dominant mode to the rock cutting mode where increase in weight on bit translate to a appropriate increase in the penetration rate. Furthermore, increase in rotational at 700rpm, maintained the same behavior with not much divergence. Which further improved at the rotary speed of 900rpm. It can be observed that the penetration rate similarly increases with increase in weight on bit. To eliminate the effect of rotational velocity, we will evaluate the effect to depth of cut. Which is simply

penetration rate divided by rotational speed, to the measure penetration rate per revolution. Figure 7.13 shows the relation between the DOC versus weight on bit (WOB) at different rotational speeds. It can be observed that WOB up to around 85N. the cutting mode is ductile. But at higher values of DOC changes to brittle mode.

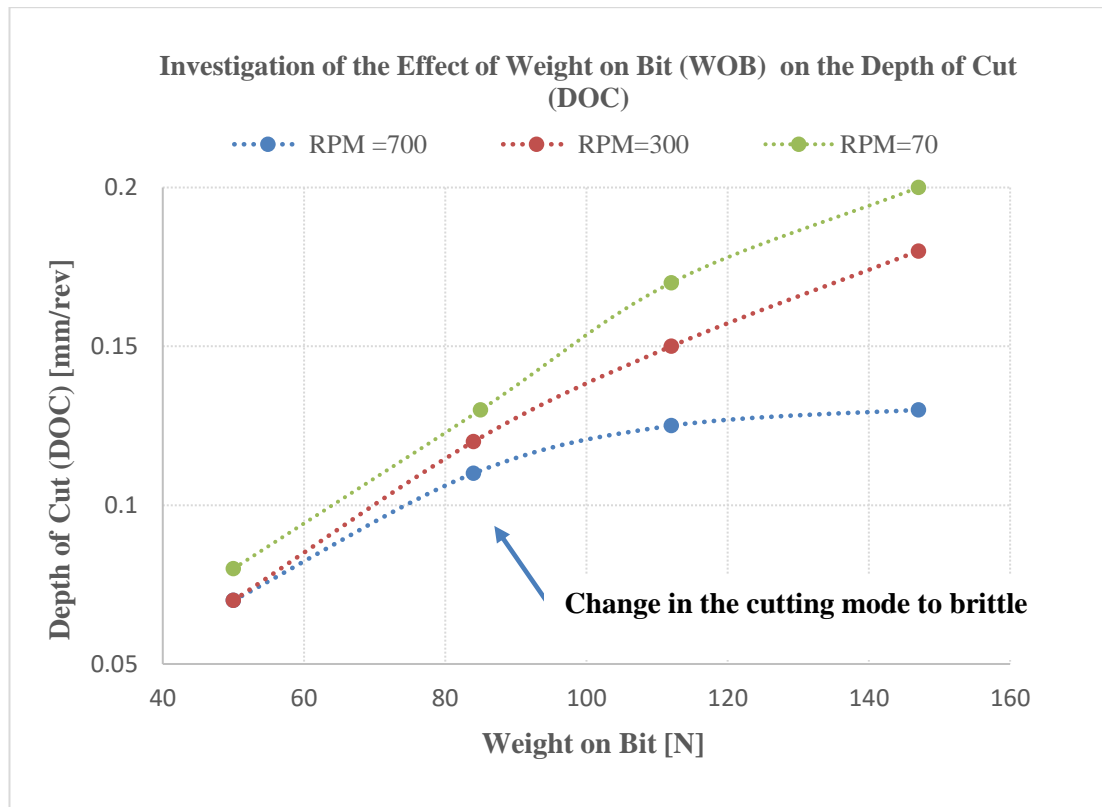


Figure 7.13: Plot of DOC versus WOB at different rotational speed

It can also be observed that lower values of rotary speed increase the DOC to maximum. This is true as the bit cutters are able to penetrate into the rock at much lower rotational speed than higher rotational values if the weight on bit is maintained the same. In the same vein the effect of increasing the rotation speed shows reduction in the depth of cut at different values of weight on bit (WOB). Therefore, a hard formation is better drilled with a low rotary speed than a high rotary speed.

7.4.5 Investigation on the Effect of change in rotational speed on rock bit interaction.

The investigation on the effect of change in rotational speed on at different values of WOB is shown in Figure 7.14. It was observed at lower WOB higher values of RPM are possible but every much limited at higher WOB (Figure 7.14)

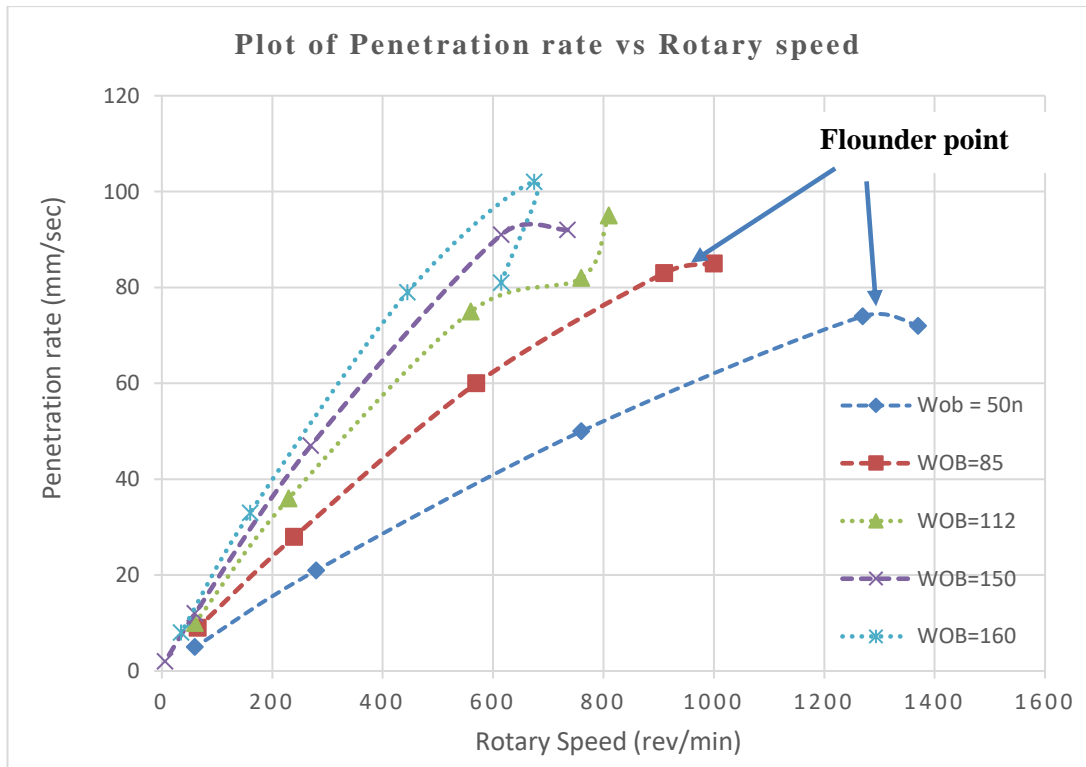


Figure 7.14: Plot of DOC versus RPM at different rotational speed

It can be observed from figure 7.14 higher depth of cut are achieved at lower rotational speed as depth of cut is seen to reduce with increasing rotational speed. Furthermore, since depth of cut is defined as penetration rate per revolution, the plot shows that penetration rate increases with increasing rotational speed. A similar separation showing the frictional and brittle dominant phase is clearly shown in the plot as well, the effect of rotary speed on penetration rate at different weight on bit

The graph shows that all values of rotary speed, increase in weight on bit (WOB) results in increase in penetration rate until a founder point is reached. A founder point is that point at which this relation does not hold. It can also be observed that at low weight on bit (50 N) endured a much longer range of rotary speed before the flounder point at 1200rpm. But at high weight on bit (160 N) the founder point will be reached at rotary speed of 675rpm. Therefore, it is evident that the founder point varies with the operating parameters and precedes the maximum penetration rate the set of parameters can achieve. Hence in the traditional drilling system a drill-off test is usually performed to identify this point and to maximum the penetration rate with the selected set of operating parameters.

7.5 Section Summary

Having performed drilling of cement plug using the designed rotary drilling rig, this section is aimed to observe rock-bit interactions in rotary drilling and subsequently observe the dynamic relationship between the input and output drilling parameters. The predictive trends observed in the data analytic part of this work. The experimental studies of the rock-bit interaction demonstrated two main drilling modes; the frictional-dominant and the cutting dominate mode.

1. The frictional mode is characterized with a very low penetration rate at low rotary speed as the rotary speed was just sufficient to overcome the frictional force due to rock-bit interaction. The cutting dominant mode occurs at higher energy in the drillstring , more (WOB, RPM) with more useful work done in the rock breaking process.

2. The experimental investigation also supports the maximum rotary speed is not the optimal as it reduces the depth of cut and increases the wear and tear of the drillstring. Therefore, the optimum rotary speed which lies with the minimum and maximum should be explored using drill-off test and/ or other optimization procedures.

The study further highlights the benefits of water (drilling fluid) during the rotary drilling process as it reduces the drillstring friction and reduces heat generated by two solid surfaces whilst rotating the drillstring. The absences of the drill fluid pose a risk of damaging the drill bit and poor cleaning of the bit face.

3. Each cement plug was drilled with a constant weight on bit which means that (the same speed of the hoisting system was maintained) for the entire distance drilled. For another weigh on bit a different cement plug with a change in the hoisting system longitudinal speed this ensure the weight on bit was constant for the run.
4. Drilling experiment performed for ROP optimization reveals valuable information about the searching of the optimal drilling parameters and need to have a benchmark to measure how relative performance to the technical limit is measured
5. The drilling of cement confirms that the point of flounder which states that higher weight on bit does not necessarily translate to higher penetration rate. At Flounder point, increase in the weight on bit actual reduces the penetration rate and causes higher stress and damage to the drilling tools.

Chapter 8

Conclusion and Future work

8.1 Conclusion

This thesis was aimed at developing predictive optimization models for an autonomous rotary drilling system. It explored the fascinating opportunities that arise when machine learning is applied to solving drilling optimization problems. The applicability of the concepts in efficient ROP prediction, UCS estimation and decision-making process in a non-linear rock drilling environment. The conclusions are provided based on research objectives as follows.

i) **Appropriate tuning parameters and their predictive performance**

Evaluation of appropriate tuning parameters and their predictive performance for self-optimizing autonomous rotary drilling systems using an artificial neural network (ANN) with actual surface operating parameters and their derived controllable energy variables. The following conclusions are reached based on the study.

- The direct use of actual surface operating parameters (WOB, RPM) as tuning parameter for autonomous system, produced a poor ROP prediction for drill rate with coefficient of determination (R^2) of 0.74, RMSE of 28 and AAPE of 106 with well-P05 dataset, suggesting the inadequacy of using these two parameters alone as tuning parameters. However, the use of derived variables (DMSE, FET) as tuning parameter gave an excellent prediction accuracy with coefficient of determination (R^2) of 0.98, RMSE of

- 7.6, and AAPE of 34 using same well-P05 dataset. Therefore, derivative variables are better and should be used as tuning parameters. The result supports the decision to use the data driven (ANN) model with derived controllable variables in the quantitative prediction of drilling rate for an autonomous drilling system.
- The precise quantitative relation between derived variables and rate of penetration will improve parameter optimization, operational efficiency, and equipment reliability.

ii) Prediction of rock strength and Maximum Achievable ROP model

To better understand the fundamental principles behind the rock-bit interaction and rock failures, which is modeled by evaluating the drilling forces for various values of rate of penetration (ROP using machine learning approach.

- To avoid misinterpreting the performance of the autonomous system by a robust model that can accurately predict instantaneous unconfined compressive strength (UCS) of heterogenous rock at the bit. It is recommended to have a benchmark system for assessing the quality perceived by a user.
- The ML methods applied in UCS prediction is globally applicable, based on fundamental principles and requires little initial calibration. Which improved the existing empirical methods that require calibration of the empirical model estimation with experimental core data or fracture pressure test on every formation stratum to improve the prediction accuracy.
- The model performance of both the ANN and Catboost algorithm showed sufficient accuracy for a qualitative UCS measurement within acceptable margin of errors. The overall performance can be further improved by additional logging datapoints

- (e.g Sonic, NPHI, RBOH) whenever available.
- The new method enables improved decision whilst drilling in many areas including determination of formation tops, early detection of reservoir core points and formation stratigraphic sequence

iii) Decision-making model for autonomous drilling system

- It is demonstrated that drill-off testing can be formulated as an MDP which intermittently analyzes a batch real-time data using Q-value algorithm to select the pair of surface operating parameters (WOB, RPM) that yield the maximum value on each episodic set.
- Modeling of experiment data showed that the proposed approach can improve decision process and realize the optimal value function irrespective of the initial state conditions.
- This research could be used as a decision-making tool in drilling operations that could provide an engineered approach for optimal operating parameter selection and improvement in the efficiency of the drilling process in terms of cost and time.

The result confirmed the obvious fact that it is neither the maximum nor the minimum operating parameters that yield the optimum result. But the optimum operating lies within the limits and can be achieved by exploration. Interestingly this optimum operating condition changes with changing environmental conditions and must therefore be explored dynamically throughout the duration of the drilling process.

iv) Investigation of the rock-bit interaction

Finally, study of the rock-bit interaction through experimental studies

The crucial tuning variables are the speed of descend of the drillstring which is a function of ROP and rotary speed energy in the drilling system.

It was observed at lower values of WOB alters the liner relationship that exist between ROP and higher WOB. At lower values of WOB a transition zone exists between the frictional dominant mode to the rock cutting mode.

The lower value of rotary speed increases the depth of cut (DOC). This is true as the bit cutters .can penetrate the rock at much lower rotational speed than higher rotational values if the weight on bit is maintained the same.

8.1 Summary of Conclusion

This work focused development of predictive optimization model for autonomous system The summary of findings in Table 4.10

Research Objectives	Options	Variables	Current practice	Research Results & Contribution
Determination of appropriate tuning parameters.	Actual Surface Parameter (WOB, RPM) with ROP	WOB, RPM	Increase in WOB, RPM denotes, increase in energy in the drilling system.	The non-linear relationship between WOB & RPM are susceptible to environmental factors such as hole drag and flounder points and not a good tuning parameter.
	Derived Controllable Variables (DMSE, FET) with ROP	DMSE, FET	Increase in WOB, RPM denotes, increase in energy in the drilling system.	Decrease in DMSE and Increase in FET results in increase in drill rate. This is not affected by environmental factors and constraints. Therefore, a suitable tuning parameter for autonomous system.
Predictive ROP Model for autonomous drilling system	Physics Based Models (PBMs)	Maurer model Bingham model B&Y model	Physics Based Models; includes (Maurer, B&Y, Bingham). In use, intermittently halt drilling to perform drill-off test to estimate formation coefficient	Maurer [$R^2=0.50$, RMSE=30] Bingham [$R^2=0.51$, RMSE=37] B&Y [$R^2=0.70$, RMSE=28] PBMs are data fitting model as formation coefficient are required to fit the model with poor accuracy in heterogenous formation.
	Data driven model (ANN) Model	ANN Model	Recent and proven technology but low application in drilling operation. Suitable for drilling automation with the benefit of big drilling data.	ANN [$R^2=0.98$, RMSE=5.8] ANN models offer the best solution, with dynamic functional relationship between input and output. The model learn by feature engineering from past events.
Real-time prediction of Instantaneous UCS Whilst drilling in an autonomous system	Core samples and empirical model using logging while drilling data	Force, Area, transit time (At)	Slowly coring technique without continuous profile of the rock UCS. Although Sonic will provide contious profile, but data is delayed due to sensor distance from the bit	UCS from core sample provides the most accurate measurement but limited due to the costly coring operation at limited sample. Both techniques unable to provide real-time instantaneous UCS required whilst drilling.
	ML Prediction of UCS from basic drilling parameters,	WOB,RPM, TOR,ROP	Acceptable Instantaneous UCS prediction within margin of error.	ANN Model performance result [$R^2=0.77$, RMSE= 0.420] Catboost [$R^2=0.70$, RMSE= 0.095]. Acceptable instantaneous UCS

8.1 Conclusion

Table 4.10 : Summary of results for ROP modeling.

Research Objectives	Options	Variable / parameters	Current practice	Research Results & Contribution
Estimation of maximum Achievable ROP Model	Use of best offset drilled well in the field	Offset well ROP	Use of offset well performance as performance benchmark in the current well	The non-linear relationship between WOB & RPM are susceptible to environmental factors such as vibration, formation change, flounder points.
	Evaluating dynamic relationship between DMSE, FET with ROP	Derivatives of WOB, RPM	The application of instantaneous UCS in the determination of optimum achievable ROP	Drilling efficiency occurs at the occurs at the region at the region of lowest DMSE
Evaluate decision making model for autonomous drilling system	Tradition manual system based on intuition and trial and error method	Manual (WOB, RPM)	Driller Performs drill-off set to select optimized parameters	Time consuming and often time uses sub-optimal parameters during most drilling operation.
	Continuous drill-off test using reinforcement learning algorithm	ANN Model	Recent and proven technology but low application in drilling operation. Suitable for drilling automation with the benefit of the big drilling data.	Demonstrates that drill-off testing can be formulated as an MDP which intermittently analyzes a batch real-time data using Q-value algorithm. The sequential decision model recursively select the optimal operating parameters that yield the optimum result.
Real-time drilling input variables vs derived variables in optimizing performance of an autonomous system	Tuning input for ANN[WOB, RPM]	WOB, RPM	Several models with 4 – 8 input drilling variables which is not suitable for autonomous system	Model performance result [$R^2= 0.74$, RMSE=28]
	Tuning input for ANN [DMSE, FET]	DMSE, FET	The concept first introduced in this research.	Model performance result [$R^2= 0.98$, RMSE=7.8] Better accuracy and low prediction error

8.2 Future work

This work has highlighted essential features of self-optimizing autonomous rotary drilling system and rock fracture mechanics. It will be interesting to carry out further studies in the areas described below to have an in-depth understanding of the phenomena: A full scale laboratory rig in the context of a drilling rig could be setup with similar instrumentation and controller system to observe the automatic drilling parameter management. All the experiments in this study were carried out at surface conditions at atmospheric temperature and pressure. The full-scale rig can be used to simulate confining pressure, in the presence of a circulating drilling fluid, whilst testing the rock failure mechanism in greater detail. A variety of actual rock samples with varying mechanical property (interbedded) are to be used for the cutting test along with using different types of drill bits such roller cone bit and PDC bit. It will be interesting to model the vibration effect by the inclusion of accelerometer and magnetometer sensors. The findings on the prediction of the formation unconfined compressive strength using basic drilling parameters and machine learning tools was phenomenal. Would develop the lesson learned with the modelling of the UCS prediction and real-time penetration rate benchmark while drilling with regional study to ascertain global conformance. The current investigation was performed with dataset from the North Sea continental shelf. On the evaluation of decision making using the Markov Decision Process (MDP), would recommend a comparative study between the Proportional Integral Derivative (PID) controller and with MDP controller to compare performance. Since the PID is a commonly used controller by control engineers in both domestic and industrial control systems.

Appendix A1 List of Nomenclatures

No.	Term	Definition	Unit
1	A_{abr}	Relative abrasiveness	f_c
2	d_b	Diameter of the bit	in.
3	D	Depth	m
4	DOC	Depth of Cut	-
5	DTOR	Downhole Torque	Kft.lbs
6	WOB	Weight on Bit	Klbs
7	ECD	Equivalent Circulation Density	pcf
8	EMQ pore	Equivalent Mud Weight	pcf
9	F	Force	N
10	F_1	Formation strength effects	N
11	F_2 & F_3	Compaction effects	N
12	F_4	Overbalance effects	N
13	F_5 & F_6	Rotary speed & bit weight effects	N
14	F_7	Tooth wear effects	N
15	F_8	Bit hydraulic effects	N
16	FD	Footage Drilled by Bit	ft.
17	F_j	Impact factor	lb
18	F_{jm}	Modified impact force	lbf
19	h_i	The output function of the ith hidden node	-
20	GPM	Gallon Per Minute	Gal/min
21	HMSE	Hydraulic Mechanical Specific Energy	Psi
22	k	Drill ability constant	N
23	DMSE	Drilling Mechanical Specific Energy	KPsi
24	NPT	Non-Productive Time	-
25	P_e	Chip hold down function	lbf
26	PID	Proportional Integral Derivative Controller	-
27	Q	Mud Flow-in-rate	Gpm
28	ROP	Rate of Penetration	ft/hr
29	RPM	Revolution Per Minutes	Rev/min
30	UCS	Unconfined compressive strength	KPsi
31	T trip	Round trip time, i.e. time-part contractor	hr
32	T bit	Bit life, i.e. time required to drill the interval	hr
33	T lost	time chargeable to non-drilling task	hr
34	TVD	True Vertical Depth	ft.
35	Y	Mud viscosity	cP
36	a, b & c	Constant of the bit	-
37	β_i	The output weight	-
38	Δ PB	Pressure Loss at Bit	Psi
39	τ	Surface Torque	Kft.lb
40	φ	Feed Rate	m/sec
41	y_i	output function of the ith hidden node	-
42			

Appendix A2 List of Acronyms

Term	Acronyms
AAPE	Average Absolute percentage error
AI	Artificial Intelligence
ANN	Artificial Neural Network
ASP	Actual Surface parameter
ANFIS	Adaptative Neuro Fuzzy Inference
BHA	Bottom Hole Assembly
CPU	Computer Processing Unit
CIT	Computational Intelligence Techniques
DCV	Derived Controllable variable
Dia	Diameter
DEO	Drilling Efficiency Optimization
DMSE	Drilling mechanical specific energy
ELM	Extreme Learning Machine
FET	Feed Thrust
GA	Genetic Algorithms
GLC	Generalized Linear Classifier
GR	Gamma-ray
IADC	International Association of Drilling Contractors
LWD	Logging While Drilling
LS-SVR	Least Square Support Vector Regression
MATLAB	Matrix Laboratory
MD	Measured Depth
ML	Machine Learning
MLP	Multi-Layer Perceptron
MWD	Measurement While Drilling
NPT	Non-Productive Time
PDA	Predictive Data-driven Analysis
PDC	Polycrystalline Diamond Compact
PDM	Predictive Data-driven modelling
QRP	Quantitative real-time prediction
RBF	Radial Basis Function
RMSE	Root Mean Square Error
ROP	Rate of penetration
RPM	Revolution per Minute
SVR	Support vector Regression
WWSLM	Wider Windows statistical learning models

Appendix B Field Drilling Mechanics Data

Table B.1 (7400-8800ft)– Field Drilling Mechanics data for **Well P05** for rate of penetration modeling

No.	Depth (ft)	ROP. (ft/hr)	WOB (Klbs.)	Torque. (Kft-lb)	RPM (rev/m)	No.	Depth (ft)	ROP. (ft/hr)	WOB (Klbs.)	Torque. (Kft-lb)	RPM (rev/m)
1	7400	10.86	18.79	16.61	125	40	8400	32.26	26.29	19.69	126
2	7430	9.91	20.49	18.02	120	41	8430	45.24	35.24	19.14	115
3	7460	22.83	25.00	18.44	114	42	8460	63.21	50.11	20.55	123
4	7490	16.13	230.69	16.42	106	43	8490	66.54	36.66	22.53	123
5	7520	17.86	237.01	0.02	1	44	8520	38.78	45.57	20.88	123
6	7550	50.92	35.27	20.22	125	45	8550	28.70	42.23	19.13	113
7	7580	104.18	50.97	23.89	136	46	8560	17.07	36.73	19.12	110
8	7610	89.42	62.44	22.76	139	47	8570	40.03	20.70	20.62	111
9	7640	89.25	48.64	22.36	140	48	8580	28.50	30.86	20.29	113
10	7670	88.22	52.08	21.98	142	49	8590	13.60	54.16	20.71	112
11	7700	141.80	62.51	23.84	141	50	8600	7.29	66.61	18.63	91
12	7750	98.04	36.76	22.32	146	51	8610	17.29	43.62	19.94	119
13	7780	82.96	48.75	22.77	140	52	8620	17.31	49.90	19.82	119
14	7810	137.87	47.89	23.84	134	53	8630	10.82	32.27	17.57	113
15	7840	96.18	52.95	22.91	137	54	8640	7.21	48.58	17.85	94
16	7870	163.39	66.59	23.85	138	55	8650	26.28	12.44	21.73	123
17	7900	130.18	56.35	24.02	140	56	8660	6.11	28.03	18.35	116
18	7930	124.33	57.68	23.03	138	57	8670	7.53	40.00	20.86	114
19	7960	78.94	52.84	20.57	136	58	8680	11.85	22.82	18.46	120
20	7990	106.13	47.91	24.39	115	59	8690	10.10	34.30	18.08	123
21	8020	67.82	46.05	21.29	125	60	8700	9.10	33.07	19.38	134
22	8050	43.44	40.92	22.44	116	61	8710	8.43	35.00	19.76	128
23	8080	52.12	45.70	23.38	122	62	8720	17.05	62.16	20.57	121
24	8110	103.57	45.06	24.04	114	63	8730	24.44	42.38	21.23	134
25	8160	17.91	48.10	19.16	116	64	8740	9.10	33.92	17.51	121
26	8190	14.24	42.99	19.21	118	65	8750	5.60	19.49	19.40	129
27	8220	17.24	37.38	19.89	96	66	8760	14.46	54.84	20.41	124
28	8250	30.39	33.12	19.24	118	67	8770	37.35	61.24	19.34	121
29	7400	10.86	18.79	16.61	125	68	8780	71.05	36.36	23.08	118
30	7430	9.91	20.49	18.02	120	69	8790	10.06	56.16	18.94	128
31	7460	22.83	25.00	18.44	114	70	8800	7.50	46.62	17.62	134
32	7490	16.13	230.69	16.42	106	71	8810	28.77	16.15	20.56	128
33	7520	17.86	237.01	0.02	1	72	8820	36.88	38.14	21.18	124
34	7550	50.92	35.27	20.22	125	73	8830	9.47	16.03	18.72	128
35	7580	104.18	50.97	23.89	136	74	8840	25.57	31.11	21.34	132
36	8280	15.75	46.84	19.75	120	75	8850	25.94	41.62	18.70	133
37	8310	22.62	41.39	20.62	124	76	8860	54.99	44.18	23.55	135
38	8340	40.67	30.76	20.35	120	77	8870	78.48	40.60	24.56	133
39	8370	19.64	50.69	20.27	115	78	8880	55.03	39.80	23.75	120

Table B.1 Continued (8800-960ft)-

No.	Depth (ft)	ROP. (ft/hr)	WOB (Klbs.)	Torque. (Kft-lb)	RPM (rev/m)	No.	Depth (ft)	ROP. (ft/hr)	WOB (Klbs.)	Torque. (Kft-lb)	RPM (rev/m)
78	8800	7.50	47	17.62	134	118	9170	6.77	48	20.72	126
80	8810	28.77	16	20.56	128	119	9180	7.76	33	19.81	124
81	8820	36.88	38	21.18	124	120	9190	16.47	36	21.11	129
82	8830	9.47	16	18.72	128	121	9200	8.58	30	19.31	129
83	8840	25.57	31	21.34	132	122	9220	3.40	33	17.08	82
84	8850	25.94	42	18.70	133	123	9230	1.26	57	15.66	103
85	8860	54.99	44	23.55	135	124	9240	12.77	58	19.25	108
86	8870	78.48	41	24.56	133	125	9250	1.03	40	14.11	70
87	8880	55.03	40	23.75	120	126	9260	6.04	41	19.82	105
88	8890	62.84	40	23.59	131	127	9270	6.90	41	18.84	120
89	8900	56.51	45	23.85	123	128	9280	6.11	37	18.60	109
90	8910	59.17	43	23.54	128	129	9290	7.44	50	18.48	99
91	8920	33.64	54	21.77	142	130	9300	1.14	51	17.79	101
92	8930	49.03	52	23.07	142	131	9310	13.24	34	19.48	113
93	8940	21.76	59	19.79	138	132	9320	7.33	61	14.77	88
94	8950	8.57	40	17.67	98	133	9330	6.16	12	16.58	79
95	8960	10.24	38	19.28	111	134	9340	27.97	27	22.17	108
96	8970	20.50	39	21.43	136	135	9350	36.93	30	24.27	117
97	8980	12.55	38	19.91	122	136	9360	43.61	38	26.78	112
98	8990	10.70	39	18.49	112	137	9370	33.75	30	23.24	142
99	9000	9.24	36	18.44	98	138	9380	74.14	33	24.15	140
100	9010	8.31	43	21.07	125	139	9390	25.74	24	21.73	141
101	9020	16.84	40	17.22	121	140	9400	51.94	12	24.18	130
102	9030	18.73	38	23.79	139	141	9410	86.48	25	25.16	137
103	9040	9.11	48	17.19	92	142	9420	72.78	23	25.52	141
104	9050	14.13	47	18.58	123	143	9430	89.63	21	26.15	135
105	9060	4.87	21	19.27	88	144	9440	16.99	8	18.51	129
106	9070	25.58	34	21.02	117	145	9450	34.95	22	22.11	141
107	9080	6.28	36	16.90	84	146	9460	27.02	18	21.73	125
108	9090	13.99	35	19.87	107	147	9470	21.59	21	21.55	125
109	9100	5.32	56	16.95	86	148	9480	15.09	31	22.02	130
110	9110	8.00	21	21.92	108	149	9490	31.71	24	21.60	134
111	9120	11.49	36	21.11	91	150	9500	18.53	33	21.39	128
112	9130	17.01	45	19.31	86	151	9510	23.58	29	21.45	126
113	9140	2.61	50	16.54	83	152	9520	50.52	25	21.79	135
114	9150	2.02	39	16.10	78	153	9530	6.62	25	18.81	119
115	8800	7.50	47	17.62	134	154	9540	5.59	23	22.74	132
116	8810	28.77	16	20.56	128	155	9550	8.15	32	18.76	121
117	8820	36.88	38	21.18	124	156	9560	25.85	27	23.58	133

Table B.2 – Field Drilling Mechanics data for **Well W1** for rate of penetration modeling

No.	Depth (ft)	ROP. (ft/hr)	WOB (Klbs).	Torque. (Kft-lb)	RPM (rev/m)	No.	Depth (ft)	ROP. (ft/hr)	WOB (Klbs).	Torque. (Kft-lb)	RPM (rev/m)
1	5606	142.45	26.17	8.23	150	40	7702	101.66	23.81	9.90	185
2	5754	107.36	19.83	7.50	147	41	7712	124.40	28.70	11.17	185
3	5813	84.71	18.35	7.22	147	42	7722	104.63	23.99	10.59	185
4	5901	137.95	12.43	7.99	147	43	7731	113.17	23.27	11.46	184
5	6019	83.97	8.02	7.60	147	44	7741	138.45	8.63	10.53	184
6	6144	162.84	31.27	8.81	145	45	7751	119.76	24.75	10.42	184
7	6153	78.74	23.92	8.80	144	46	7898	140.78	27.60	9.04	148
8	6311	174.06	49.71	8.78	148	47	7908	75.20	17.12	8.85	148
9	6321	147.54	45.81	8.39	146	48	7918	81.89	14.02	8.77	148
10	6449	162.31	6.56	11.32	138	49	7928	67.67	19.05	10.07	147
11	6458	148.68	9.38	12.19	134	50	8075	85.23	10.70	9.11	149
12	6600	149.48	22.16	11.50	143	51	8712	41.19	22.18	10.76	176
13	6609	158.28	19.34	9.93	146	52	8722	28.95	22.05	10.66	179
14	6619	149.16	14.63	8.80	149	53	8948	50.88	23.67	12.58	157
15	6777	72.18	18.56	13.44	159	54	8958	51.69	22.53	12.04	178
16	6787	117.01	5.63	9.37	171	55	8968	44.41	18.39	10.66	180
17	6885	112.53	18.09	9.39	181	56	8978	38.28	15.49	10.44	178
18	6888	94.82	19.09	8.61	180	57	9194	22.06	19.50	10.47	179
19	6889	97.33	18.30	8.97	181	58	9204	26.74	13.10	10.71	179
20	6889	100.77	14.98	9.34	179	59	9214	33.27	13.10	10.82	178
21	6898	169.37	18.56	9.42	180	60	9224	35.14	20.55	11.78	177
22	6908	122.78	7.61	8.68	180	61	9234	23.79	10.56	10.46	178
23	6918	83.49	14.32	9.27	180	62	9234	23.94	13.33	12.55	170
24	6928	262.08	17.90	8.70	180	63	9243	25.70	9.16	12.48	175
25	7033	144.09	22.39	9.06	177	64	9253	39.25	16.10	11.79	176
26	7042	110.91	12.00	9.18	181	65	9263	33.22	26.09	9.93	179
27	7052	75.85	27.18	8.28	181	66	9273	39.55	13.83	10.86	179
28	7180	95.75	30.37	8.27	179	67	9283	25.55	17.65	9.97	178
29	7289	64.05	32.24	8.84	179	68	9578	47.34	16.60	10.71	180
30	7298	152.73	17.47	8.82	179	69	9588	40.48	19.15	10.66	180
31	7308	109.48	19.41	9.09	178	70	9598	35.62	19.21	12.28	178
32	7318	145.16	17.32	8.27	178	71	9608	30.24	20.30	12.63	179
33	7328	57.47	19.90	9.48	178	72	9614	41.24	25.03	10.66	178
34	7338	93.70	25.71	8.62	178	73	9755	22.71	28.00	12.34	174
35	7348	101.16	37.76	9.04	179	74	9765	23.50	30.00	11.12	174
36	7357	70.73	16.95	8.54	178	75	9765	15.33	12.27	9.77	175
37	5606	142.45	26.17	8.23	150	76	9766	14.89	20.52	10.05	174
38	5754	107.36	19.83	7.50	147	77	9766	15.78	20.98	12.18	175
39	5813	84.71	18.35	7.22	147	78	9767	15.79	20.91	10.52	176

Table B.2 – Field Drilling Mechanics data for Well W1 for rate of penetration modeling

No.	Depth (ft)	ROP. (ft/hr)	WOB (Klbs).	Torque. (Kft-lb)	RPM (rev/m)	No.	Depth (ft)	ROP. (ft/hr)	WOB (Klbs).	Torque. (Kft-lb)	RPM (rev/m)
78	9807	23.09	17.43	11.96	177	118	10009	19.01	16.48	11.86	176
80	9812	23.14	32.95	10.99	178	119	10067	51.53	17.47	12.62	180
81	9813	21.79	31.06	11.43	179	120	10068	49.76	19.14	12.02	181
82	9813	23.12	29.17	11.68	179	121	10068	48.14	20.51	11.33	181
83	9814	23.44	30.66	11.52	175	122	10069	48.29	24.75	13.51	182
84	9814	22.49	27.64	11.37	178	123	10069	49.87	23.31	12.93	181
85	9826	19.13	28.21	11.91	178	124	10070	53.23	26.96	13.02	180
86	9826	19.55	22.00	12.88	179	125	10070	55.72	27.87	10.81	181
87	9827	20.57	29.32	11.78	179	126	10087	65.56	28.17	12.94	183
88	9827	21.95	26.60	11.93	178	127	10087	67.85	32.78	13.12	179
89	9828	22.23	35.56	10.29	178	128	10088	61.41	22.62	11.09	181
90	9828	29.17	22.72	12.50	178	129	10088	66.15	18.27	10.86	181
91	9841	24.19	30.92	13.69	175	130	10089	57.14	20.35	10.07	180
92	9841	26.11	32.91	13.64	181	131	10184	45.82	40.57	12.75	181
93	9842	29.17	22.93	10.63	179	132	10184	44.23	41.90	13.56	175
94	9842	27.62	28.39	10.57	178	133	10185	38.98	39.86	13.51	169
95	9843	27.78	34.37	11.16	179	134	10185	34.10	32.67	12.12	182
96	9843	28.63	33.99	11.89	179	135	10186	32.74	36.70	13.28	177
97	9858	23.57	22.17	9.86	180	136	10186	34.91	35.30	12.96	181
98	9858	22.23	29.97	9.93	181	137	10187	30.47	26.68	11.39	182
99	9859	22.36	35.97	11.40	181	138	10215	19.12	29.43	12.73	180
100	9859	23.40	35.28	10.98	181	139	10243	25.25	26.11	13.37	177
101	9860	23.57	38.46	10.71	181	140	10284	48.94	27.25	14.97	173
102	9860	27.45	42.77	11.75	182	141	10800	61.01	13.60	12.02	177
103	9861	26.32	40.37	10.85	181	142	10947	128.84	35.19	13.04	182
104	9861	25.00	31.80	11.87	182	143	11020	46.94	18.98	11.46	179
105	9871	18.47	34.63	11.13	181	144	11065	66.79	5.26	9.66	179
106	9871	18.10	35.34	14.89	151	145	11210	27.76	7.71	10.62	180
107	9872	19.94	26.02	15.71	159	146	11375	84.98	11.97	10.33	164
108	9872	22.56	34.96	13.69	174	147	11520	54.88	31.41	11.36	177
109	9873	22.46	30.29	11.54	181	148	11640	13.04	18.13	10.59	146
110	9879	23.21	40.63	11.89	182	149	11647	7.13	22.85	10.43	19
111	9880	23.94	26.74	9.99	179	150	11648	6.96	24.49	11.35	43
112	9880	16.55	33.74	10.67	178	151	10009	19.01	16.48	11.86	176
113	9881	16.15	28.76	12.84	179	152	10067	51.53	17.47	12.62	180
114	9881	16.93	29.88	13.62	172	153	10068	49.76	19.14	12.02	181
115	9890	26.87	32.91	12.59	172	154	10068	48.14	20.51	11.33	181
116	9890	26.94	27.10	10.27	177	155	10069	48.29	24.75	13.51	182
117	9891	27.87	25.63	12.01	178	156	10069	49.87	23.31	12.93	181

Table B.3 – Field Drilling Mechanics data for Well-2 for Formation UCS Prediction while Drilling

No.	Hole Depth (ft)	ROP. (ft/hr)	WOB (Klbs).	Torque. (Kft-lb)	RPM (rev/m)	NPHI	UCS. (Oyler) (Kpsi)	UCS (CB) (Kpsi)	DMSE (Kpsi)	UCS (DMSE) (Kpsi)
1	10416	21.93	2.48	16.11	130	0.100	11607	11.73	79.34	27.77
2	10430	27.56	2.43	16.80	130	0.106	10705	11.00	66.05	23.12
3	10471	16.16	2.96	13.88	130	0.114	14534	14.06	92.45	32.36
4	10481	13.39	3.76	14.07	130	0.139	10737	10.73	113.17	39.61
5	10491	13.39	10.66	13.81	129	0.166	8016	8.36	110.85	38.80
6	10501	12.94	11.51	14.65	130	0.118	12157	12.00	121.78	42.62
7	10521	13.33	10.54	16.06	130	0.120	9913	10.24	129.86	45.45
8	10530	18.77	11.89	15.92	129	0.107	11681	10.46	91.23	31.93
9	10540	19.85	10.74	15.09	130	0.105	12356	12.12	81.89	28.66
10	10550	19.51	9.04	14.19	130	0.134	8577	8.67	78.36	27.42
11	10571	37.20	17.62	16.21	129	0.091	11920	12.26	46.88	16.41
12	10621	50.00	18.04	17.75	130	0.101	11694	11.83	38.36	13.43
13	10640	58.82	21.81	18.54	130	0.105	11052	10.54	34.07	11.93
14	10660	64.52	20.88	18.23	130	0.118	9216	9.77	30.52	10.68
15	10662	65.22	20.36	17.92	129	0.126	9007	9.30	29.58	10.35
16	10663	65.45	20.19	18.56	130	0.140	8336	8.94	30.55	10.69
17	10665	65.45	20.12	18.51	130	0.148	8776	9.07	30.57	10.70
18	10667	65.22	21.49	20.52	129	0.127	9806	10.11	33.88	11.86
19	10668	65.34	21.01	17.83	129	0.118	10694	10.57	29.32	10.26
20	10670	65.22	22.64	18.08	130	0.106	11441	12.03	30.03	10.51
21	10671	65.22	21.97	18.19	130	0.107	11478	11.70	30.12	10.54
22	10673	64.06	21.30	19.12	129	0.114	9997	9.81	32.15	11.25
23	10675	64.29	21.98	20.10	129	0.112	11148	10.66	33.46	11.71
24	10676	64.40	21.56	18.32	130	0.110	11511	11.16	30.67	10.73
25	10681	64.28	20.91	19.91	129	0.135	7914	8.13	33.25	11.64
26	10683	64.57	25.88	18.77	130	0.099	13192	12.57	31.46	11.01
27	10701	64.63	21.04	17.38	129	0.149	8137	8.91	28.88	10.11
28	10801	65.22	19.05	20.18	129	0.142	7476	7.88	33.22	11.63
29	10840	64.63	15.64	18.71	130	0.149	8137	7.80	31.19	10.92
30	10860	81.45	18.17	19.40	129	0.128	9908	9.44	25.56	8.94
31	10881	81.60	18.84	19.55	130	0.129	10591	9.75	25.84	9.04
32	10921	81.82	16.96	18.60	129	0.148	7968	7.96	24.46	8.56
33	10940	81.82	17.53	18.87	130	0.139	8237	8.25	24.94	8.73
34	10960	97.60	20.23	20.07	129	0.157	8038	8.66	22.12	7.74
35	11001	97.82	19.30	20.43	129	0.159	6993	6.99	22.42	7.85

Table B.4 – Field Drilling Mechanics data for Determination of Optimum ROP Baseline from Well-2

No.	Hole Depth (ft)	ROP. (ft/hr)	WOB (Klbs).	Torque. (Kft-lb)	RPM (rev/m)	NPHI	UCS. (Oyler) (Kpsi)	UCS (CB) (Kpsi)	ROP LBL (ft/hr)	ROP HBL (ft/hr)
1	10416	21.93	2.48	16.11	130	0.100	11607	11.73	46.36	57.95
2	10430	27.56	2.43	16.80	130	0.106	10705	11.00	51.73	64.66
3	10471	16.16	2.96	13.88	130	0.114	14534	14.06	33.20	41.50
4	10481	13.39	3.76	14.07	130	0.139	10737	10.73	44.14	55.17
5	10491	13.39	10.66	13.81	129	0.166	8016	8.36	55.50	69.38
6	10501	12.94	11.51	14.65	130	0.118	12157	12.00	41.04	51.30
7	10521	13.33	10.54	16.06	130	0.120	9913	10.24	52.82	66.02
8	10530	18.77	11.89	15.92	129	0.107	11681	10.46	51.13	63.92
9	10540	19.85	10.74	15.09	130	0.105	12356	12.12	41.89	52.36
10	10550	19.51	9.04	14.19	130	0.134	8577	8.67	55.11	68.89
11	10571	37.20	17.62	16.21	129	0.091	11920	12.26	44.41	55.51
12	10621	50.00	18.04	17.75	130	0.101	11694	11.83	50.60	63.25
13	10640	58.82	21.81	18.54	130	0.105	11052	10.54	59.33	74.16
14	10660	64.52	20.88	18.23	130	0.118	9216	9.77	62.91	78.63
15	10662	65.22	20.36	17.92	129	0.126	9007	9.30	64.75	80.94
16	10663	65.45	20.19	18.56	130	0.140	8336	8.94	69.78	87.23
17	10665	65.45	20.12	18.51	130	0.148	8776	9.07	68.85	86.06
18	10667	65.22	21.49	20.52	129	0.127	9806	10.11	68.16	85.20
19	10668	65.34	21.01	17.83	129	0.118	10694	10.57	56.53	70.66
20	10670	65.22	22.64	18.08	130	0.106	11441	12.03	50.78	63.48
21	10671	65.22	21.97	18.19	130	0.107	11478	11.70	52.41	65.51
22	10673	64.06	21.30	19.12	129	0.114	9997	9.81	65.51	81.88
23	10675	64.29	21.98	20.10	129	0.112	11148	10.66	62.98	78.73
24	10676	64.40	21.56	18.32	130	0.110	11511	11.16	55.23	69.04
25	10681	64.28	20.91	19.91	129	0.135	7914	8.13	82.01	102.51
26	10683	64.57	25.88	18.77	130	0.099	13192	12.57	50.42	63.03
27	10701	64.63	21.04	17.38	129	0.149	8137	8.91	65.36	81.69
28	10801	65.22	19.05	20.18	129	0.142	7476	7.88	85.76	107.20
29	10840	64.63	15.64	18.71	130	0.149	8137	7.80	80.69	100.87
30	10860	81.45	18.17	19.40	129	0.128	9908	9.44	68.83	86.04
31	10881	81.60	18.84	19.55	130	0.129	10591	9.75	67.43	84.29
32	10921	81.82	16.96	18.60	129	0.148	7968	7.96	78.42	98.03
33	10940	81.82	17.53	18.87	130	0.139	8237	8.25	77.13	96.41
34	10960	97.60	20.23	20.07	129	0.157	8038	8.66	77.75	97.19
35	11001	97.82	19.30	20.43	129	0.159	6993	6.99	97.85	122.32

Appendix C List of experiments

Table C.1 – List of Experiments with uniaxial test Machine

No.	Rock/ Core type	Definition	Unit
1	Cement Core	UCS	
2	Cement Core	UCS	
3	Cement Core	UCS	
4	Cement Core	UCS	
5	Cement Core	UCS	

Table C.2 – List of Experiments on 3.5in Drill bit on effect of Changing weight on Bit (WOB)

No.	Rock/ Core type	Rotational speed [RPM]	WOB [N]
1	Cement Core	70-100	50
2	Cement Core	70-100	85
3	Cement Core	70-100	112
4	Cement Core	70-100	147
5	Cement Core	70-100	160
6	Cement Core	300	50
7	Cement Core	300	85
8	Cement Core	300	112
9	Cement Core	300	147
10	Cement Core	300	160
11	Cement Core	700	50
12	Cement Core	700	85
13	Cement Core	700	112
14	Cement Core	700	147
15	Cement Core	700	160
16	Cement Core	900	50
17	Cement Core	900	85
18	Cement Core	900	112
19	Cement Core	900	147
20	Cement Core	900	160

Table C.3 – List of Experiments on 3.5in Drill bit on effect of Changing rotational speed (RPM) at constant weight on Bit

No.	Rock/ Core type	Weight on Bit (WOB)	Rotational speed [RPM]
1	Cement Core	50	1370
2	Cement Core	50	1270
3	Cement Core	50	760
4	Cement Core	50	280
5	Cement Core	50	60
6	Cement Core	85	1000
7	Cement Core	85	910
8	Cement Core	85	570
9	Cement Core	85	240
10	Cement Core	85	65
11	Cement Core	112	810
12	Cement Core	112	760
13	Cement Core	112	560
14	Cement Core	112	230
15	Cement Core	112	60
16	Cement Core	150	735
17	Cement Core	150	615
18	Cement Core	150	270
19	Cement Core	150	60
20	Cement Core	150	6

Appendix D Programming

D.1 : Reinforcement Learning code.

```
%% Load('MDP2')

I = 10; %number of iteration
K=5; %How many K
J=I;
V_int = zeros(I,1); % Intial V
n_end=10;
n_now=1;
v=V_int;
ind_all=[];

qi =[7161.82 7430.09 5009.24 2056.31 498.15;
8278.23 8500.39 6036.86 2827.92 854.43;
7831.99 9450.55 7471.69 3568.89 995.89;
9228.49 9141.06 4731.06 1192.48 142.72;
8061.25 10198.16 7858.75 3344.22 758.47;
8909.61 10270.01 6290.49 1871.15 262.34;
9622.59 10449.93 7090.61 2841.58 658.41;
10206.75 10166.77 5848.13 1845.82 313.76;
9206.44 10927.64 7327.75 2556.97 451.9;
9701.99 10842.65 6355.54 1810.01 244.43];

%rand(I,K); %values of p
qij = zeros(I,J,K); %values of pij
for k=1:K
    for i=1:10
        qij(i,:,k) =MDP2(5*(i-1)+k,2:end);
    end
end
%%
sumij=zeros(I,K);

v_all=zeros(I,n_end);

for n=n_end-1:-1:n_now
    for k=1:K
        sumij(:,k) = qi(:,k)+ qij(:, :,k)*v;
    end

    for i=1:I
        [v(i),ind]=max(sumij(i,:));
        ind_all(i)=ind;
    end
    v_all(:,n)=v;
    v_all(:,end)=ind_all;
end
```

D.2 : ANN Code for Neutral Network ROP Prediction

```
% Solve an Input-Output Fitting problem with a Neural Network
% for ROP Prediction using surface drilling parameters or derivatives
%
% This script assumes these variables are defined:
%
% data_1 - input data.
% data_2 - target data.

x = data_1';
t = data_2';
% Choose a Training Function
% For a list of all training functions type: help nntrain
% 'trainlm' is usually fastest.
% 'trainbr' takes longer but may be better for challenging problems.
% 'trainscg' uses less memory. Suitable in low memory situations.
trainFcn = 'trainlm'; % Levenberg-Marquardt backpropagation.

% Create a Fitting Network
hiddenLayerSize = 10;
net = fitnet(hiddenLayerSize,trainFcn);

% Setup Division of Data for Training, Validation, Testing
net.divideParam.trainRatio = 70/100;
net.divideParam.valRatio = 15/100;
net.divideParam.testRatio = 15/100;

% Train the Network
[net,tr] = train(net,x,t);

% Test the Network
y = net(x);
e = gsubtract(t,y);
performance = perform(net,t,y)

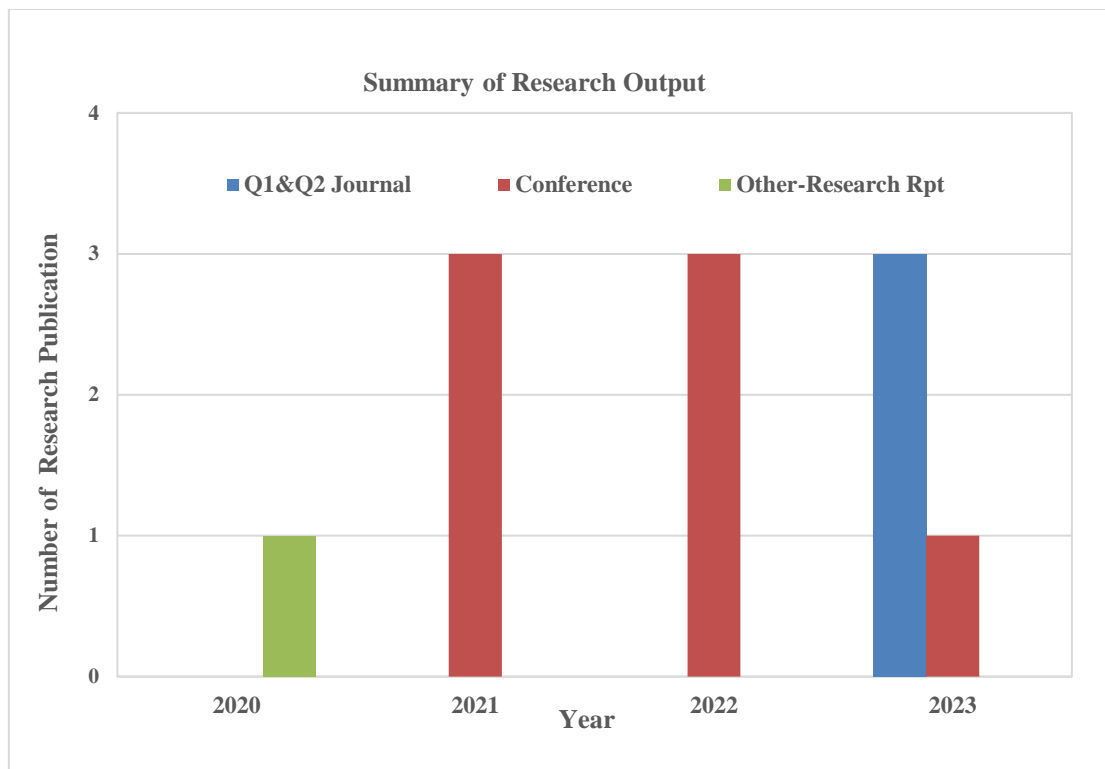
% View the Network
view(net)

% Plots
% Uncomment these lines to enable various plots.
%figure, plotperform(tr)
%figure, plottrainstate(tr)
%figure, ploterrhist(e)
%figure, plotregression(t,y)
%figure, plotfit(net,x,t)
```

Appendix E List of Published Work

1. **Amadi, K.W** Iyalla, I., Alsaba, M., Prahbu, R., Waly, M., (2023); Development of Predictive Optimization Model for Autonomous Rotary Drilling System Using Machine Learning Approach. *Journal of Petroleum Exploration and Production technology* (Q2)
2. **Amadi, K.W** Iyalla, I., Alsaba, M., Prahbu, R., Waly, M., (2023); Continuous Dynamic Drill-off Test Whilst Drilling Using Reinforcement Learning in Autonomous Rotary Drilling System. *European Journal of Engineering and technology research* (Q1)
3. **Amadi, K.W** Iyalla, I., Alsaba, M., Prahbu, R., Waly, M. (2023); Machine Learning Techniques for Real-time Prediction of Essential Rock Properties Whilst Drilling. Paper presented in NAICE Nigerian Annual International Conference and Exhibition, Lagos, Nigeria. 31 July – 3rd August 2023.
4. **Amadi, K.W**, Iyalla, I. Alsaba, M., Elgaddafi., Waly, M., (2022); Investigation of the Effect of Mud Lubricant on Drilling Mechanics. 2022 MedGU Annual Meeting and Conference, Marrakech 27-31st – Nov, 2022.
5. **Amadi, K.W** Iyalla, I., Alsaba, M., Prahbu, R., Waly, M., (2022); Continuous Dynamic Drill-off Test Whilst Drilling Using Reinforcement Learning in Autonomous Rotary Drilling System. 2022 ADIPEC Technical Conference & Exhibition, Abu Dhabi. October 31st – November 3rd
6. **Amadi, K.W** I. Iyalla, I Prahbu, R., (2021) Modelling and Predicting Performance of Autonomous Rotary Drilling System Using Machine Learning Techniques. 2021 NAICE Nigerian Annual International Conference and Exhibition, Lagos, Nigeria. 2-6 August 2021.

7. **Amadi, K., W.,** Iyalla, I., Liu, Y., Alsaba, M., Kuten, D., (2021); Evaluation of Derived Controllable Variables for Predicting ROP using Artificial Intelligence in Autonomous Downhole Rotary Drilling System 2021 SPE/IADC Middle East Drilling Technology Conference and Exhibition, Abu Dhabi, UAE.25-27 May 2021.



References

- ABBAS, A. K., RUSHDI, S. and ALSABA, M., 2018 "Modeling Rate of Penetration for Deviated Wells Using Artificial Neural Network," Abu Dhabi International Petroleum Exhibition and Conference (ADIPEC), Abu Dhabi, UAE, Nov. 12–15, Paper No. SPE-192875-MS. <https://doi.org/10.2118/192875-MS>
- ABDULRAHEEM A, AHMED M, VANTALA A, PARVEZ, T., 2009; Prediction of rock mechanical parameters for hydrocarbon reservoirs using different artificial intelligence techniques. In: SPE Saudi Arabia section technical symposium. Society of Petroleum Engineer. <https://doi.org/10.2118/126094-MS>
- AHMED, A.; ELKATATNY, S.; ALI, A.; MAHMOUD, M.; ABDULRAHEEM, 2018. A New Model Pore Pressure Prediction While Drilling Using Artificial Neural Networks. *Arabian J. Sci. Eng* 2018, 44, 6079–6088. <http://doi.org/10.1007/s13369-018-3574-7>
- AHMED, A. et al., 2019. New Model for Pore Pressure Prediction While Drilling Using Artificial Neural Networks. *Arabian Journal for Science and Engineering*, 44(6).
- AHMED, O., ADENIRAN, A. and SAMSURI, A., 2018. Rate of Penetration Prediction Utilizing Hydromechanical Specific Energy. *Drilling*.
- AKGUN, F. 2002. How to Estimate the Maximum Achievable Drilling Rate without Jeopardizing Safety. In Proceedings of the SPE-78567 MS Was Presented at Abu Dhabi International Petroleum Exhibition and Conference, Abu Dhabi, UAE, 13–16 October 2002. <https://doi.org/10.2118/78567-MS>
- Al Dushaishi, M. F., M. Alsaba, T, Tarshtoush (2021); Stick-slip investigation of dual drilling and reaming bottom hole assembly. *Proceedings of the Institution of Mechanical Engineers, Part C: Journal of Mechanical Engineering Science*. Volume 236, Issue 3 July 2021.
- ALFRED R. J. 1983. *Rock mechanics*. Clausthal-Zellerfeld, Federal Republic of Germany: Trans Tech Publications, Gulf Pub. Co., 2nd edition,
- AMADI, K.; IYALLA, I, PRABHU, R., ALSABA, M., WALY, M. 2022. Continuous Dynamic Drill-off Test Whilst Drilling Using Reinforcement Learning in Autonomous Rotary Drilling System SPE-211723-MS presented at 2022 Abu Dhabi International Petroleum Exhibition and Conference. 31st – 3rd Nov. 2023. <https://doi.org/10.2118/211723-MS>
- AMADI, K. and IYALLA, I., 2012. Application of mechanical specific energy techniques in reducing drilling cost in deepwater development. In: Society of Petroleum Engineers - SPE Deepwater Drilling and Completions Conference 2012. pp. 626–635.
- AMANI A, SHAHBAZI K (2013); Prediction of rock strength using drilling data and sonic logs. *Int J Comput Appl* 81(2):5–10. <https://doi.org/10.5120/13982-1986>
- AMER M.M, DAHAS A.S, and EL-SAYED, A.H (2017); An ROP Predictive Model in Nile Delta using Artificial Neural Networks. SPE-187969-MS Presented at the SPE Kingdom of Saudi Arabia Annual Technical Symposium and Exhibition. <https://doi.org/10.2118/187969-MS>
- ARABJAMALOEI, R.; SHADIZADEH, (2011); S. Modeling and Optimizing Rate of Penetration Using Intelligent Systems in an Iranian Southern Oil Field (Ahwaz Oil Field). *Pet. Sci. Technol.* 2011, 29, 1637–1648. <https://doi.org/10.1080/10916460902882818>
- ANTONIO, L.M. and COELLO, C.A.C., 2018. Coevolutionary Multiobjective Evolutionary Algorithms: Survey of the State-of-the-Art. *IEEE Transactions on Evolutionary Computation*, 22(6).
- ARMENTA, M; (2008); Identifying inefficient drilling conditions using drilling specific energy. SPE Annual Technical conference and Ex. 2008 Denver, Colorado. <https://doi.org/10.2118/116667-MS>
- ARMENTA, M; 2008; Identifying inefficient drilling conditions using drilling specific energy. SPE Annual Technical conference and Ex. 2008 Denver, Colorado. <https://doi.org/10.2118/116667-MS>
- ASADI, A (2017); Application of artificial neural networks in prediction of uniaxial compressive strength of rocks using well logs and drilling data. *Proc Eng* 191:279–286
- AWOTUNDE, A.A. and MUTASIEM, M.A., 2014. Efficient Drilling Time Optimization with Differential Evolution. In: SPE Nigeria Annual International Conference and Exhibition.
- BAKERHUGHES, 2020. World rig count. <https://rigcount.bakerhughes.com/rig-count-overview>.
- BARBOSA, L.F.F.M. et al., 2019. Machine learning methods applied to drilling rate of penetration prediction and optimization - A review. *Journal of Petroleum Science and Engineering*, 183.
- BATAEE, M. and MOHSENI, S., 2011. Application of Artificial Intelligent Systems in ROP Optimization: a Case Study. In: SPE Middle East Unconventional Gas Conference and Exhibition. Society of Petroleum Engineers.
- BILGESU, H.I. et al., 1997. A New Approach for the Prediction of Rate of Penetration (ROP) Values. In: Proceedings of the SPE-39231-MS Was Presented at SPE Eastern Regional Meeting,.
- BINGHAM, M.G., 1965. A new approach to interpreting- rock drillability. *Petroleum Pub.*

- BISHOP, C.M., 1995. *Neural Networks for Pattern Recognition*. Oxford University Press.
- BISHOP, C.M., 2006. *Pattern recognition and machine learning*. Springer-Verlag,
- BODAGHI, A., ANSARI, H.R. and GHOLAMI, M., 2015. Optimized support vector regression for drilling rate of penetration estimation. *Open Geosciences*, 7(1).
- BOURGOYNE, A.T. and YOUNG, F.S., 1974. A Multiple Regression Approach to Optimal Drilling and Abnormal Pressure Detection. *Society of Petroleum Engineers Journal*, 14(04).
- BP, 2014. *world energy review*. world energy review.
- BAHARI, A.; BARADARAN SEYED, A. (2007); Trust-Region Approach to Find Constants of Bourgoyne and Young Penetration Rate Modeling Khangiran Iranian Gas Field. In Proceedings of the SPE-107520-MS Was Presented at Latin American & Caribbean Petroleum Engineering Conference, Buenos Aires, Argentina, 15–18 April 2007. <https://doi.org/10.2118/107520-MS>
- BATAEE, M.; MOHSENI, S. (2011); Application of Artificial Intelligent Systems in ROP Optimization: A Case Study. In Proceedings of the SPE-140029-MS was Presented at SPE Middle East Unconventional Gas Conference and Exhibition, Muscat, Oman, 31 January–2 February 2011. <https://doi.org/10.2118/140029-MS>
- BHOWMIK, S., PANUA, R., DEBROY, D., and PAUL, A., (2017); “Artificial Neural Network Prediction of Diesel Engine Performance and Emission Fueled with Diesel–Kerosene–Ethanol Blends: A Fuzzy-Based Optimization,” *ASME J. Energy Resour. Technol.*, 139(4), p. 042201. <https://doi.org/10.1115/1.4035886>
- BILGESU, H.I.; TETRICK, L.T.; ALTMIS, U.; MOHAGHEGH, S.; AMERI, S. (1997); A New Approach for the Prediction of Rate of Penetration (ROP) Values. In Proceedings of the SPE-39231-MS Was Presented at SPE Eastern Regional Meeting, Lexington, KY, USA, 22–24 October 1997. <https://doi.org/10.2118/39231>
- BILGESU, H, COX Z.D, ELSHEHABI, C., IDOWU, G.O, ;(2017); A Realtime interactive drill-off test utilizing artificial intelligence algorithms for DSAT Drilling automation university competition 2017 <https://doi.org/10.2118/185730-MS>
- BINGHAM, M.G (1965); A New Approach to Interpreting—Rock Drillability; Petroleum Pub. Co.: Tulsa, OK, USA.
- BODAGHI, A.; ANSARI, H.R.; GHOLAMI, M. (2015); Optimized support vector regression for drilling rate of penetration estimation. *Open Geoscience*. 2015. <https://doi.org/10.1515/geo-2015-0054>
- BUNTINE, W. (1992); Learning classification trees. *Statistics computing* 2 (2)63-67 <https://doi.org/10.1007/BF01889584>
- BURGOYNE, A.T.; YOUNG, F.S (1974); Multiple Regression Approach to Optimal Drilling and Abnormal Pressure Detection. *J. SPE* 1974, 14, 371–384. <https://doi.org/10.2118/4238-PA>
- CAVANOUGH G.L; KOCHANNEK, M; CUNNINGHAM, J.B; GIPPS, I.D ;2008. A self-optimizing control system for Hard rock percussive drilling, *IEEE/ASME transactions on Mechatronics* 2008,1, 1083-4435. <https://doi.org/10.1109/TMECH.2008.918477>
- CHANG C., (2006): Empirical rock strength logging in boreholes penetrating sedimentary formations. *J. Eng. Geol.* 7(3):174–183
- CHAU K., T, WONG R.H., (1996); Uniaxial compressive strength and point load strength of rocks. *Int J Rock Mech Min Sci Geomech Abstracts* 33(2):183–188. [https://doi.org/10.1016/01489062\(95\)00056-9](https://doi.org/10.1016/01489062(95)00056-9).
- CHIRANTH, H, DAIGLE, H, MILLWATER, H, and GRAY, K; 2017. Analysis of the rate of penetration (ROP) prediction in drilling using physic-based and data driven Models. *Journal of petroleum science and Engineering*, 2017, 159, 295-306. <https://doi.org/10.1016/j.petrol.2017.09.020>
- CHOPRA, S.,MARBURT, K., J., and SHARMA, R., K., (2019) Unsupervised machine learning facies classification in the Delaware Basin and its comparison with supervised Bayesian facies classification
- CAPUANO (2016); *Geothermal Well Drilling for Power generation*
- CAO, J. et al., 2015. Extreme Learning Machine for Reservoir Parameter Estimation in Heterogeneous Sandstone Reservoir. *Mathematical Problems in Engineering*, 2015.
- CCOICCA, Y.J., 2013. Applications of Support Vector Machines in the Exploratory Phase of Petroleum and Natural Gas: a Survey. *International Journal of Engineering & Technology*, 2(2).
- CHIANDUSSI, G. et al., 2012. Comparison of multi-objective optimization methodologies for engineering applications. *Computers & Mathematics with Applications*, 63(5).
- CORTES, C. and VAPNIK, V., 1995. Support-vector networks. *Machine Learning*, 20(3).
- CUI, Y. et al., 2017. Review: Multi-objective optimization methods and application in energy saving. *Energy*, 125.
- DASHEVSKIY, D., DUBINSKY, V. and MACPHERSON, J.D., 1999. Application of Neural Networks for Predictive Control in Drilling Dynamics. In: *SPE Annual Technical Conference and Exhibition*. Society of

Petroleum Engineers.

- Deng, Y., Chen, M., Jin, Y., Zhang, Y., Zou, D., Lu, Y., 2016. Theoretical and experimental study on the penetration rate for roller cone bits based on the rock dynamic strength and drilling parameters. *J. Nat. Gas Sci. Eng.* 36, 117–123. <https://doi.org/10.1016/j.jngse.2016.10.019>.
- DESMETTE et al 2009. *Drilling optimization manual : Diamant Drilling services*
- DRUCKER, H. et al., 1997. *Support Vector Regression Machines*.
- EATON, A.N. et al., 2017. Real time model identification using multi-fidelity models in managed pressure drilling. *Computers & Chemical Engineering*, 97, pp. 76–84.
- ELKATATNY, S.M. et al., 2017. Optimization of Rate of Penetration using Artificial Intelligent Techniques. In: *Optimization of Rate of Penetration Using Artificial Intelligent Techniques*. American Rock Mechanics Association.
- EMERY C. L. (1966); The strain in rocks in relation to highway design. *Rock Mechanics*, (135):1–9. <http://onlinepubs.trb.org/Onlinepubs/hrr/1966/135/135-001.pdf>
- ENGBROKS, L. et al., 2018. Applying forward dynamic programming to combined energy and thermal management optimization of hybrid electric vehicles. *IFAC-PapersOnLine*, 51(31), pp. 383–389.
- ESKANDARIAN, S., BAHRAMI, P. and KAZEMI, P., 2017. A comprehensive data mining approach to estimate the rate of penetration: Application of neural network, rule based models and feature ranking. *Journal of Petroleum Science and Engineering*, 156.
- Ganasan, R., Tan, C.,G., Ibrahim, Z. (2021); Crack Width Prediction Models for RC Beam-Column Joint Subjected to Lateral Cyclic Loading Using Machine Learning. *Appl. Sci.* 2021, 11, 7700. <https://doi.org/10.3390/app11167700>
- GAO, Z., SUN, T. and XIAO, H., 2019. Decision-making method for vehicle longitudinal automatic driving based on reinforcement Q-learning. *International Journal of Advanced Robotic Systems*, 16(3), pp. 172988141985318–172988141985318.
- GENDELMAN, O. V., 2012. Analytic treatment of a system with a vibro-impact nonlinear energy sink. *Journal of Sound and Vibration*, 331(21).
- Golubev, A, Rabinovich G (1976); Resultaty primeneia apparturny akusticeskogo karotasa dlja predeleina proconstych svoystv gornych porod na mestorosdeniaach tverdykh isjopaemykh. *Prikl. Geofiz. Moskva* 73:109–116
- Gowida, A., Elkatatny, S. & Gamal, H. (2021); Unconfined compressive strength (UCS) prediction in real-time while drilling using artificial intelligence tools. *Neural Comput. Appl.* <https://doi.org/10.1007/s00521-020-05546-7> (2021).
- Gullu, and Hazirbaba (2010); Unconfined compressive strength and post-freeze–thaw behavior of fine-grained soils treated with geofiber and synthetic fluid. *Int J Cold Regions Science and Technology* 62 (2010) 142
- GURIA, C., GOLI, K.K. and PATHAK, A.K., 2014. Multi-objective optimization of oil well drilling using elitist non-dominated sorting genetic algorithm. *Petroleum Science*, 11(1), pp. 97–110.
- Hamrick T.R.(2011) *Optimization of Operating Parameters for Minimum Mechanical Specific Energy in Drilling* MSc Thesis. (West Virginia University, USA)
- HARELAND, G. and HOBEROCK, L.L., 1993. Use of Drilling Parameters To Predict In-Situ Stress Bounds. In: *SPE/IADC Drilling Conference*. Society of Petroleum Engineers.
- Hariharan, P R, and Azar, J J. (1996); PDC bit hydraulics design, profile are key to reducing balling. *United States: N. p.*, 1996. Web.
- HAYKIN, S.; HAKIN, S., (1998); *The Neural Networks a Comprehensive Foundation*; Macmillan College Publishing Company: Stuttgart, Germany, 1998.
- HESTER, T., LOPES, M. and STONE, P., 2013. *Learning Exploration Strategies in Model-Based Reinforcement Learning*. Available from: <http://www.ifaamas.org>.
- HEGDE, C. et al., 2017. Analysis of rate of penetration (ROP) prediction in drilling using physics-based and data-driven models. *Journal of Petroleum Science and Engineering*, 159.
- HEGDE, C.M., WALLACE, S.P. and GRAY, K.E., 2015. Use of Regression and Bootstrapping in Drilling Inference and Prediction. In: *SPE Middle East Intelligent Oil and Gas Conference and Exhibition*. Society of Petroleum Engineers. <https://doi.org/10.2118/176791-MS>
- HEGDE, C., SOARES, C. and GRAY, K.E., 2018. Rate of Penetration (ROP) Modeling Using Hybrid Models: Deterministic and Machine Learning. In: *Proceedings of the 6th Unconventional Resources Technology Conference*. American Association of Petroleum Geologists. <https://doi.org/10.15530/urtec-2018-2896522>
- HUANG, G.-B., ZHU, Q.-Y. and SIEW, C.-K., 2006. Extreme learning machine: Theory and applications. *Neurocomputing*, 70(1–3).
- HUANG, H. and DETOURNAY, E., 2008. Intrinsic Length Scales in Tool-Rock Interaction. *International*

- Journal of Geomechanics, 8(1).
- JEFFERY, C. and CREEGAN, A., 2020. Adaptive Drilling Application Uses AI To Enhance On-Bottom Drilling Performance. *Journal of Petroleum Technology*, 72(08), pp. 45–47.
- Jahanbakhshi, R.; Keshavarzi, R.; Jafarnejhad, (2012) A. Real-time Prediction of Rate of Penetration during Drilling Operation in Oil and Gas Wells. In Proceedings of the ARMA-2012-244 Was Presented at 46th U.S. Rock Mechanics Geomechanics Symposium, Chicago, IL, USA, 24–27 June 2012
- JIANG, W. and SAMUEL, R., 2016. Optimization of Rate of Penetration in a Convoluted Drilling Framework using Ant Colony Optimization. In: IADC/SPE Drilling Conference and Exhibition. Society of Petroleum Engineers. <https://doi.org/10.2118/178847-MS>
- KHOUKHI, A.; Ibrahim, A. (2012); Rate of Penetration prediction and Optimization using Advancing Artificial Neural NETWORKS, a Comparative Study. In Proceedings of the 4th International Joint Conference on Computational Intelligence, Barcelona, Spain, 5–7 October 2012
- KONDERITE, W.L.; WEIS, J.A (2005) REAL-TIME IMPLEMENTATION OF MSE. IN PROCEEDINGS OF THE AADE NATIONAL TECHNICAL CONFERENCE AND EXHIBITION, HOUSTON, TX, USA, 5–7 APRIL 2005.
- KUMAMOTO University (2010) Lecture Note .<http://www.cs.kumamoto-u.ac.jp/epslab/ICinPS/Lecture-2.pdf>
- LECUN, Y., BENGIO, Y. and HINTON, G., 2015. Deep learning. *Nature*, 521(7553).
- LINDQVIST (1982); Rock fragmentation by indentation and disc cutting some theoretical and experimental studies.
- LYONS, W., PLISGA, G. and LORENZ, M., 2004. standard Handbook of Petroleum and Natural Gas Engineering.
- MANSHAD, A., ROSTAMI, H. and TOREIFI, H., 2017. Optimization of Drilling Penetration Rate in Oil Fields Using Artificial Intelligence Technique. *Heavy Oil.: Characteristics, Production and Emerging Technologies*; Nova Science Publishers: Hauppauge, NY, USA, 2017; pp. 255–269
- MANTHA, B. and SAMUEL, R., 2016. ROP Optimization Using Artificial Intelligence Techniques with Statistical Regression Coupling. In: SPE Annual Technical Conference and Exhibition. Society of Petroleum Engineers.
- MAZZINI, A., NERMOEN, A., KROTKIEWSKI, M., PODLADCHIKOV, Y., PLANKE, S., SVENSEN, H.,(2009);2009. Strike-slip faulting as a trigger mechanism for overpressure release through piercement structures. Implications for the LUSI mud volcano,Indonesia. *Marine and Petroleum Geology* 26, 1751–1765.
- MCKENNA, I, PAN, R, KOEDERITZ, W, (2015); The Application of Real-Time Stochastic Analysis for Autonomous Drilling Optimization. *Oil Gas European Magazine* (2015) 41(1) 21-23
- Norwegian Oil Industry Association, (2006); Integrated operation enhance value creation. Equinor Norway.
- MOTAHHARI, H.R. et al., 2007. Method of Optimizing Motor and Bit Performance for Maximum ROP. In: Canadian International Petroleum Conference. Petroleum Society of Canada.
- MAURER, W.C., 1962. The ‘Perfect - Cleaning’ Theory of Rotary Drilling. *Journal of Petroleum Technology*, 14(11). <https://doi.org/10.2118/408-PA>
- MORAN, D.P.; IBRAHIM, H.F.; PURWANTO, A; (2010); Osmond, J. Sophisticated ROP Prediction Technology Based on Neural Network Delivers Accurate Results. In Proceedings of the SPE-132010-MS Was Presented at IADC/SPE Asia Pacific Drilling Technology Conference and Exhibition, Ho Chi Minh City, Vietnam, 1–3 November 2010. <https://doi.org/10.2118/132010-MS>
- MORAVEJI, M.K. and NADERI, M., (2016). Drilling rate of penetration prediction and optimization using response surface methodology and bat algorithm. *Journal of Natural Gas Science and Engineering*, 31.
- MOSTOFI M, RAHIMZADEH H, SHAHBAZI K (2011) The development of a new sonic correlation for UCS estimation from drilling data. *Pet Sci Technol* 29(7):728–734. <https://doi.org/10.1080/10916460903452025>
- MITZER H, STOLL R (1973); Einige Beitrageder geophysics zur primadatenerfassung im Bergbau. *Neue Bergbautechnik*, pp 21–25
- Nabaei M, Shahbazi K (2012) A new approach for predrilling the unconfined rock compressive strength prediction. *Pet Sci Technol* 30(4):350–359. <https://doi.org/10.1080/10916461003752546>
- Neter J, Kutner M, Nachtsheim C, Wasserman W (1996) *Applied linear statistical models*. McGraw-Hill Companies, Inc, NY
- Norwegian Oil Industry Association, (2006) Integrated operation enhance value creation. Equinor Norway
- Oyler DC, Mark C, Melinda GM (2010) In situ estimation of roof rock strength using sonic logging. *Int J Coal Geol* 83:484–490
- PAVKOVIC, D., 2017. Current Trends in Oil Drilling Systems R&D with Emphasis on Croatian Oil Drilling Sector-A Review Isolated DC microgrids View project Advanced Systems for Drilling Control at

References

- Hydrocarbon Exploration Facilities View project. Available from: <https://www.researchgate.net/publication/316789728>.
- PAYETTE, G.S. et al., 2017. A Real-Time Well-Site Based Surveillance and Optimization Platform for Drilling: Technology, Basic Workflows and Field Results. In: SPE/IADC Drilling Conference and Exhibition. Society of Petroleum Engineers.
- PERERA, A.T.D. and KAMALARUBAN, P., 2021. Applications of reinforcement learning in energy systems. *Renewable and Sustainable Energy Reviews*, 137, p. 110618.
- Perrin, V.P.; Mensa-Wilmot, G.; Alexander, W.L (1997): Drilling index-a new approach to bit performance evaluation. In Proceedings of the SPE/IADC Drilling Conference, Amsterdam, The Netherlands, 4–6 March 1997.
- PETTER O, K., ROLLER and RAGNAR, T.,(2007): Productivity in Exploration Drilling Robert Gordon University (2008): Subsurface Engineering course note.
- Rashidi, M. & Asadi, A (2018); An artificial intelligence approach in estimation of formation pore pressure by critical drilling data. In 52nd U.S. Rock Mechanics/Geomechanics Symposium (2018).
- Sanjay K. Shrivastava, Ahmad Javed, K. Krishna Pratap (2013) Assessing Rock Compressive Strength and Predicting Formation Drillability using Sonic, Gamma & Density Logs. 10th Biennial International Conference & Exposition
- SEIFABAD, M.C. and EHTESHAMI, P., 2013. Estimating the drilling rate in Ahvaz oil field. *Journal of Petroleum Exploration and Production Technology*, 3(3).
- SHADIZADEH, S. R., KARIMI, F., and ZOVEIDAVIANPOOR, M., (2010); “Drilling Stuck Pipe Prediction in Iranian Oil Fields: An Artificial Neural Network Approach,” *Iran J. Chem. Eng.*, 7(4), pp. 29–41.
- SHI, X. et al., 2016. An Efficient Approach for Real-Time Prediction of Rate of Penetration in Offshore Drilling. *Mathematical Problems in Engineering*, 2016. <https://doi.org/10.1155/2016/3575380>
- SOARES, C., GRAY, K., (2019); Real-time predictive capabilities of analytical and machine learning rate of penetration (ROP) models.*J.Pet.Sci.Eng.* <https://doi.org/10.1016/j.petrol.2018>.
- SOARES, C., DAIGLE, H. and GRAY, K., 2016. Evaluation of PDC bit ROP models and the effect of rock strength on model coefficients. *Journal of Natural Gas Science and Engineering*, 34.
- SPENCER, S.J. et al., 2017. Estimation and control for efficient autonomous drilling through layered materials. In: 2017 American Control Conference (ACC). IEEE. pp. 176–182.
- SPRLJAN, P., PAVKOVIC, D. and KOLAR, 2020. Automation Systems Design and Prototyping Aimed at Mature Petroleum Drilling Rig Retrofitting. *Tehnicki Vjesnik - Technical Gazette*,27(1).
- SUTTON, R.S. and BARTO, A.G., (2020). Reinforcement Learning: An Introduction Second edition, in progress.
- SUYKENS, J.A.K. et al., 2002. Weighted least squares support vector machines: robustness and sparse approximation. *Neurocomputing*, 48(1–4).
- TEALE, R (1965); the concept of specific energy in rock drilling. *International journal of rock mechanics science*.2 (1) 57- 73. [https://doi.org/10.1016/0148-9062\(65\)90022-7](https://doi.org/10.1016/0148-9062(65)90022-7)
- TLEGENOV, Y., SAN, W. and SOON, H., 2015. Adaptive Feed Rate Policies for Spiral Drilling Using Markov Decision Process. *CoRR*, abs/1512.0, pp. 1–20.
- WARREN, T.M., 1987. Penetration Rate Performance of Roller Cone Bits. *SPE Drilling Engineering*, 2(01). <https://doi.org/10.2118/13259-PA>
- WEE, W. and KALOGERAKIS, N., 1989. Modelling Of Drilling Rate For Canadian Offshore Well Data. *Journal of Canadian Petroleum Technology*, 28(06).
- WEI, X, SHAHANI, N, ZHENG, X (2023); Predictive Modeling of the Uniaxial Compressive DStrengths of rock Using Artificial Neural Network. *MPDI Journal* <https://doi.org/10.3390/math11071650>.
- XU, X. et al., 2019. A Reinforcement Learning Approach to Autonomous Decision Making of Intelligent Vehicles on Highways. *IEEE Transactions on Systems, Man, and Cybernetics: Systems*.
- Xia, Y., He, L, Li, Y, Liu, N., and Ding, Y., (2019) Predicting Loan Default in Peer-to-Peer Lending using Narrative Data. *Journal of Forecasting*. Pp.1–21, 2019. <https://doi.org/10.1002/for.2625>
- YUSWANDARI, A., PRAYOGA, A. and PURBA, D., n.d. Rate of Penetration (ROP) Prediction Using Artificial Neural Network to Predict ROP for Nearby Well in a Geothermal Field. In: PROCEEDINGS.
- Zausa, F., Civolani, L., Brignoli, M. and Santarelli, F. J. (1997); Analyzing oil well stability in real time during the drilling process. *The Indentation Technique and other mechanical*
- ZHANG, X. and JIANG, H., 2021. Automated optimal control in energy systems: the reinforcement learning approach. In: *New Technologies for Power System Operation and Analysis*. Elsevier. pp. 275–318.
- ZHOU, A. et al., 2011. Multiobjective evolutionary algorithms: A survey of the state of the art. *Swarm and Evolutionary Computation*, 1(1).